THESIS for Ph.D. in ENGINEERING

"On the Range and Application of Arched Plate Theory"

by

CHARLES M. MOIR, B.Sc.(Lond.)

November, 1933.

ABSTRACT.

This paper deals with the effects of symmetrical loading on thin shells of uniform thickness; cyclical loads are not included. The equations of equilibrium and stress-strain relations are established for a portion of thin curved plate subject to tangential and radial loading. From these are derived the particular sets of equations for circular flat plates, cylindrical, conical and spherical walls. The distortion and stress equations for the different sets are presented in expressions of similar type. In conical and spherical walls, experimental corroboration has been obtained for the more complicated expressions, which are believed to appear for the first time. The applications include important practical engineering problems on the separate and combined forms. A comparison of the probable effects between welded and riveted joints in the cylindrical wall with a hemispherical dished end serves as an introduction to a final discussion of the elliptical and double segmental end.

C O N T E N T S.

------ oOo ------

The distortions and stresses in thin curved plates have been the subject of many mathematical researches. In his standard work[1] Professor Love has given references to the more notable contributions, and his theory on thin shells may be taken as the most advanced and comprehensive work of the present day. He has dealt very fully with the immediate cases which concern this paper; the cylindrical, conical and spherical shells. While the expressions derived in the treatment satisfy the mathematician, they are of little value to the engineer who considers the worth of formulae on a basis of simplicity and adaptability. To him there remains the task of interpreting these expressions and reducing them to such a form that their applications to problems in engineering design present little difficulty. Papers demonstrating how the final expressions of these mathematical researches may be extended, recast and so applied, are very few. The lack of publications must be attributed to the difficult methods adopted in derivation and the complicated form in which the theory appears.

A brief survey may assist, in the reading of this paper, to distinguish between what is presented as original work and what has appeared elsewhere. It is necessary, of course, that a paper of this order should include theories which have appeared before; these are indicated. In many cases, however, the methods of derivation are new and the final forms entirely different.

The case of circular flat plates has received much attention both analytically and experimentally. In a recent paper[2], a line of investigation by the former method presented a mode of treatment which differed from the established method of derivation, resulting in the equations for direct and bending stresses being formulated in expressions of similar type/

1. "Mathematical Theory of Elasticity" A.E.H. Love, 3rd Edition, 1920.

2. "Direct and Bending Stresses in Circular Flat Plates" Prof. W. Kerr, Ph.D., Journal R.T.C., 1930.

type. These expressions are not only identical, they are also simple and possess a wide range of application. This work has been embodied in this Thesis because the circular flat disc is one of the extreme cases in arched plate theory; and also, an illustration is given of the method of procedure in the application of the results to an important engineering problem.

The theory of cylindrical walls is well known and has been included in many books. The application of the theory has, however, been restricted to a very small range, and particular cases outwith this range have been the subjects of isolated papers. These various investigations on an essentially similar problem, with degrees of variation in the conditions, have been carried out on different lines. All lead to important conclusions in engineering design, but the varying methods of derivation obscure and complicate the problem of the cylindrical wall. For design purposes this is not satisfactory.

The direct or membrane stresses due to the effects of internal pressure in a spherical shell have been included in many publications. The equations of stress due to edge forces do not appear so frequently, and where they are mentioned, the equations have been adapted from those for the cylindrical wall, giving results which are approximately correct only for the hemispherical shell. Equations of stress due to the loading of a conical wall do not seem to have appeared in any publication. In spite of the lack of information from engineering research on these simple forms, elliptical and double segmental dished ends have been the subjects recently of much investigation in America and Germany. To attack such complicated forms with no more guidance than what can be given by the cylindrical equations, and these not fully developed, is a very doubtful procedure. It would appear more satisfactory to lead up to these solutions after the equations for conical

and/

and spherical shells have been established.

In the present paper, from a general development, the stress-strain relations and equations of equilibrium for the forms, circular flat plate, cylindrical, conical and spherical walls are derived. Each set shows very clearly the nature of the successive complications that arise with the change of form. Nevertheless, when the equations of distortions and stresses are formulated, they show, for each case, a similarity of type which is remarkable and constitutes an aid to investigation.

The appearance of so many constants in the final equations would appear to constitute a real difficulty in their application. All that is required, however, is an effective method of handling large and, at times, clumsy expressions.

In circular flat plates the bending and direct stresses are evaluated separately. The equations expressing these types of stress, being developed from identical equations, allow the use of one mode of attack which greatly simplifies the work.

In cylindrical walls the extensional and edge effects, analogous to direct and bending effects in flat plates, can also be expressed separately. While the two sets of equations are not at all similar, this step is advantageous in breaking up the constants into two groups. The extensional equations, not unlike the equations for circular plates, contain two constants and their solutions are not difficult. The edge effect equations include four constants and much work is entailed in determining their values. Whatever the conditions of the problem may be, these values are obtained by solving four simultaneous equations. To facilitate the application of the results the values have been fully determined and tabulated for a wide range of cases.

The values of the constants for conical walls are determined by an identical procedure, but they cannot be reduced to the neat and simple terms which express the cylindrical constants. A straight-forward evaluation of stress for each example, reaching a numerical solution by the most direct route is to be preferred. Owing to the form, the constants for the extensional and edge effects in spherical walls cannot be determined separately. While the equations expressing these effects may be so determined, in the evaluation of the constants it is necessary in most cases to combine the two solutions. The handling of the constants constitutes an important part of this paper, and the different cases are discussed under their particular sections.

While some of the applications are new, there are others which have appeared in recent publications. As regards the latter, the methods of derivation employed here are different; in one case only partial agreement is obtained in the conclusions. The whole endeavour of this paper is to demonstrate how problems on plate forms - flat and arched - can be solved by similar methods, although specific conditions may vary widely.

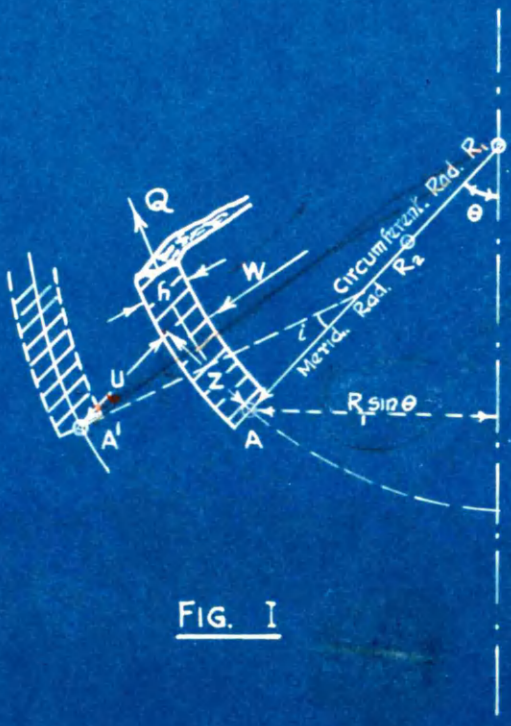

FIG. I

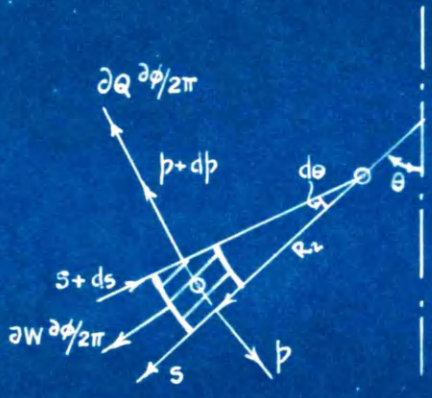

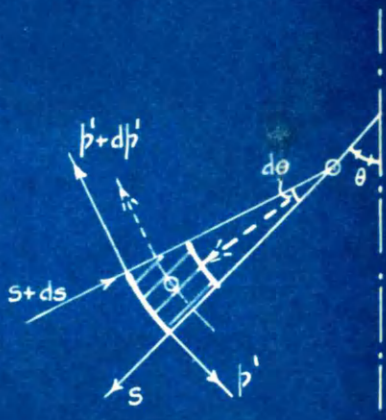

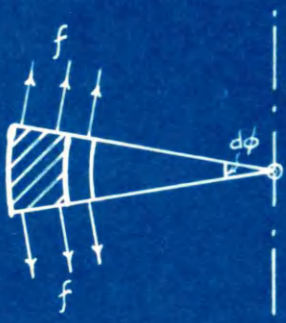

FIG. 2a.

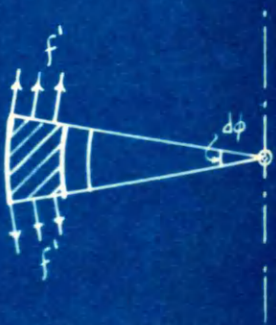

FIG. 2b.

General Development of Theory.

Consider the portion of thin curved plate of uniform thickness h as shown in Fig. I. The meridional and circumferential radii at point A are denoted by R_2 and R_1 respectively. Under the actions of the radial force W and the tangential force Q, A strains to A^1. The tangential displacement is Z and the radial displacement U. The change of slope, i, assumed positive in the direction shown, is then equal to $-\frac{du}{R_2 d\theta} + \frac{z}{R_2}$. The circumferential strain of the outer fibres is:-

$$\frac{2\pi\{R_1 \sin\theta + Z\cos\theta + U\sin\theta + h/2 \cdot \sin(\theta+i) - R_1\sin\theta - h/2\cdot\sin\theta\}}{2\pi\{R_1\sin\theta + h/2\cdot\sin\theta\}}$$

$$= \frac{z}{R_1}\cot\theta + \frac{u}{R_1} + \frac{h}{2R_1}\cdot i\cdot\cot\theta$$

The meridional strain of the outer fibres is:-

$$\frac{1}{R_2}\cdot\frac{dz}{d\theta} + \frac{u}{R_2} + \frac{h}{2R_2}\cdot\frac{di}{d\theta}$$

Observing that $\left(\frac{z}{R_1}\cot\theta + \frac{u}{R_1}\right)$ and $\left(\frac{1}{R_2}\cdot\frac{dz}{d\theta} + \frac{u}{R_2}\right)$ are due to direct stresses and $h/2R_1\cdot(i\cot\theta)$ and $h/2R_2\cdot\frac{di}{d\theta}$ due to bending stresses, the stress-strain relations are obtained as follows:-

Direct Effects.	Bending Effects.
$\frac{z}{R_1}\cdot\cot\theta + \frac{u}{R_1} = f - \sigma p$	$\frac{h}{2R_1}\cdot(i\cot\theta) = f' - \sigma p'$
$\frac{1}{R_2}\cdot\frac{dz}{d\theta} + \frac{u}{R_2} = p - \sigma f$	$\frac{h}{2R_2}\cdot\frac{di}{d\theta} = p' - \sigma f'$

where f and f^1 are the circumferential direct and bending stresses respectively; p and p^1, the radial direct and bending stresses; E, the modulus and σ, Poisson's ratio.

The equilibrium equations are obtained in the usual manner. In Fig. 2(a), ∂Q and ∂W are respectively the tangential and radial forces on the complete annular element of length $R_2 d\theta$. The condition of tangential equilibrium for the element subtending an angle $\partial\phi$ at the centre gives:-

$$(p+dp)(R_1+dR_1)\sin(\theta+d\theta)\,h\,d\phi\cos d\theta - pR_1\sin\theta\,h\,d\phi - (s+ds)(R_1+dR_1)\sin(\theta+d\theta)\,h\,d\phi\sin d\theta$$

$$-fR_2\,d\theta\,h\,d\phi\cos\theta + dQ\,d\phi/2\pi\cdot\cos d\theta = 0$$

$$\therefore \frac{d}{d\theta}(pR_1\sin\theta) - fR_2\cos\theta - sR_1\sin\theta = -\frac{1}{2\pi h}\cdot\frac{dQ}{d\theta}$$

Consideration of the forces radially gives:-

$$-(p+dp)(R_1+dR_1)\sin(\theta+d\theta)\,h\,d\phi\sin d\theta - (s+ds)(R_1+dR_1)\sin(\theta+d\theta)\,h\,d\phi\cos d\theta$$

$$+(sR_1)\sin\theta\cdot h\cdot d\phi - fR_2\,d\theta\,h\,d\phi\sin\theta - dQ\cdot\frac{d\phi}{2\pi}\cdot\sin d\theta + dW\cdot\frac{d\phi}{2\pi} = 0$$

$$\therefore pR_1\sin\theta + fR_1\cos\theta + \frac{d}{d\theta}(sR_1\sin\theta) = \frac{1}{2\pi h}\cdot\frac{dW}{d\theta}$$

From Fig 2(b), by taking moments about point O, we have

$$\frac{h^2}{6}(p'+dp')(R_1+dR_1)\sin(\theta+d\theta)\,d\phi - \frac{h^2}{6}p'R_1\sin\theta\cdot d\phi + (s+ds)(R_1+dR_1)\sin(\theta+d\theta)\,h\,d\phi\,R_2\frac{d\theta}{2}$$

$$+sR_1\sin\theta\cdot h\cdot d\phi\cdot R_2\frac{d\theta}{2} - \frac{h^2}{6}\cdot f'\cdot R_2\,d\theta\cdot d\phi\cdot\cos\theta = 0$$

$$\therefore sR_1R_2\sin\theta = -\frac{h}{6}\cdot\frac{d}{d\theta}(p'R_1\sin\theta) + \frac{h}{6}\cdot f'R_2\cos\theta$$

The complete set of equations for the general development may now be written down as follows:-

$$E\left(\frac{z\cot\theta}{R_1} + \frac{u}{R_1}\right) = f - \sigma p$$

$$E\left(\frac{1}{R_2}\cdot\frac{dz}{d\theta} + \frac{u}{R_2}\right) = p - \sigma f$$

$$E\cdot\frac{h}{2}\cdot\frac{i\cot\theta}{R_1} = f' - \sigma p'$$

$$E\cdot\frac{h}{2}\cdot\frac{1}{R_2}\frac{di}{d\theta} = p' - \sigma f'$$

$$\frac{d}{d\theta}(pR_1\sin\theta) - fR_2\cos\theta - sR_1\sin\theta = -\frac{1}{2\pi h}\cdot\frac{dQ}{d\theta}$$

$$pR_1\sin\theta + fR_2\sin\theta + \frac{d}{d\theta}(sR_1\sin\theta) = \frac{1}{2\pi h}\cdot\frac{dW}{d\theta}$$

$$sR_1R_2\sin\theta = -\frac{h}{6}\cdot\frac{d}{d\theta}(p'R_1\sin\theta) + \frac{h}{6}f'R_2\cos\theta$$

$$i = -\frac{1}{R_2}\cdot\frac{du}{d\theta} + \frac{z}{R_2}$$

From these relations a set of equations for different forms may be derived.

SECTION I.

CIRCULAR FLAT PLATES.

Theoretical Development:

Application:

Circular Flat Plates[2]

In this case $\theta = 0$, $R_1 = R_2 = \infty$. Put $R_2 d\theta = dr$, $R_1 \sin\theta = r$, where dr is the thickness of an annular element of radius r. The general equations become:-

$$\left.\begin{aligned} E\frac{z}{r} &= f - \sigma p \\ E\frac{dz}{dr} &= p - \sigma f \\ E\cdot\frac{h}{2}\cdot\frac{i}{r} &= f' - \sigma p' \\ E\cdot\frac{h}{2}\cdot\frac{di}{dr} &= p' - \sigma f' \end{aligned}\right\} \cdots (1) \qquad \left.\begin{aligned} \frac{d}{dr}(pr) - f &= -\frac{1}{2\pi h}\cdot\frac{dQ}{dr} \\ sr &= \frac{W}{2\pi h} \\ sr &= -\frac{h}{6}\cdot\frac{d}{dr}(p'r) + \frac{h}{6}\cdot f' \\ i &= -\frac{du}{dr} \end{aligned}\right\} \cdots (2)$$

These equations may be broken up into two separate groups and appear as:-

For Direct Conditions.

$$\left.\begin{aligned} E\cdot\frac{z}{r} &= f - \sigma p \\ E\frac{dz}{dr} &= p - \sigma f \\ f &= \frac{d}{dr}(pr) + \frac{1}{2\pi h}\cdot\frac{dQ}{dr} \end{aligned}\right\} \cdots (3)$$

For Bending Conditions.

$$\left.\begin{aligned} E\frac{u'}{r} &= f' - \sigma p' \\ E\frac{du'}{dr} &= p' - \sigma f' \\ f' &= \frac{d}{dr}(p'r) + \frac{3}{\pi h^2}\cdot W \end{aligned}\right\} \cdots (4)$$

where $u' = h/2 \cdot i$ Similarity will be exact when the last terms in the third equation of each group are written:-

$$\frac{1}{2\pi h}\cdot\frac{dQ}{dr} = m_2 + n_2 r + K_2 r^2 \cdots\cdots\cdots\cdots (5)$$

and $$\frac{3}{\pi h^2} W = m'_2 + n'_2 r + K'_2 r^2 \cdots\cdots\cdots (6)$$

These expressions refer to a general state of loading and in the Q equation only the third term is required for rotational effects. In the W equation the first term is necessary for ring loads and the third term for uniform loading.

Formation of Basic Equation.

Considering the direct set of equations alone, elimination of Z between the first and second equations and substitution of f from:-

$$f = \frac{d}{dr}(pr) + m_2 + n_2 r + K_2 r^2 \cdots\cdots\cdots (7)$$

leads on reduction to:-

$$r^2\cdot\frac{d^2}{dr^2}(pr) + r\frac{d}{dr}(pr) - (pr) = -(1+\sigma)m_2 r - (2+\sigma)n_2 r^2 - (3+\sigma)K_2 r^3 \cdots (8)$$

Ibid.

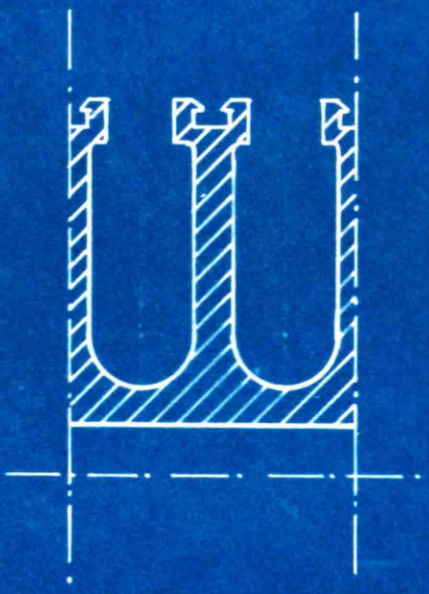

FIG. 3a.

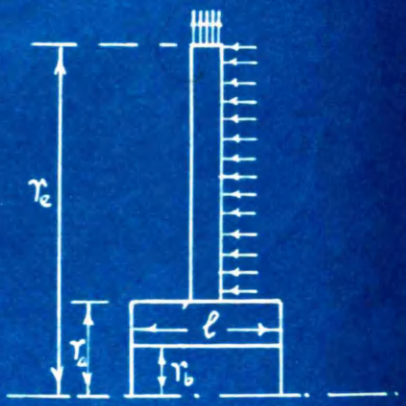

FIG. 3b.

The solutions for the direct stresses p and f are found as:-

$$p = A + \frac{B}{r^2} - \left(\frac{1+\sigma}{2}\right) m_2 \log_e r - \left(\frac{2+\sigma}{3}\right) n_2 r - \left(\frac{3+\sigma}{8}\right) K_2 r^2 \qquad \text{-----(9)}$$

$$f = A - \frac{B}{r^2} + \left(\frac{1-\sigma}{2}\right) m_2 - \left(\frac{1+\sigma}{2}\right) m_2 \log_e r - \left(\frac{1+2\sigma}{3}\right) n_2 r - \left(\frac{1+3\sigma}{8}\right) K_2 r^2 \qquad \text{- - - -(10)}$$

$$E\frac{u}{r} = f - \sigma p \qquad \text{- - - -(11)}$$

The solutions for the bending stresses follow and are:-

$$p' = A' + \frac{B'}{r^2} - \left(\frac{1+\sigma}{2}\right) m_2' \log_e r - \left(\frac{2+\sigma}{3}\right) n_2' r - \left(\frac{3+\sigma}{8}\right) K_2' r^2 \qquad \text{- - - - (12)}$$

$$f' = A' - \frac{B'}{r^2} + \left(\frac{1-\sigma}{2}\right) m_2' - \left(\frac{1+\sigma}{2}\right) m_2' \log_e r - \left(\frac{1+2\sigma}{3}\right) n_2' r - \left(\frac{1+3\sigma}{8}\right) K_2' r^2 \qquad \text{- - - -(13)}$$

$$E\frac{u'}{r} = E \cdot \frac{h}{2} \cdot \frac{i}{r} = f' - \sigma p' \qquad \text{- - - -(14)}$$

A and B, A' and B' are integration constants.
In these equations the accented symbols refer always to bending values and are to be contrasted with the same symbols unaccented for the direct conditions.

Sign Convention.

Tensile stresses are in all cases positive. The bending stresses are then at the outer fibres. The solutions obtained for p^1, f^1, and u^1 refer to the lower side of a horizontal plate, so that positive values would indicate bending concave upwards. The lateral pressure is positive if downwards.

The following example illustrates the method of procedure in the application of these results to a typical problem which maintains general expressions throughout. For any specific example a straight-forward evaluation of stress is simpler.

Investigation of Stresses in a High Speed Turbine Disc under Pressure.

This problem is an investigation of the stresses in a high speed turbine disc, machined from the solid, as shown in Fig. 3(a). It carries a lateral pressure, W, together with peripheral radial stresses, and is taken as directionally fixed at both outer and inner radii, Fig. 3(b).

This/

This case is developed in three separate steps, viz., consideration of:-

(I) the direct stresses in the disc;

(II) the direct stresses in the cylinder, treating the cylinder as a disc;

(III) the bending stresses in the disc.

(I). If Q be the radial loading due to rotation, then at any radius r,

$$dQ = \frac{\rho \cdot 2\pi r \cdot dr \cdot h \cdot \omega^2 r}{g} \; ; \; \therefore \; \frac{1}{2\pi h} \cdot \frac{dQ}{dr} = \frac{\rho \cdot \omega^2 r^2}{g} \; ; \; \therefore K_2 = \frac{\rho \omega^2}{g}$$

where ρ is the density and ω is the angular velocity. Also $m_2 = n_2 = 0$:-

$$\therefore p = A + \frac{B}{r^2} - \frac{3+\sigma}{8} \cdot K_2 r^2 \qquad \text{(15)}$$

$$\therefore f = A - \frac{B}{r^2} - \frac{1+3\sigma}{8} \cdot K_2 r^2 \qquad \text{(16)}$$

$$E\frac{U}{r} = f - \sigma p \qquad \text{(17)}$$

where U is the radial expansion at a radius r. The boundary conditions are:-

$$p = p_e \text{ at } r = r_e \; ; \qquad p = p_a \text{ at } r = r_a .$$

hence:-

$$p_e = A + \frac{B}{r_e^2} - \frac{3+\sigma}{8} \cdot K_2 r_e^2 \qquad \text{(18)}$$

$$p_a = A + \frac{B}{r_a^2} - \frac{3+\sigma}{8} \cdot K_2 r_a^2 \qquad \text{(19)}$$

From (18) and (19) the integration constants A and B are found as:-

$$A = -\frac{p_a r_a^2}{r_e^2 - r_a^2} + \frac{p_e r_e^2}{r_e^2 - r_a^2} + C_1 (r_e^2 + r_a^2) \qquad \text{(20)}$$

$$B = \frac{r_a^2 r_e^2}{r_e^2 - r_a^2} (p_a - p_e) - C_1 r_a^2 r_e^2 \qquad \text{(21)}$$

where $C_1 = \frac{3+\sigma}{8} K_2$. Substituting the values of A and B in (16) we obtain at $r = r_a$:-

$$f_a = -\frac{p_a (r_a^2 + r_e^2)}{r_e^2 - r_a^2} + \frac{2 p_e r_a^2}{r_e^2 - r_a^2} + C_1 \{2 r_e^2 + r_a^2\} - C_2 r_a^2 \qquad \text{(22)}$$

where $C_2 = \frac{1+3\sigma}{8} \cdot K_2$

(II). Rotational stresses only are considered in the cylinder and/

and to cover these effects $K_2 = \frac{\rho\omega^2}{g}$ is used and the equations can be written:-

$$p = A + \frac{B}{r^2} - \frac{3+\sigma}{8} K_2 r^2 \quad \ldots\ldots\ldots (23)$$

$$f = A - \frac{B}{r^2} - \frac{1+3\sigma}{8} K_2 r^2 \quad \ldots\ldots\ldots (24)$$

$$E\frac{u}{r} = f - \sigma p \quad \ldots\ldots\ldots (25)$$

The boundary conditions for the cylinder are:-

$$p = p_a \frac{h}{\ell} \text{ at } r = r_a \; ; \qquad p = 0 \text{ at } r = r_b$$

Substituting in (23) therefore:-

$$p_a \frac{h}{\ell} = A + \frac{B}{r_a^2} - C_1 r_a^2 \quad \ldots\ldots (26)$$

$$0 = A + \frac{B}{r_b^2} - C_1 r_b^2 \quad \ldots\ldots (27)$$

From (26) and (27) the values A and B are obtained as:-

$$A = -p_a \cdot \frac{h}{\ell} \cdot \frac{r_a^2}{r_b^2 - r_a^2} + C_1 (r_a^2 + r_b^2) \quad \ldots\ldots (28)$$

$$B = p_a \cdot \frac{h}{\ell} \cdot \frac{r_a^2 r_b^2}{r_b^2 - r_a^2} - C_1 (r_a^2 \times r_b^2) \quad \ldots\ldots (29)$$

The radial hoop stress in the cylinder at $r = r_a$ is found by substituting the values above in (24), giving:-

$$f = -p_a \cdot \frac{h}{\ell} \cdot \frac{r_a^2 + r_b^2}{r_b^2 - r_a^2} + C_1 \{r_a^2 + 2r_b^2\} - C_2 r_a^2 \quad \ldots\ldots (30)$$

The connecting condition between the disc and the cylinder is that the radial expansion is the same for both at $r = r_a$. Hence:-

$$(f - \sigma p) \text{ for disc} = (f - \sigma p) \text{ for cylinder}$$

For the disc the value of f is found in equation (22) and $p = p_a$. For the cylinder f is as in (30) and $p = p_a \cdot h/\ell$. We finally obtain:-

$$p_a \left\{ \left(\frac{r_c^2 + r_a^2}{r_c^2 - r_a^2} + \sigma \right) + \left(\frac{r_a^2 + r_b^2}{r_a^2 - r_b^2} - \sigma \right) \frac{h}{\ell} \right\} = 2p_c \cdot \frac{r_c^2}{r_c^2 - r_a^2} + C_1 \left\{ 2r_a^2 - 2r_b^2 \right\} \quad \ldots (31)$$

p_a can therefore be found and hence all radial strains and stresses in the disc and cylinder.

(III). The pressure difference W on the disc within any area of radius r is $W = \{\pi\omega^2(r^2 - r_a^2) - P\}$ where P is the lateral restraint at the bore. Hence:-

$$\frac{3}{\pi h^2} \cdot W = \frac{3}{\pi h^2} \{\pi\omega^2(r^2 - r_a^2) - P\} \quad \therefore m_2' = \left\{ \frac{3P}{\pi h^2} + \frac{3\omega}{h^2} \cdot r_a^2 \right\} ; \quad \therefore K_2' = \frac{3\omega}{h^2}$$

The stress equations may now be written as:-

$$p' = A' + \frac{B'}{r^2} - \left(\frac{1+\sigma}{2}\right) m_2' \log_e r - \left(\frac{3+\sigma}{8}\right) K_2' r^2 \quad \ldots\ldots (32)$$

$$f' = A' - \frac{B'}{r^2} - \left(\frac{1+\sigma}{2}\right) m_2' \log_e r - \left(\frac{1+3\sigma}{8}\right) K_2' r^2 + \left(\frac{1+\sigma}{2}\right) m_2' \quad \ldots\ldots (33)$$

$$E \frac{\delta_r}{2} \cdot \frac{i}{r} = f' - \sigma p' \quad \ldots\ldots (34)$$

The boundary conditions are, that the slopes at $r = r_e$ and $r = r_a$ are zero. Substituting in (34) the particular values of f^1 and p^1 at the above radii, two equations are obtained from which the integration constants are found as:-

$$A' = \frac{1+\sigma}{2} \cdot m_2' \left\{ \frac{r_e^2}{r_e^2 - r_a^2} \log_e \frac{r_e}{r_a} + \log_e r_a \right\} + \frac{K_2'}{8}(1+\sigma)(r_e^2 + r_a^2) - \frac{m_2'}{2} \quad \ldots (35)$$

$$B' = \frac{1-\sigma}{2} m_2' \cdot \frac{r_e r_a}{r_e^2 - r_a^2} \log_e \frac{r_e}{r_a} + \frac{K_2'}{8}(1+\sigma) r_e^2 r_a^2 \quad \ldots\ldots (36)$$

Substituting these values in (32) the radial bending stress at $r = r_a$ is found as:-

$$p_a = m_2' \frac{r_e^2}{r_e^2 - r_a^2} \cdot \log_e \frac{r_e}{r_a} + \frac{K_2'}{4}\left\{ r_e^2 - r_a^2 \right\} - \frac{m_2'}{2} \quad \ldots (37)$$

Generally, high radial stresses occur at the junction of the disc and cylinder. Superimposing the radial direct stress as found from (31) on the radial bending stress as in (37), the maximum stress at this radius may be found.

SECTION II.

THIN CYLINDRICAL WALLS.

Theoretical Development: Page.

Applications:

Thin Cylindrical Walls.

Restatement of the general equations:-

$$\left.\begin{aligned} E\left(\frac{Z\cot\theta}{R_1}+\frac{u}{R_1}\right) &= f-\sigma p \\ E\left(\frac{1}{R_2}\frac{dz}{d\theta}+\frac{u}{R_2}\right) &= p-\sigma f \\ E\cdot\frac{h}{2}\cdot\frac{i\cot\theta}{R_1} &= f'-\sigma p' \\ E\cdot\frac{h}{2}\cdot\frac{1}{R_2}\cdot\frac{di}{d\theta} &= p'-\sigma f' \end{aligned}\right\} \qquad \left.\begin{aligned} \frac{d}{d\theta}(pR_1\sin\theta)-fR_2\cos\theta-sR_1\sin\theta &= -\frac{1}{2\pi h}\cdot\frac{dQ}{d\theta} \\ pR_1\sin\theta+fR_2\sin\theta+\frac{d}{d\theta}(sR_1\sin\theta) &= \frac{1}{2\pi h}\cdot\frac{dW}{d\theta} \\ sR_1R_2\sin\theta &= -\frac{h}{6}\cdot\frac{d}{d\theta}(p'R_1\sin\theta)+\frac{h}{6}f'R_2\cos\theta \\ i &= -\frac{1}{R_2}\cdot\frac{du}{d\theta}+\frac{Z}{R_2} \end{aligned}\right\}$$

Derivation of stress-strain relations from general equations.

For the cylindrical wall $\theta = 90^\circ$, $R_2 = \infty$, $R_1 = r$, r = constant. Putting $R_2 d\theta = dx$, the general equations become:-

$$\left.\begin{aligned} E\frac{u}{r} &= f-\sigma p \quad (1) \\ E\frac{dz}{dx} &= p-\sigma f \quad (2) \\ E(0) &= f'-\sigma p' \quad (3) \\ E\frac{h}{2}\cdot\frac{di}{dx} &= p'-\sigma f' \quad (4) \end{aligned}\right\} \qquad \left.\begin{aligned} \frac{dp}{dx} &= -\frac{1}{2\pi hr}\cdot\frac{dQ}{dx} \quad (5) \\ f &= \frac{1}{2\pi h}\cdot\frac{dW}{dx}-\frac{d}{dx}(sr) \quad (6) \\ (sr) &= -\frac{1}{6}\cdot h\cdot\frac{d}{dx}(p'r) \quad (7) \\ i &= -\frac{du}{dx} \quad (8) \end{aligned}\right\}$$

Formation of basic equation.

The reduction of these equations is effected by equating the double differentiation of (1) to (4), eliminating the terms containing p and f by means of (5), (6), and (7), and observing $f' = \sigma p'$, $i = -\dfrac{du}{dx}$. This leads to the equation:-

$$\frac{d^4p'}{dx^4}+\left\{\frac{12(1-\sigma^2)}{h^2r^2}\right\}p' = -\frac{3}{\pi rh^2}\cdot\frac{d^3W}{dx^3}-\frac{3\sigma}{\pi h^2r^2}\frac{d^2Q}{dx^2} \qquad \ldots\ldots (9)$$

If the variation of W and Q is such that there are no third and second derivatives respectively, then, where $n^4 = \dfrac{3(1-\sigma^2)}{h^2r^2}$

$$\frac{d^4p'}{dx^4}+4n^4p' = 0 \qquad \ldots\ldots (10)$$

The solution of equation (10) is:-

$$p' = e^{nx}\{A\cos nx+B\sin nx\}+e^{-nx}\{C\cos nx+D\sin nx\}$$

where A, B, C, and D are integration constants. When p' is known, all other quantities may be found. Substituting $\alpha = nx$, the complete set is given as:-

$$p' = e^{\alpha}\{A\cos\alpha + B\sin\alpha\} + e^{-\alpha}\{C\cos\alpha + D\sin\alpha\} \quad (11)$$

$$f' = \sigma p' \quad (12)$$

$$i = -\frac{1}{6}\rho n^3 r^2\left[e^{\alpha}\{2(B-A)\cos\alpha - 2(B+A)\sin\alpha\} + e^{-\alpha}\{2(D+C)\cos\alpha + 2(D-C)\sin\alpha\}\right] \quad (13)$$

$$s = -\frac{1}{6}\rho n\left[e^{\alpha}\{(B+A)\cos\alpha + (B-A)\sin\alpha\} + e^{-\alpha}\{(D-C)\cos\alpha - (D+C)\sin\alpha\}\right] \quad (14)$$

$$u = \frac{r}{2\pi h E}\left[\frac{dW}{dx} - \sigma\int_0^x \frac{dQ}{dx}\cdot dx\right] - \frac{\sigma a_1 r}{E} + \frac{1}{6}\frac{\rho n^2 r^2}{E}\left[e^{\alpha}\{2B\cos\alpha - 2A\sin\alpha\} + e^{-\alpha}\{-2D\cos\alpha + 2C\sin\alpha\}\right] \quad (15)$$

$$p = -\frac{1}{2\pi h r}\int_0^x \frac{dQ}{dx}\cdot dx + a_1 \quad (16)$$

$$f = E\frac{u}{r} + \sigma p \quad (17)$$

$$z = -\frac{1}{2\pi h r E}\left[\int_0^x\left\{\int_0^x \frac{dQ}{dx}\cdot dx\right\}dx - \sigma r\int_0^x \frac{dW}{dx}\cdot dx\right] + \frac{a_1 x}{E} + b_1 + \frac{\sigma r s}{E} \quad (18)$$

Omitting the equations for circumferential stress in the group above, the remaining six supply the necessary conditions from which the values of the integration constants may be determined.

Extensional Equations.

Where the boundary conditions are suitable[1], i.e. implying no shear or bending conditions at the edges, equation (6) may be written, $f = \frac{1}{2\pi h}\cdot\frac{dW}{dx}$; the term $\frac{d}{dx}(sr)$ being negligible. The following group of equations comprise the extensional effects:-

$$p = -\frac{1}{2\pi h r}\int_0^x \frac{dQ}{dx}\cdot dx + a_1 \quad (19)$$

$$f = \frac{1}{2\pi h}\cdot\frac{dW}{dx} \quad (20)$$

$$u = \frac{r}{2\pi h E}\left[\frac{dW}{dx} - \sigma\int_0^x \frac{dQ}{dx}\cdot dx\right] - \frac{\sigma a_1 r}{E} \quad (21)$$

$$z = -\frac{1}{2\pi h r E}\left[\int_0^x\left\{\int_0^x \frac{dQ}{dx}\cdot dx\right\}dx - \sigma r\int_0^x \frac{dW}{dx}\cdot dx\right] + \frac{a_1 x}{E} + b_1 \quad (22)$$

These equations include all external loading effects.

Edge effect Equations.

When the conditions at the boundaries include bending and shear effects, the permissible step of breaking up equation (6) and the above development allow the omission of all external load actions on whose effects those resulting from the forces at the edges may be superposed. Rewriting equation (6) thus, $f = -\frac{d}{dx}(sr)$, the stresses and movements due to edge effects are written:-

[1] Ibid. p.560.

$$p' = e^{\alpha}\left\{A\cos\alpha + B\sin\alpha\right\} + e^{-\alpha}\left\{C\cos\alpha + D\sin\alpha\right\} \tag{23}$$

$$f' = \sigma p' \tag{24}$$

$$i = -\frac{1}{6}\rho n^3 r^2\left[e^{\alpha}\left\{2(B-A)\cos\alpha - 2(B+A)\sin\alpha\right\} + e^{-\alpha}\left\{2(D+C)\cos\alpha + 2(D-C)\sin\alpha\right\}\right] \tag{25}$$

$$s = -\frac{1}{6}\rho n\left[e^{\alpha}\left\{(B+A)\cos\alpha + (B-A)\sin\alpha\right\} + e^{-\alpha}\left\{(D-C)\cos\alpha - (D+C)\sin\alpha\right\}\right] \tag{26}$$

$$u = \frac{1}{6}\frac{\rho n^2 r^2}{E}\left[e^{\alpha}\left\{2B\cos\alpha - 2A\sin\alpha\right\} + e^{-\alpha}\left\{-2D\cos\alpha + 2C\sin\alpha\right\}\right] \tag{27}$$

$$f = E\frac{u}{r} \tag{28}$$

$$Z = \frac{\sigma r}{E}\cdot s \tag{29}$$

The integration constants a_1 and b_1 are omitted from the above group of equations, as their inclusion would merely give results obtained in the preceding group. The condition equations for a_1 and b_1 are (20) and (22), and for A, B, C, and D, (23), (25), (26) and (27). The group of equations, (19-22), give what is called extensional effects; the group (23-28), give edge effects. The above procedure simplifies the application of the equations.

Sign convention.

It is important in arithmetical solutions to note the convention of signs adopted in the development. Internal pressures and direct tensile stresses, positive; bending tensile stresses on the outer edge of the wall, positive; shear stresses are positive when the radius of the shell at the origin tends to increase.

Evaluation of the Constants.

The evaluation of the integration constants, a_1 and b_1, in the extensional solution is straightforward and need not be discussed. Owing to the variety of combinations of the end terminal conditions and the solution of four simultaneous equations, the determination of the constants A, B, C, and D in the edge effect group is more involved. The following procedure is given:-

The equations for axial bending stress, shear stress, slope/

slope and radial deflection at the origin and at the end, may be written:-

At origin		At end, L	
$P_o = A+C$	(30)	$P_L = A + a'B + \frac{C}{\xi} + a'\frac{D}{\xi}$	(31)
$H_o = -A-B+C-D$		$H_L = A + b'B - b'\frac{C}{\xi} + \frac{D}{\xi}$	
$K_o = -B+D$		$K_L = A - c'B - \frac{C}{\xi} + c'\frac{D}{\xi}$	
$L_o = A-B-C-D$		$L_L = A - d'B - d'\frac{C}{\xi} - \frac{D}{\xi}$	

where,

at origin, $p' = p'_o$, $s = s_o$, $i = i_o$, $u = u_o$.

and $P_o = p'_o$, $H_o = \frac{s_o}{\frac{1}{6}\hbar n}$, $K_o = -\frac{u_o E}{2(\frac{1}{6}\hbar n^2 r^2)}$, $L_o = \frac{i_o}{2(\frac{1}{6}\hbar n^3 r^2)}$

at end, L, $p' = p'_L$, $s = s_L$, $i = i_L$, $u = u_L$.

and

$$P_L = \frac{p'_L}{q\sqrt{\xi}}, \qquad K_L = -\frac{u_L E}{2(\frac{1}{6}\hbar n^2 r^2)\sqrt{\xi}\cdot b}$$

$$H_L = -\frac{s_L}{\frac{1}{6}\hbar n\sqrt{\xi}(q-b)}, \qquad L_L = \frac{i_L}{2(\frac{1}{6}\hbar n^3 r^2)\sqrt{\xi}\cdot(q+b)}$$

and $b = \sin\alpha_L$, $q = \cos\alpha_L$, $\xi = e^{2\alpha_L}$, $a' = \frac{b}{q}$, $b' = \frac{q+b}{q-b}$, $c' = \frac{q}{b}$, $d' = \frac{q-b}{q+b}$

Any combination of four equations, two from the origin group and two from the end L group, will suffice to give values to the constants A, B, C, and D. Three tabular schemes containing the more common conditions have been drawn up. In table I, the conditions are all of an essentially different nature; in tables II and III the conditions appearing at both ends are similar, but not necessarily equal.

TABLE I.

Conditions - at origin, $u = u_0$, $i = 0$;

at end, L, $s = s_L$, $p' = p'_L$.

Constant.	Coeff. of $K_0 \cdot \frac{1}{N}$	Coeff. of $H_L \cdot \frac{\sqrt{\epsilon}\,(q-b)}{N}$	Coeff. of $P_L \cdot \frac{\sqrt{\epsilon}\,q}{N}$
$A\sqrt{\epsilon}$ -	$-\frac{1}{\sqrt{\epsilon}}(2b^2-2bq-1)-\frac{1}{\epsilon\sqrt{\epsilon}}$	$-b-\frac{b-2q}{\epsilon}$	$q+b+\frac{3q+b}{\epsilon}$
$B\sqrt{\epsilon}$ -	$+\frac{1}{\sqrt{\epsilon}}(2b^2+2bq-3)-\frac{1}{\epsilon\sqrt{\epsilon}}$	$+q+\frac{q}{\epsilon}$	$-q+b+\frac{q+b}{\epsilon}$
C - -	$-1-\frac{1}{\epsilon}(2b^2+2bq-$ illegible	$-\frac{2q+b}{\sqrt{\epsilon}}-\frac{b}{\epsilon\sqrt{\epsilon}}$	$\frac{3q-b}{\sqrt{\epsilon}}+\frac{q-b}{\epsilon\sqrt{\epsilon}}$
D - -	$+1-\frac{1}{\epsilon}(2b^2-2bq-3)$	$+\frac{q}{\sqrt{\epsilon}}+\frac{q}{\epsilon\sqrt{\epsilon}}$	$\frac{q+b}{\sqrt{\epsilon}}+\frac{3q+b}{\epsilon\sqrt{\epsilon}}$

$$N=\left\{1-\frac{1}{\epsilon}(4b^2-6)+\frac{1}{\epsilon^2}\right\}$$

TABLE II.

Conditions - at origin, $p' = p'_0$, $s = s_0$;

at end, L, $p' = p'_L$, $s = s_L$.

Const.	Coeff. of $P_0 \cdot \frac{1}{N_1}$	Coeff. of $P_L \cdot \frac{\sqrt{\epsilon}\cdot q}{N_1}$	Coeff. of $H_0 \cdot \frac{1}{N_1}$	Coeff. of $H_L \cdot \frac{\sqrt{\epsilon}\,(q-b)}{N_1}$
$A\sqrt{\epsilon}$	$-\frac{1+2bq+2b^2}{\sqrt{\epsilon}}+\frac{1}{\epsilon\sqrt{\epsilon}}$	$q+b-\frac{q+b}{\epsilon}$	$+\frac{2b^2}{\sqrt{\epsilon}}$	$-b+\frac{b}{\epsilon}$
$B\sqrt{\epsilon}$	$\frac{1+2bq-2b^2}{\sqrt{\epsilon}}-\frac{1}{\epsilon\sqrt{\epsilon}}$	$-q+b+\frac{q-3b}{\epsilon}$	$+\frac{1-2bq}{\sqrt{\epsilon}}-\frac{1}{\epsilon\sqrt{\epsilon}}$	$+q-\frac{q+2b}{\epsilon}$
C	$1-\frac{1-2bq+2b^2}{\epsilon}$	$-\frac{q+b}{\sqrt{\epsilon}}+\frac{q-b}{\epsilon\sqrt{\epsilon}}$	$-\frac{2b^2}{\epsilon}$	$+\frac{b}{\sqrt{\epsilon}}-\frac{b}{\epsilon\sqrt{\epsilon}}$
D	$1-\frac{1-2bq-2b^2}{\epsilon}$	$-\frac{q+3b}{\sqrt{\epsilon}}+\frac{q+b}{\epsilon\sqrt{\epsilon}}$	$-1+\frac{1+2bq}{\epsilon}$	$-\frac{q-2b}{\sqrt{\epsilon}}+\frac{q}{\epsilon\sqrt{\epsilon}}$

$$N_1=\left\{1-\frac{1}{\epsilon}(4b^2+2)+\frac{1}{\epsilon^2}\right\}$$

TABLE III.

Conditions - at origin, $u = u_o$, $i = 0$;

at end, L, $u = u_L$, $i = 0$.

Constant	Coeff. of $K_0 \cdot \frac{1}{N_1}$	Coeff. of $K_L \cdot \frac{\sqrt{\epsilon} \cdot b}{N_1}$
$A\sqrt{\epsilon}$ -	$-\frac{2b^2-2bq-1}{\sqrt{\epsilon}} - \frac{1}{\epsilon\sqrt{\epsilon}}$	$-q+b+\frac{q-3b}{\epsilon}$
$B\sqrt{\epsilon}$ -	$+\frac{2b^2+2bq+1}{\sqrt{\epsilon}} - \frac{1}{\epsilon\sqrt{\epsilon}}$	$-q-b+\frac{q-b}{\epsilon}$
C - -	$-1-\frac{2b^2+2bq-1}{\epsilon}$	$+\frac{q+3b}{\sqrt{\epsilon}} - \frac{q+b}{\epsilon\sqrt{\epsilon}}$
D - -	$+1-\frac{2b^2-2bq+1}{\epsilon}$	$-\frac{q+b}{\sqrt{\epsilon}} + \frac{q-b}{\epsilon\sqrt{\epsilon}}$

$$N_1 = \left\{1 - \frac{1}{\epsilon}(4b^2+2) + \frac{1}{\epsilon^2}\right\}$$

The reason for giving the coefficients of $A\sqrt{\xi}$ and $B\sqrt{\xi}$ is that in any subsequent work for the determination of a movement or stress at some intermediate section of a particular cylinder, the constants A and B are modified by the ratio $\frac{\sqrt{\xi_x}}{\sqrt{\xi}}$, whereas the constants C and D are modified only by $\frac{1}{\sqrt{\xi_x}}$. Again, if $\frac{1}{\sqrt{\xi}}$ were included in the coefficients of the constants A and B, it would appear that when ξ is very large $A = B = 0$, which is not the case.

The limitations of these tables are contained in the facts that the bending stress condition is always associated with the shear stress condition, and the radial deflection condition with the slope condition, and that the slope condition is zero. The argument for the first statement is the frequency with which such combinations appear in practice, and for the second that the condition of a particular slope is not generally useful. The only time that the slope condition may be of value is when an uncertain fixity of the edge exists and such a case can be solved with a fair degree of accuracy by combining the slope condition with a factor m, varying from

zero/

zero for a free edge to unity for a fixed edge, as was shown in the paper on flat circular discs[3]. Generally, however, whatever the conditions in a problem may be, the values of the constants can be obtained by solving the four appropriate equations from groups (29) and (30). In any tabular scheme inappropriate coefficients, i.e. coefficients associated with zero conditions, automatically drop out.

---

[3] "Load and Temperature Stresses in Circular Flat Plates" McBroom and Moir. Journal R.T.C., 1932.

Application to Pipes reinforced by Steel Rings and subject to Internal Pressure,

The behaviour of pipes reinforced by steel rings[4] is given as an example to illustrate the procedure in the application of the above development. The problem shows how pipes reinforced in this way maintain the strength, with a considerable reduction of thickness, given by plain pipes. That there are definite limits for the distance between the reinforcement rings can be clearly shown; but the immediate exercise is merely a demonstration of the determination of the stress values for definite lengths.

Let r be the mean radius of the pipe, h the thickness, and p the internal pressure. The breadth of the rings is C, the thickness t, and the mean radius is taken as r, the mean radius of the pipe. The clear length between the rings is L.

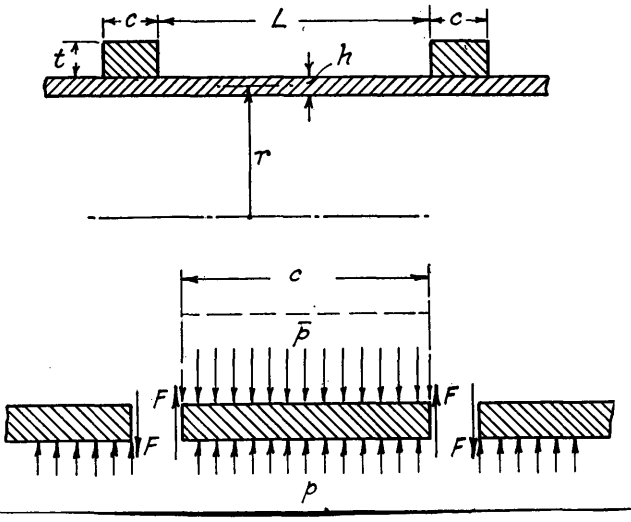

FIG. 4.

E denotes the modulus, and σ Poisson's ratio. The forces acting on the ring and cylinder are given in Fig. 4, $\bar{p}$ being the interface pressure and F the shear force per unit length of the circumference. In this particular problem axial effects are not considered, and the only important equations from the extensional solution are:-

$$u = \frac{r}{2\pi hE} \cdot \frac{dW}{dx} = \frac{pr^2}{hE} \quad \text{and} \quad f = \frac{1}{2\pi h} \cdot \frac{dW}{dx} = E \cdot \frac{u}{r}.$$

These values may be incorporated in the edge effect equations, which then give:-

$$u = u_f + \frac{1}{6}\frac{hn^2r^2}{E}\left[e^{\alpha}\left\{2B\cos\alpha - 2A\sin\alpha\right\} + e^{-\alpha}\left\{-2D\cos\alpha + 2C\sin\alpha\right\}\right] \quad (32)$$

$$f = E \cdot \frac{u}{r} \quad (33)$$

[4] Prof. Cook, Report of British Association, 1923, p.345.

where $u_f = \frac{pr^2}{hE}$

Equivalent pressure in the cylinder due to ring effect =

$$\left(p - \bar{p} + \frac{2F}{c} \right) \qquad (1_1)$$

Let radial expansion at origin = $\bar{u}_o$ Then

$$\bar{u}_o = \frac{r^2}{Eh} \left\{ p - \bar{p} + \frac{2F}{c} \right\} \qquad (2_1)$$

Let $\bar{s}$ = shrinkage, then stress in ring = $E\left(\frac{\bar{s} + \bar{u}_o}{r}\right)$

$$\therefore \bar{p} = E\left(\frac{\bar{s} + \bar{u}_o}{r}\right) \cdot \frac{t}{r} \qquad (3_1)$$

F = shear force per unit length. $\therefore$ shear stress, $s = \frac{F}{h}$.

From equation (26)

$$s = -\frac{1}{6} \cdot hn \left[e^{\alpha} \left\{ (B+A)\cos\alpha + (B-A)\sin\alpha \right\} + e^{-\alpha} \left\{ (D-C)\cos\alpha - (D+C)\sin\alpha \right\} \right]$$

In this case there is obtained at x = 0,

$$F = \frac{h^2 n}{6} \left\{ B + A + D - C \right\} \qquad \ldots\ldots \qquad (4_1)$$

The conditions for this problem are, at origin $u = \bar{u}_0$, $i = 0$; at end, L, $u = \bar{u}_L = \bar{u}_0$, $i = 0$. Table III furnishes the values of the constants for these particular conditions, but in this case, due to the alteration in the general equations,

$$K_o = -\frac{u_f(k-1)E}{2\left(\frac{1}{6} \cdot hn^2 r^2\right)}, \text{ where } k = \frac{u_o}{u_f} + 1 = \frac{\bar{u}_o}{u_f}$$

Let the values of the coefficients, including the N_1 value, for the constants $A\sqrt{\varepsilon}$, $B\sqrt{\varepsilon}$, C, and D be a_0, b_0, c_0, and d_0. Then

$$F = \frac{h^2 n}{6} \cdot K_o \cdot e_o \quad \text{where} \quad e_o = \frac{1}{\sqrt{2}}(a_o + b_o) - (c_o - d_o)$$

$$= \frac{Eh}{2\pi r^2} \cdot u_f \left\{ 1 - k \right\} \cdot e_o \qquad \ldots\ldots (5_1)$$

and $$\bar{p} = E\left(\frac{\bar{s} + \bar{u}_o}{r}\right) \cdot \frac{t}{r} = \frac{Et}{r^2}\left\{ \bar{s} + k \cdot u_f \right\} \qquad \ldots (6_1)$$

Inserting the values of (5_1) and (6_1) in (1_1), we obtain

$$\bar{u}_o = k u_f = \frac{pr^2}{Eh} - \frac{t\bar{s}}{h} - \frac{t}{h} \cdot k \cdot u_f + \frac{k u_f}{hcn}(1-k)e_o$$

giving

$$k = \frac{1 - \frac{Et\bar{s}}{pr^2} + \frac{e_o}{cn}}{1 + \frac{t}{n} + \frac{e_o}{cn}} \qquad (7_1)$$

The radial bending stress from equation (23) is

$$p' = e^{\alpha}\left\{ A\cos\alpha + B\sin\alpha \right\} + e^{-\alpha}\left\{ C\cos\alpha + D\sin\alpha \right\} \qquad \ldots\ldots (8_1)$$

The/

The maximum bending stress will occur at x = 0

$$\therefore \quad p'_{max.} = A + C = K_0\left(\frac{a_0}{\sqrt{2}} + c_0\right) = 1{\cdot}815\,(1-k)\left(\frac{a_0}{\sqrt{2}} + c_0\right)\frac{pr}{h} \quad \ldots(8_1)$$

where Poisson's ratio, $\sigma = 0.3$.

The circumferential direct stress from equation (32) is

$$f = \frac{pr}{h} + \frac{1}{6}hrn^2\left[e^{\alpha}\left\{2B\cos\alpha - 2A\sin\alpha\right\} + e^{-\alpha}\left\{-2D\cos\alpha + 2C\sin\alpha\right\}\right]$$

The maximum circumferential direct stress will occur at $x = \frac{L}{2}$

$$\therefore f_{max.} = \frac{pr}{h} + \frac{1}{6}\cdot hrn^2\left[2K_0\cdot g_0\right]$$

where $$g_0 = e^{-\frac{nL}{2}}\left\{b_0\cos\frac{nL}{2} - a_0\sin\frac{nL}{2}\right\} + e^{-\frac{nL}{2}}\left\{-d_0\cos\frac{nL}{2} + c_0\sin\frac{nL}{2}\right\}$$

$$\therefore f_{max} = \left\{1 + \overline{1-k}\cdot g_0\right\}\frac{pr}{h} \quad \ldots(9_1)$$

The ring stress $p_0 = E\left(\frac{\bar{s} + \bar{u}_0}{r}\right) = E\frac{\bar{s}}{r} + k\cdot\frac{pr}{h}$ $\ldots(10_1)$

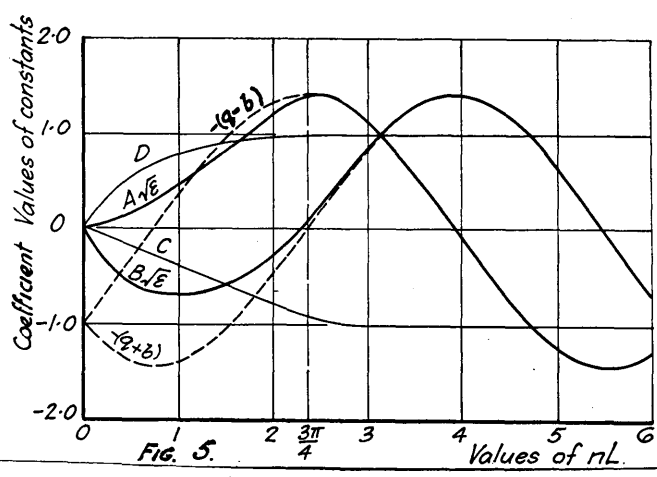

FIG. 5.

With p, r, and h fixed, relative differences in the stress values of equations (8_1), (9_1) and (10_1) may be obtained by varying the shrinkage $\bar{s}$ and the distance between the rings, L. The coefficients of the constants are independent of $\bar{s}$ and their values have been plotted on a base "nL" varying from 0 to 6, as shown in Fig. 5. From these graphs e_0 and g_0 may be obtained for any particular value of "nL." With a definite shrinkage allowance, the ratio k may then be calculated for the same value of "nL."

The problem quoted in the paper cited gives the following figures:- Diam. of pipe = 80 in., t = 1.575 in., h = 0.63 in., p = 278 lb. per in.^{2}, L = 6.6 in., c = 4.45 in.

$$\therefore n = \sqrt[4]{\frac{3(1-\sigma^2)}{h^2r^2}} = 0{\cdot}255\,, \quad \therefore nL = 1{\cdot}682 \quad \therefore e^{nL} = \sqrt{2} = 5{\cdot}38$$

From/

From the graphs of the coefficients of the constants we obtain:-

$$a_o = +0.968, \quad b_o = -0.511, \quad c_o = -0.626, \quad d_o = +0.9$$

$$\therefore e_o = \frac{1}{\sqrt{2}}(a_o + b_o) - (c_o - d_o) = 1.611$$

$$\therefore g_o = e^{-\frac{nL}{2}}\left\{b_o \cos\frac{nL}{2} - a_o \sin\frac{nL}{2}\right\} + e^{-\frac{nL}{2}}\left\{-d_o \cos\frac{nL}{2} + c_o \sin\frac{nL}{2}\right\} = -0.920$$

Let shrinkage fit $\bar{s} = 0.016$, and $E = 30 \times 10^6$ lb. per in.^{2}

$$\therefore k = \frac{1 - \frac{Et\bar{s}}{pr^2} + \frac{e_o}{cn}}{1 + \frac{t}{n} + \frac{e_o}{cn}} = 0.1502$$

$\therefore$ Axial bending stress,

$$p'_o = (1-k)\left(\frac{a_o}{\sqrt{2}} + c_o\right) 1.815 \frac{pr}{h} = -12,200 \text{ lb. per in.}^2$$

$\therefore$ Circumferential direct stress,

$$f = (1 + \sqrt{1-k}\cdot g_o)\cdot\frac{pr}{h} = +3890 \text{ " " "}$$

$\therefore$ Ring stress,

$$p_o = \frac{E\bar{s}}{r} + k\cdot\frac{pr}{h} = +14565 \text{ " " "}$$

The latter two results are in close agreement with those obtained by Professor Cook, who, however, has made no mention of the axial bending stress which appears to be the main stress in the pipe. Consequently, the first conclusions in his paper are somewhat incomplete. With the major stress values reduced to such formulae and with the aid of the graphs to obtain the values of the constants, it is a simple matter to extend the various points in a problem of this order.

The Factor 'nL'.

In any actual application the constants are associated with coefficients whose values depend entirely upon the length, radius of the cylinder and the thickness of the wall. In the general expressions the dimensions combine to form a ratio, $nL = \sqrt[4]{\frac{3(1-\sigma^2)}{h^2r^2}}\cdot L$ and when this ratio exceeds a certain value, which varies slightly for different conditions, the coefficients of the constants become $\pm$ unity or even zero. Hence, in not a few cases, certain of the constants disappear from the expressions, simplifying/

simplifying the work entailed in determining the edge effects throughout the cylinder. In the example above the principal terms in the $A\sqrt{\epsilon}$ and $B\sqrt{\epsilon}$ coefficients are $-(q - b)$ and $-(q + b)$, and in the C and D coefficients, + unity and - unity respectively. The graphs of these quantities are indicated in Fig. 5 by the broken lines. When "nL" = π, the full values of the coefficients and the above values are synonymous, showing that beyond this value all the terms containing $\sqrt{\epsilon}$ or ϵ are negligible. The explanation of this important point is found in Table III and may be interpreted as the conditions at either end having no influence on the movements and stresses at the other. This allows the breaking up of groups (29) and (30); the constants A and B being omitted from the former and the C and D constants from the latter. For the conditions at the origin the two appropriate equations may be written down and solved for C and D; similarly with the appropriate equations at end, L, for the evaluation of the constants $A\sqrt{\epsilon}$ and $B\sqrt{\epsilon}$. All the constants are retained in the stress and movement equations for any intermediate section. When, however, $nL \geqq 2\pi$ any intermediate stress or movement may be obtained by evaluating only half the terms in the equation, depending upon which end the section is nearest, i.e., for axial bending stress at $\frac{L}{4}$, evaluate terms containing the constants C and D; but for a similar stress at $\frac{3L}{4}$, evaluate the terms containing A and B. When $\frac{3\pi}{4} < nL < \pi$, all the terms may be omitted from the coefficient values except those influenced by unity or $\frac{1}{\sqrt{\epsilon}}$. With these points established the following tentative table is drawn up, and may be used for any conditions existing at the edges of a cylinder.

(1) When $nL \geqq 2\pi$

The four simultaneous equations necessary for the determination of the constants may be broken up into two pairs, and the appropriate pair solved for the C and D and the A and B

constants/

constants respectively. In any intermediate movement or stress equation, terms containing A and B or C and D respectively may be omitted depending on the relative position of the section to the ends of the cylinder.

(11) when $\pi < nL < 2\pi$

As in case (1) except that for the movement or stress at any intermediate section, all the constants must be retained in the appropriate expression.

(111) when $\frac{3\pi}{4} < nL < \pi$

Simplification in the actual procedure of determining the constants is permissible. The final expressions for the coefficients of the constants will include terms containing only unity and/or $\frac{1}{\sqrt{2}}$.

(1V) when $nL < \frac{3\pi}{4}$

Full values of the constants must be obtained in the manner outlined. Taking the conditions, say, at origin, $p' = p'_o$, $s = s_o$; at end, L, $p' = p'_L$, $s = s_L$, insert sufficient arithmetical values in the general conditions equations in order to obtain a table of the type.

CONSTANT	coeff. of p'_o	coeff. of S_o	coeff. of p'_L	coeff. of S_L
$A\sqrt{2}$, $B\sqrt{2}$ C , D.	-	-	-	-

In cases (1), (11), and (111) maintain the general expressions throughout; a table similar to the one above, containing the arithmetical coefficients may be drawn up finally.

Any cylinder to which case (1) applies is generally known as a "long" cylinder. The term is rather misleading, in that it is possible to have two cylinders of equal length with one pertaining to case (1V) and the other to case (1). It would appear that before a cylinder can be classified in any one of the above cases, the group ratio "nL", which includes all the dimensions of the cylinder, and which controls the constants and their method of evaluation, must be computed.

Application to Overhung Rim of Rotating Wheel loaded by Centrifugal Force.[5]

This application illustrates, for different rim lengths, (1) the ratios between the radial displacement at the disc and the free edge of the rim; (11) the increase of bending stress at the disc fixture as the length of rim is extended. The rim is assumed to have a constant thickness, h, a mean radius, r, and a length L, as shown in Fig. 6.

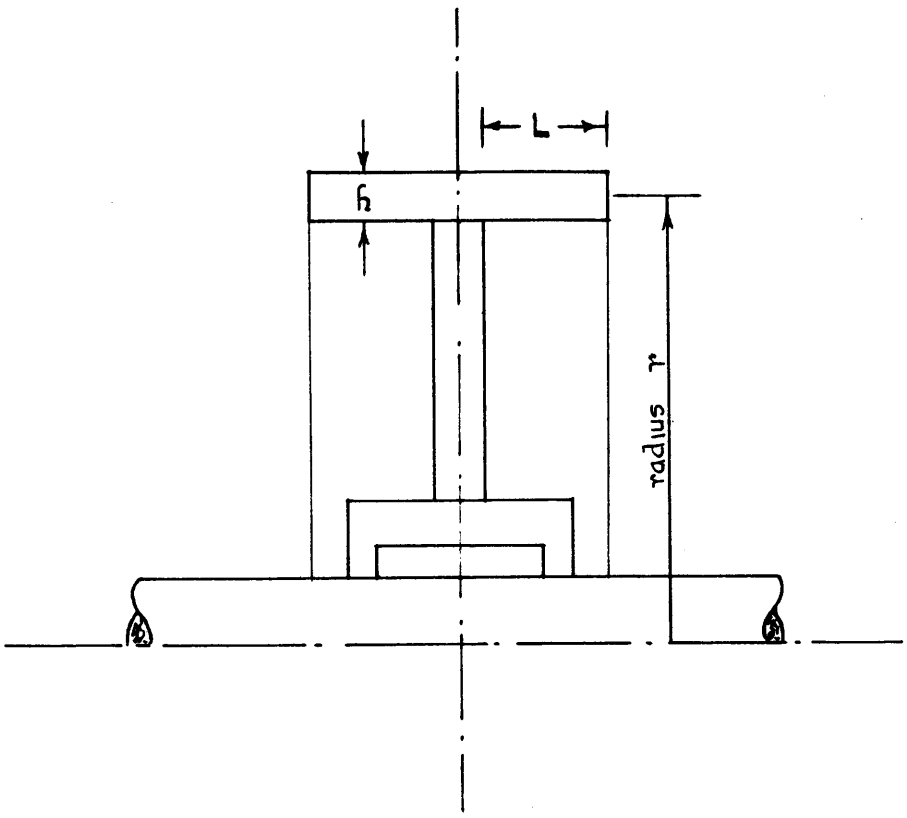

FIG. 6.

Let the radial displacement at the disc be $\bar{U}$. The conditions for the problem are then

at the disc fixture $U = \bar{U}$, $i = o$,

at the free end $s = o$, $p' = o$

the origin being at the disc.

With no internal pressure or axial loads the radial deflection is given by

$$U = \frac{1}{6}\frac{hD^2x^2}{E}\left[\sqrt{\xi}\left\{2B\cos\alpha - 2A\sin\alpha\right\} + \frac{1}{\sqrt{2}}\left\{-2D\cos\alpha + 2C\sin\alpha\right\}\right] \qquad (1_2)$$

[5] Engineering Vol. 121 June 1926. p.649.

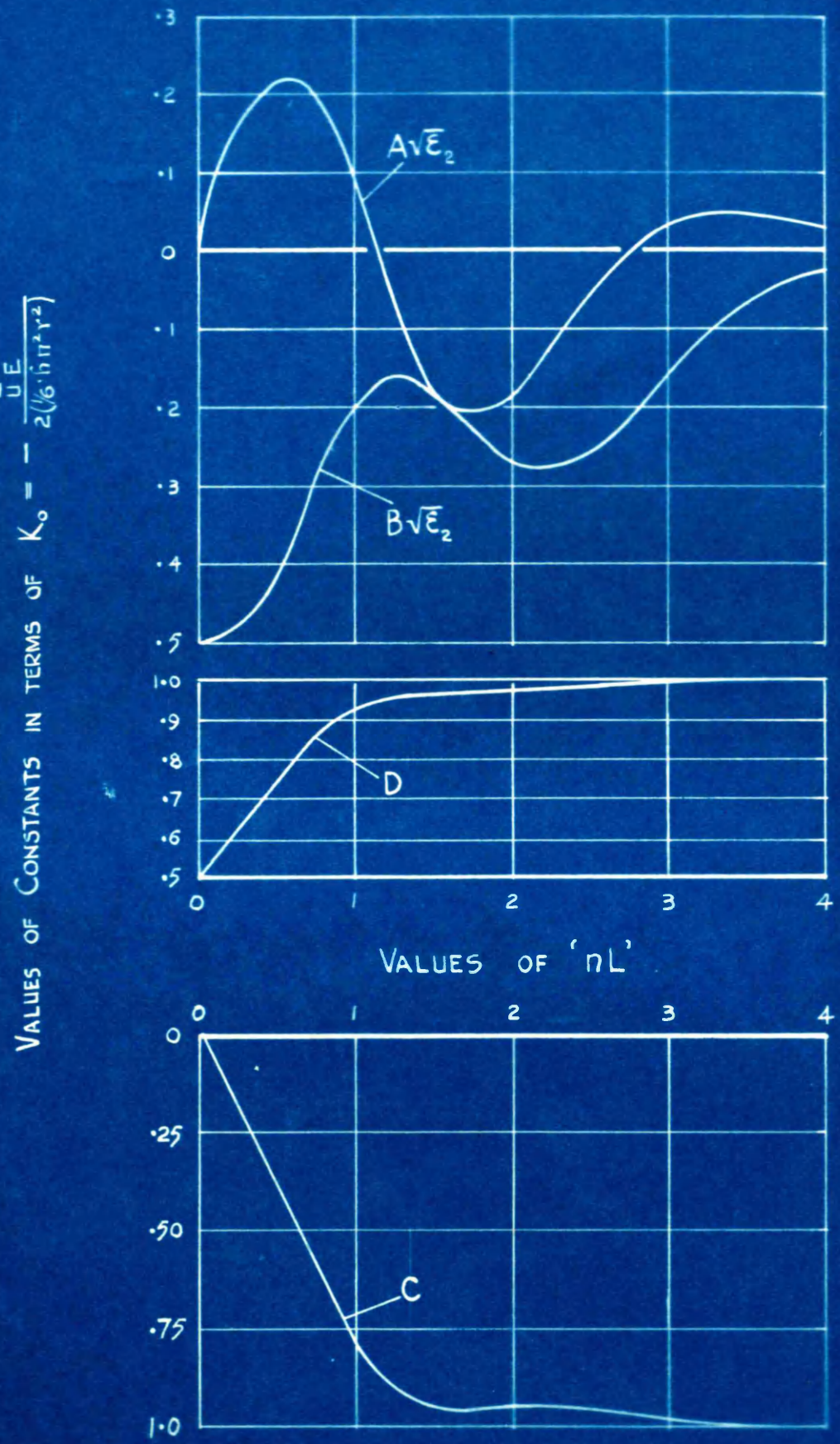
VALUES OF CONSTANTS IN TERMS OF $K_0 = -\frac{\bar{U}E}{2(\frac{1}{6}\cdot\hbar\pi^2\gamma^2)}$
·3
·2
·1
0
·1
·2
·3
·4
·5
$A\sqrt{\bar{\epsilon}_2}$
$B\sqrt{\bar{\epsilon}_2}$
1·0
·9
·8
·7
·6
·5
D
0
1
2
3
4
VALUES OF 'nL'
0
·25
·50
·75
1·0
C

FIG. 7

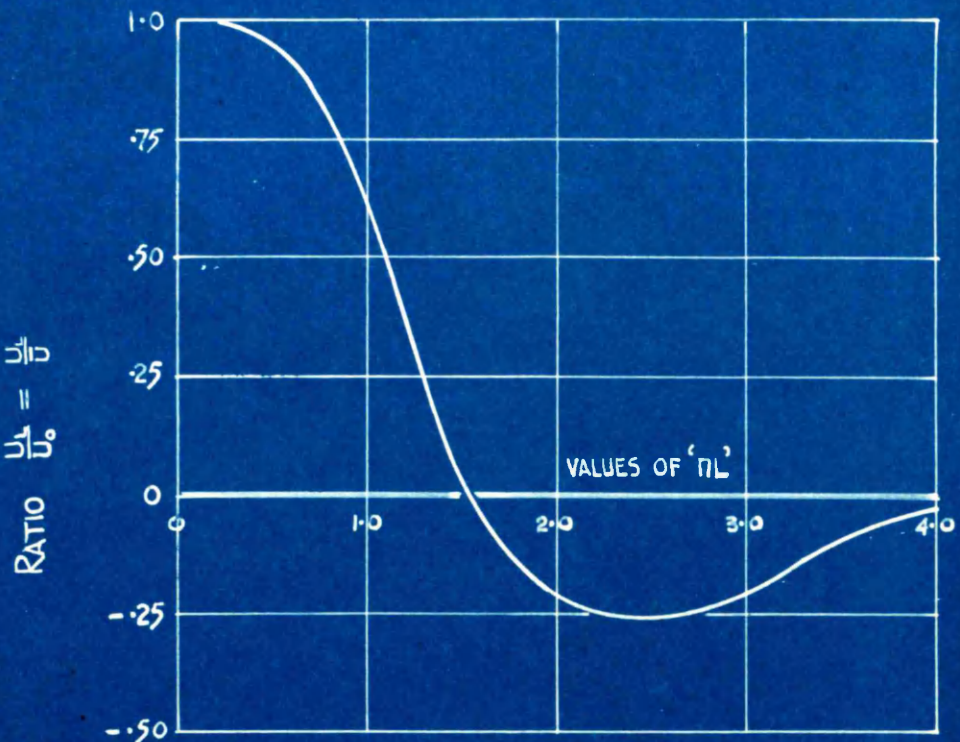

FIG. 8a

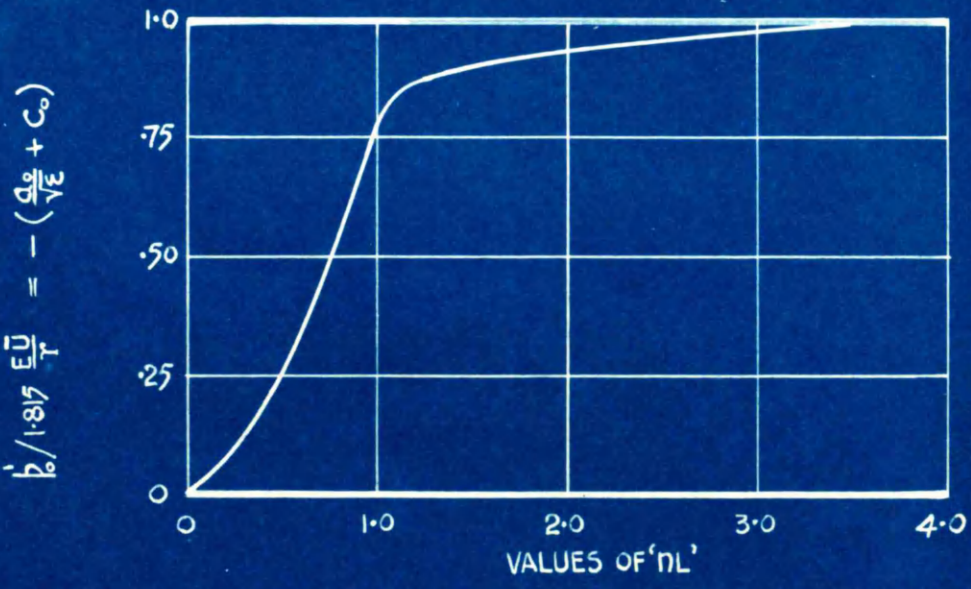

VARIATION OF BENDING STRESS p'_o

FIG. 8b.

at $x = L$

$$u_L = \frac{1}{6}\frac{\rho n^2 r^3}{E}\left[\sqrt{\xi_L}\left\{2B\cos\alpha_L - 2A\sin\alpha_L\right\} + \frac{1}{\sqrt{\xi_L}}\left\{-2D\cos\alpha_L + 2C\sin\alpha_L\right\}\right] \qquad (2_2)$$

The coefficients for the constants are selected from Table I, (in this case they may be obtained from column 1). Let the coefficients of $A\sqrt{\xi_L}$, $B\sqrt{\xi_L}$, C and D, in terms of $K_o = -\frac{\bar{u}E}{2(\frac{1}{6}\rho n^2 r^3)}$ be a_o, b_o, c_o, and d_o. The radial displacement at L may then be written:-

$$u_L = \frac{1}{6}\frac{\rho n^2 r^3}{E}\left\{-\frac{\bar{u}E}{2(\frac{1}{6}\rho n^2 r^3)}\right\}\left[2\sqrt{\xi_L}\left\{b_o\cos\alpha_L - a_o\sin\alpha_L\right\} + \frac{2}{\sqrt{\xi_L}}\left\{-d_o\cos\alpha_L + c_o\sin\alpha_L\right\}\right] \qquad (3_2)$$

$$\therefore \frac{u_L}{\bar{u}} = -(b_o\cos\alpha_L - a_o\sin\alpha_L) - (-d_o\cos\alpha_L + c_o\sin\alpha_L)/\sqrt{\xi_L}$$

$$= \sin\alpha_L\left(a_o - \frac{c_o}{\sqrt{\xi_L}}\right) - \cos\alpha_L\left(b_o - \frac{d_o}{\sqrt{\xi_L}}\right) \qquad \cdots\cdots (4_2)$$

The values of the coefficients selected from Table I, p.18, for values of nL from 0, 4 are given in Fig. 7. The ratios $\frac{u_L}{\bar{u}}$ are then easily computed and are given for the same range of nL values in Fig. (8a). A study of this graph shows that the condition for a good design is nL = 0.5; and that for a recessed hub, a similar problem, to ensure a good grip between shaft and hub, the condition is, $2 < nL < 3$.

Treating this example as a statical problem in which a cylindrical wall is subject to the same conditions, there is the interesting feature that when nL = 2.5 the difference between the edge deflections is a maximum. Where the cylindrical wall forms part of a more extensive arrangement, this particular point may be of importance in fixing the 'best length' of the cylindrical wall.

The radial/bending stress is given by:-

$$p' = \sqrt{\xi}\left(A\cos\alpha + B\sin\alpha\right) + \frac{1}{\sqrt{\xi}}\left(C\cos\alpha + D\sin\alpha\right) \qquad \cdots\cdots (5_2)$$

When $x = o$

$$p' = A + C = -\frac{\bar{u}E}{2(\frac{1}{6}\rho n^2 r^3)}\left\{\frac{a_o}{\sqrt{\xi}} + c_o\right\}$$

$$\therefore \frac{p'_o}{1{\cdot}815\frac{E}{r}\cdot\bar{u}} = -\left\{\frac{a_o}{\sqrt{\xi}} + c_o\right\}$$

The quantity $-\left\{\frac{a_o}{\sqrt{\xi}} + c_o\right\}$ is also graphed in Fig. (8b) and possesses/

$\left\{\frac{a_o}{\sqrt{\xi}}\right.$

possesses to some degree the same characteristics as the quantity $\frac{u_L}{\bar{u}}$. In actual practice, of course, $\bar{u}$ would be negative and hence the radial bending stress would be negative, indicating compression on the outside face.

SECTION III.

THIN CONICAL WALLS.

Thin Conical Walls.

Restatement of general equations:-

$$\left.\begin{aligned} E\left(\frac{z\cot\theta}{R_1}+\frac{u}{R_1}\right) &= f-\sigma p \\ E\left(\frac{1}{R_2}\cdot\frac{dz}{d\theta}+\frac{u}{R_2}\right) &= p-\sigma f \\ E\cdot\frac{h}{2}\cdot\frac{i\cot\theta}{R_1} &= f'-\sigma p' \\ E\,\frac{h}{2}\cdot\frac{1}{R_2}\cdot\frac{di}{d\theta} &= p'-\sigma f' \end{aligned}\right\} \qquad \left.\begin{aligned} \frac{d}{d\theta}(pR_1\sin\theta)-fR_2\cos\theta-sR_1\sin\theta &= -\frac{1}{2\pi h}\cdot\frac{dQ}{d\theta} \\ pR_1\sin\theta+fR_2\sin\theta+\frac{d}{d\theta}(sR_1\sin\theta) &= \frac{1}{2\pi h}\cdot\frac{dW}{d\theta} \\ sR_1R_2\sin\theta &= -\frac{h}{6}\cdot\frac{d}{d\theta}(p'R_1\sin\theta)+\frac{h}{6}f'R_2\cos\theta \\ i &= -\frac{1}{R_2}\cdot\frac{du}{d\theta}+\frac{z}{R_2} \end{aligned}\right\}$$

Derivation of stress-strain relations from general equations.

For the conical wall $\theta=(90^\circ-\lambda)$ where 2λ is the cone angle at the apex. $R_2=\infty$, $R_1=r=x\tan\lambda$, where x is the distance measured from the apex of the cone to any section. Putting $R_2d\theta=dx$, the complete set of equations may be written:-

$$\left.\begin{aligned} E\left(\frac{z}{x}+\frac{u\cot\lambda}{x}\right) &= f-\sigma p \\ E\left(\frac{dz}{dx}\right) &= p-\sigma f \\ E\left(\frac{h}{2}\cdot\frac{i}{x}\right) &= f'-\sigma p' \\ E\left(\frac{h}{2}\cdot\frac{di}{dx}\right) &= p'-\sigma f' \end{aligned}\right\} \qquad \left.\begin{aligned} &(1)\quad \frac{d}{dx}(px)-f=-\frac{1}{2\pi h\sin\lambda}\cdot\frac{dQ}{dx} && (5)\\ &(2)\quad f-\frac{d}{dx}(sx\tan\lambda)=\frac{1}{2\pi h\cos\lambda}\cdot\frac{dW}{dx} && (6)\\ &(3)\quad (sx)=-\frac{h}{6}\cdot\frac{d}{dx}(p'x)+\frac{h}{6}f' && (7)\\ &(4)\quad i=-\frac{du}{dx} && (8) \end{aligned}\right\}$$

Extensional Equations.

As before, the omission of the shear term in (6) enables the necessary equations for extensional effects to be found, and they are given as:-

$$p=\frac{Pr}{2h}+\frac{a_1}{x} \qquad (9)$$

$$f=\frac{Pr}{h} \qquad (10)$$

$$u=\frac{3Pr^2}{4hE}-\frac{a_1\tan\lambda}{E}(\sigma+\log_e x)-b_1\tan\lambda \qquad (11)$$

$$z=\frac{(1-2\sigma)}{4hE}Pr\cdot x+\frac{a_1}{E}\log_e x+b_1 \qquad (12)$$

where a_1 and b_1 are integration constants, and P the internal pressure.

Edge effect Equations.

Due to the presence of the term $\frac{h}{6}\cdot f'$ in equation (7), the reduction of the equations for edge effects is somewhat more/

more complicated than the similar procedure in the cylindrical wall case. Omitting the load terms and integration constants we obtain:-

From (5) and (6) $$\frac{d}{dx}(px) = f = -\frac{d}{dx}(sx)\tan\lambda \qquad (13)$$

From (1) $$Ez = (fx) - \sigma(px) - E\cot\lambda \cdot u \qquad (14)$$

$$\therefore E\frac{dz}{dx} = \frac{d}{dx}(fx) - \sigma\frac{d}{dx}(px) - E\cot\lambda \cdot \frac{du}{dx} \qquad (15)$$

Substituting from (2)

$$p - \sigma f = \frac{d}{dx}(fx) - \sigma\frac{d}{dx}(px) - E\cot\lambda \cdot \frac{du}{dx} \qquad (16)$$

Hence from (13)

$$E\cot\lambda \cdot i = -\frac{(sx)}{x}\tan\lambda + \tan\lambda \cdot \frac{d}{dx}\left\{x \cdot \frac{d}{dx}(sx)\right\} \qquad (17)$$

$$\therefore \frac{d^2s}{dx^2} + \frac{3}{x}\cdot\frac{ds}{dx} - \frac{Ei}{x^2\tan^2\lambda} = 0 \qquad (18)$$

From equations (3) and (4)

$$f' = \frac{Eh}{2(1-\sigma^2)}\left\{\frac{i}{x} + \sigma\frac{di}{dx}\right\}; \qquad p' = \frac{Eh}{2(1-\sigma^2)}\left\{\frac{di}{dx} + \sigma\frac{i}{x}\right\}$$

$$\therefore \frac{d}{dx}(p'x) = \frac{Eh}{2(1-\sigma^2)} \cdot \frac{d}{dx}\left(x \cdot \frac{di}{dx}\right) + \frac{\sigma Eh}{2(1-\sigma^2)} \cdot \frac{di}{dx} \qquad (19)$$

Substituting for $\frac{d}{dx}\cdot(p'x)$ and f' in equation (7).

$$\therefore (sx) = -\frac{h}{6} \cdot \frac{Eh}{2(1-\sigma^2)}\left\{\frac{d}{dx}\left(x \cdot \frac{di}{dx}\right) - \frac{i}{x}\right\} \qquad (20)$$

$$\therefore \frac{d^2i}{dx^2} + \frac{1}{x}\cdot\frac{di}{dx} - \frac{i}{x^2} + \frac{12}{h^2}\cdot\frac{1-\sigma^2}{E}\cdot s = 0 \qquad (21)$$

Putting $\eta = \frac{1-\sigma^2}{E}(sx)$ and $x = \frac{R^2}{2}$ equations (18) and (21) may be written:-

$$\left.\begin{aligned} \frac{d^2\eta}{dR^2} + \frac{1}{R}\cdot\frac{d\eta}{dR} - \frac{4\eta}{R^2} - \frac{2(1-\sigma^2)}{\tan^2\lambda}\cdot i &= 0 \\ \frac{d^2i}{dR^2} + \frac{1}{R}\cdot\frac{di}{dR} - \frac{4i}{R^2} + \frac{24}{h^2}\cdot\eta &= 0 \end{aligned}\right\} \qquad (22)$$

The solutions of the equations in (22) are:-

$$i = \frac{1}{\sqrt{R}}\left[e^{n'R}\left\{K\cos n'R + H\sin n'R\right\} + e^{-n'R}\left\{K_1\cos n'R + H_1\sin n'R\right\}\right] \qquad (23)$$

$$\eta = \frac{Q}{\sqrt{R}}\left[e^{n'R}\left\{-H\cos n'R + K\sin n'R\right\} + e^{-n'R}\left\{H_1\cos n'R - H_1\sin n'R\right\}\right] \qquad (24)$$

where K, H, K_1 and H_1 are integration constants; $n' = \sqrt[4]{\frac{12(1-\sigma^2)}{h^2\tan^2\lambda}}$

$Q = \frac{(1-\sigma^2)}{(n'\tan\lambda)^2}$, and $R = \sqrt{2x}$. With i and η known, all other quantities may be found.

The tangential bending stress, $p' = \frac{Eh}{2(1-\sigma^2)}\left\{\frac{di}{dx} + \frac{\sigma i}{x}\right\}$

$$p' = \frac{Eh}{2(1-\sigma^2)}\cdot\frac{n'}{(R)^{3/2}}\left[e^{n'R}\left\{(K+H)\cos n'R - (K-H)\sin n'R\right\} + e^{-n'R}\left\{-(K_1-H_1)\cos n'R - (K_1+H_1)\sin n'R\right\}\right]$$

To/

[1] Ibid., p.583 et seq.

To obtain an expression similar to that for the axial bending stress in thin cylindrical walls, it is necessary to put $\frac{Eh}{2(1-\sigma)} \cdot n' \cdot \{K+H\} = A$; similarly for the terms containing $(K-H)$, (K_1-H_1) and (K_1+H_1) in terms of B, C and D respectively. Hence

$$\beta' = \frac{e^{n'R}}{R^{3/2}}\{A\cos n'R + B\sin n'R\} + \frac{e^{-n'R}}{R^{3/2}}\{C\cos n'R + D\sin n'R\}$$

$$= \sqrt{2}\{A\cos\theta + B\sin\theta\} + \frac{1}{\sqrt{2}}\{C\cos\theta + D\sin\theta\}$$

where $n'R = \theta$ and ξ, associated with A and B $= e^{2n'R}/(R)^3$

and ξ_1, " " C " D $= e^{2n'R} \cdot R^3$.

Putting $\nu = \sqrt{3(1-\sigma^2)}$, the edge effect equations are:-

$$\beta' = \sqrt{2}(A\cos\theta + B\sin\theta) + \frac{1}{\sqrt{2}}(C\cos\theta + D\sin\theta) \quad (25)$$

$$\beta' = \sigma\beta' \quad (26)$$

$$S = -\frac{\nu}{6}\sqrt{\frac{h}{r}}\left[\sqrt{2}\{(B+A)\cos\theta + (B-A)\sin\theta\} + \frac{1}{\sqrt{2}}\{(D-C)\cos\theta - (D+C)\sin\theta\}\right] \quad (27)$$

$$i = -\frac{\nu^3}{6E}\sqrt{\frac{r}{h}}\left[\sqrt{2}\{2(B-A)\cos\theta - 2(B+A)\sin\theta\} + \frac{1}{\sqrt{2}}\{2(D+C)\cos\theta + 2(D-C)\sin\theta\}\right] \quad (28)$$

$$u = \frac{\nu^2 r}{6E}\left[\sqrt{2}\{2B\cos\theta - 2A\sin\theta\} + \frac{1}{\sqrt{2}}\{-2D\cos\theta + 2C\sin\theta\}\right] \quad (29)$$

$$f = E\frac{u}{r} \quad (30)$$

$$\beta = -S\tan\lambda \quad (31)$$

$$Z = \frac{\sigma r S}{E} \quad (32)$$

The cylindrical equations may be reduced to a similar form; but, whereas the radius, r, in the cylindrical plate is constant, in the above equations it is variable.

Evaluation of the Constants.

The procedure for the determination of the constants A, B, C and D is similar to that given for the cylindrical wall. For that case, however, when $x = 0$, $e^{nx} = 1$, resulting in simple equations for the conditions at the origin. In truncated cones, the conditions always appear at sections x_1 and x_2, these values representing the distance of the sections from the origin or apex of the cone. Consequently the eight conditions equations for the conical wall are of a nature similar to those of the cylindrical wall at end, L, and the full expressions for the coefficients of the constants are too long to be of

practical/

practical use.

The essential difference in the coefficients of the two cases depends on the value e^{nL} for the cylinder and $\left(\frac{R_1}{R_2}\right)^{\frac{3}{2}} \cdot e^{n'(R_2-R_1)}$ for the cone. Taking a cylindrical wall and a conical wall of equal length and thickness and the radius of the cylinder equal to the horizontal radius at the base of the cone, a comparison of the above quantities may be effected and results in

$$\sqrt{\xi} = e^{nL}$$

$$\sqrt{\frac{\xi_2}{\xi_1}} = \sqrt[4]{m^3} \cdot e^{nL_1\left\{\frac{1-\sqrt{m}}{1-m}\right\}2\sqrt{\cos\lambda}}$$

where $n = \sqrt[4]{\frac{3(1-\sigma^2)}{h^2r^2}}$; $m = \frac{x_1}{x_2}$ and $L = L_1$

In order that the criterion for the four cases indicated in the cylindrical wall development may be adopted, it is merely necessary to determine the value "nL_1" by equating $\xi = \frac{\xi_2}{\xi_1}$. This amounts to reducing the length of conical wall to a corresponding length of cylindrical wall and selecting the appropriate method of procedure for the determination of the constants. When case (IV) applies, the table drawn up, corresponding to that for the cylindrical wall, is of the type:-

Conditions, at x_1, $p = p'_1$, $s = s_1$;

at x_2, $p' = p'_2$, $s = s_2$.

CONSTANT.	Coeff. of p'_1.	Coeff. of s_1.	Coeff. of p'_2.	Coeff. of s_2.	
$A\sqrt{\xi_2}$, $B\sqrt{\xi_2}$					
$C/\sqrt{\xi_1}$, $D/\sqrt{\xi_1}$	•	•	•	•	

An interesting observation on the above ratio is that when λ tends to zero, m approaches unity and $\frac{\xi}{\xi_2/\xi_1} >$ unity showing that when a cylindrical wall becomes a truncated conical wall, the edge effects are not so rapidly damped out. When $\lambda \to \frac{\pi}{2}$, $\frac{\xi}{\xi_2/\xi_1} \to \infty$, which is the case of a circular flat disc slightly coned, where the boundary conditions cause distortions and stresses throughout the plate.

METHOD OF APPLYING LOAD AND MEASURING DEVICES USED FOR CONICAL AND SPHERICAL THIN SHELLS

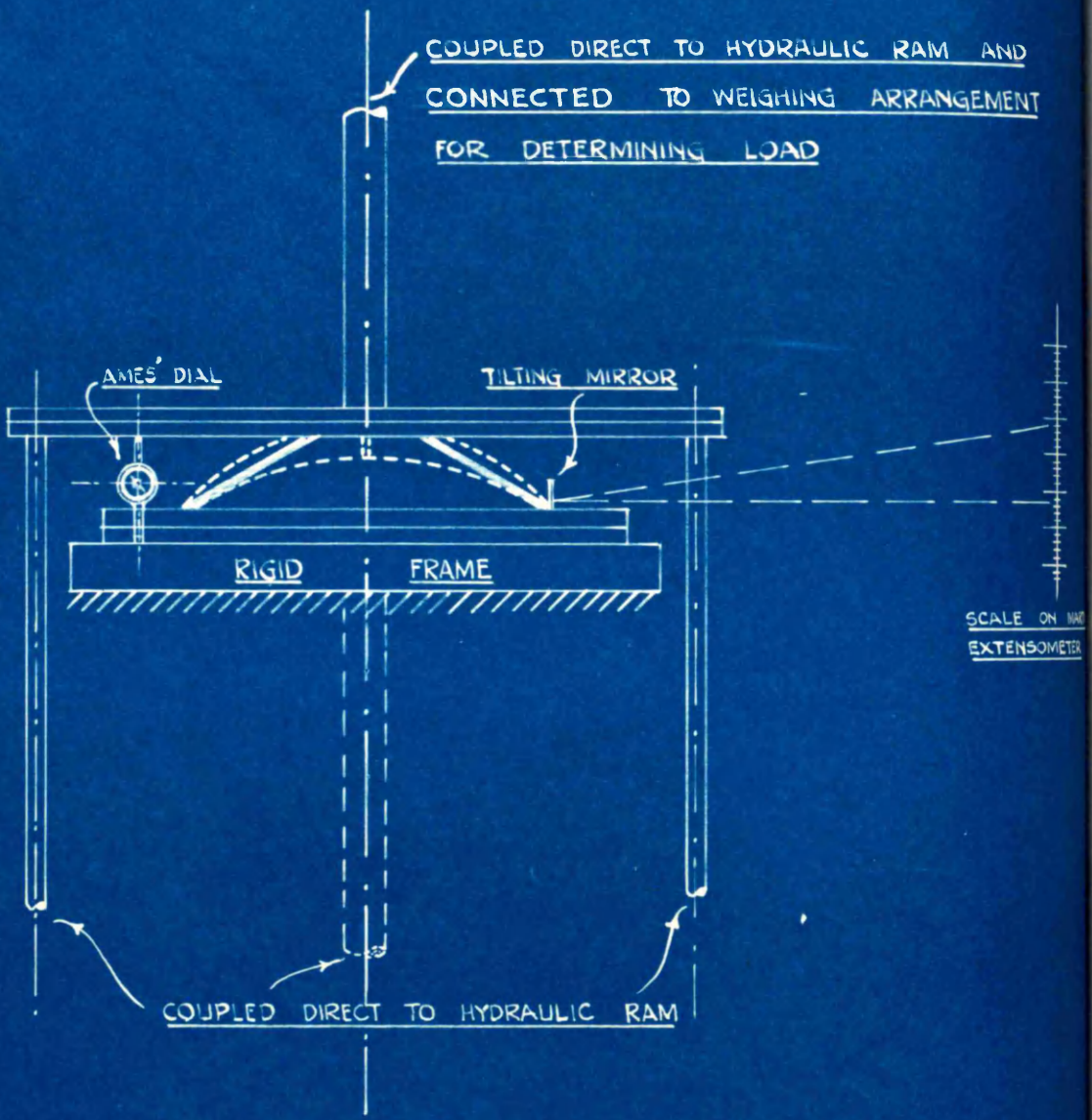

FIG. 10.

Applications to Experimental Cases.

(1) Vertical Ring Load on a Conical Wall. An application of these equations is given for a test on a truncated cone carried out in the laboratory. The details of the plate are as shown in Fig. 9. A vertical ring load P is applied at edge (A). The base of the cone is simply supported; the surfaces in contact being highly polished, frictional forces were assumed to be zero.

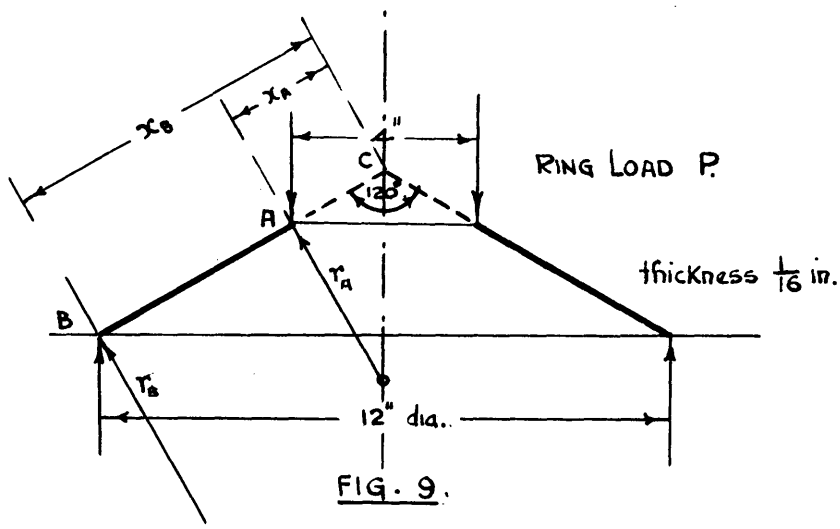

FIG. 9.

Experimental Observations. The simplest experimental readings to observe as a check on any results are the relative vertical displacement between the edges (A) and (B), and the slope at (B). The former was obtained by means of an Ames' dial reading to $\frac{1}{1000}$ in., the latter by a Martin's extensometer. These tests were carried out in the Laboratory of the Mechanics and Mechanical Engineering Department at the Royal Technical College, Glasgow. A diagram of the apparatus is shown in Fig. 10.

The readings are shown in Figs. 12 and 11 respectively. The slope of the graph in Fig. 12 gives $\frac{19.6}{1000}$ in. per ton, and in Fig. 11, $\frac{19.65}{1000}$ radians per ton.

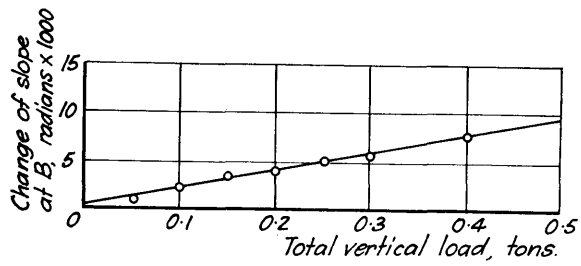

FIG. 11.

Change of Slope at B.

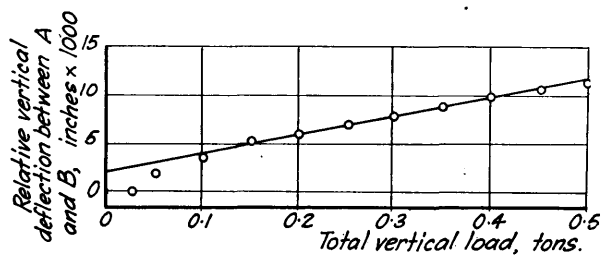

FIG. 12.

Relative Vertical Deflection between A and B.

The first two readings in Fig. 12 which are obviously not correct theoretically, may be explained as due to a slight non-parallelism of the edges (A) and (B), and therefore a non-equal distribution of the load round the edge A, which continued until a load of 0.1 tons was applied. Another reading observed was the extension of a chord of length 8.993 in. under full load, and this was found to be in close agreement with the theoretical calculation.

Analytical Investigation.

Length of conical plate 4.62 in., $x_A = 2.31$ in., $x_B = 6.93$ in.,

$$\therefore m = \frac{x_A}{x_B} = 0.333.$$

Corresponding length of cylindrical wall, L = 3.72 in.

$$n = \sqrt[4]{\frac{3(1-\sigma^2)}{\beta^2 r^2}} = 2.1, \text{ where}$$

$\therefore nL = 2.1 \times 3.72 = 7.8$, which is $> 2\pi$; hence for edge effects, case (1) applies.

Edge Effects.

The conditions for the problem are:-

$$\text{at } x_A, \quad \beta' = 0, \quad s = s_A.$$

$$\text{at } x_B, \quad \beta' = 0, \quad s = s_B.$$

The necessary equations for the evaluation of the constants are then - for A and B,

$$\therefore \quad 0 = \sqrt{\varepsilon_B}\left(A\cos\theta_B + B\sin\theta_B\right)$$
$$S_B = -\frac{\nu}{6}\sqrt{\frac{h}{r_B}}\left[\sqrt{\varepsilon_B}\left\{(B+A)\cos\theta_B + (B-A)\sin\theta_B\right\}\right] \quad \Bigg\} \text{ -- (1)}$$

for C and D.

$$0 = \frac{1}{\sqrt{\varepsilon_A}}\left(C\cos\theta_A + D\sin\theta_A\right)$$
$$S_A = -\frac{\nu}{6}\sqrt{\frac{h}{r_A}}\left[\frac{1}{\sqrt{\varepsilon_A}}\left\{(D-C)\cos\theta_A - (D+C)\sin\theta_A\right\}\right] \quad \Bigg\} \text{ -- (2)}$$

From which we obtain the constants,

$$A\sqrt{\varepsilon_B} = \frac{S_B b_B}{\frac{\nu}{6}\sqrt{h/r_B}}, \qquad B\sqrt{\varepsilon_B} = -\frac{S_B q_B}{\frac{\nu}{6}\sqrt{h/r_B}}$$

$$C/\sqrt{\varepsilon_A} = \frac{S_A b_A}{\frac{\nu}{6}\sqrt{h/r_A}}, \qquad D/\sqrt{\varepsilon_A} = -\frac{S_A q_A}{\frac{\nu}{6}\sqrt{h/r_A}}$$

Where $b = \sin\theta$, $q = \cos\theta$.

When determining the distortions and stresses at an edge, it is not necessary to evaluate the constants. Substituting the above constants in the appropriate expressions we obtain:-

At edge (A)

$$\text{Radial deflection, } u = \frac{V^2 r_A}{6E}\left[\frac{1}{\sqrt{\varepsilon_A}}\left(-2Dq_A + 2Cb_A\right)\right]$$
$$= -\frac{P\nu\tan\lambda}{\pi h E\sqrt{h/r_A}}$$
$$= -\frac{7.97}{1000} \text{ in. per ton (inwards).}$$

$$\text{Circumferential direct stress, } f = E\frac{u}{r_A} = -22.9 \text{ tons per in.}^2 \text{ per ton.}$$

$$\text{Change of slope, } i = -\frac{V^3}{6E}\sqrt{\frac{r_A}{h}}\left[\frac{1}{\sqrt{\varepsilon_A}}\left\{2(D+C)q_A + 2(D-C)b_A\right\}\right]$$
$$= -\frac{P\nu^2\tan\lambda}{\pi h^2 E}$$
$$= -\frac{20.3}{1000} \text{ radians per ton.}$$

At edge (B), it follows

$$\text{Radial deflection, } u = \frac{P\nu\tan\lambda}{\pi h E\sqrt{h/r_B}} = +\frac{13.8}{1000} \text{ in. per ton}$$

$$\text{Circumferential direct stress, } f = E\frac{u_B}{r_B} = +13.2 \text{ tons per in.}^2 \text{ per ton.}$$

$$\text{Change of slope, } i = -\frac{P\nu^2\tan\lambda}{\pi h^2 E} = -\frac{20.3}{1000} \text{ radians per ton.}$$

$$\text{Experimental reading, } i = -\frac{19.65}{1000} \text{ radians per ton.}$$

For intermediate sections it is necessary to draw up a tabular scheme. The best method is to determine the effects of the forces at edges separately, the final result at any section being obtained by addition. According to the ratio nL, the forces at the edges in this case have no effect at sections beyond a distance of 2 in., which means roughly that the sections in the middle sixth of the plate are not affected by the conditions at either edge.

The following table gives the method of computation for the tangential bending stresses induced at sections within a distance of 2 in. from the edge (2).

Tangential bending stress, $p' = \sqrt{z}\,(Aq + Bb)$

$$A' = A\sqrt{z_B} = \frac{s_B b_B}{\frac{\nu}{6}\sqrt{r/r_B}} = -23.75 \; ; \; B' = B\sqrt{z_B} = -\frac{s_B q_B}{\frac{\nu}{6}\sqrt{r/r_B}} = -1.52$$

x''	R_x	n'	θ_x	$\theta_x - \theta_B$	$\left(\frac{R_B}{R_x}\right)^{\frac{3}{2}}$	$\sqrt{\frac{z_x}{z_B}}$	$\cos\theta_x$	$\sin\theta_x$	$A'\cos\theta_x$	$B'\cos\theta_x$	p'
6.93	3.73	5.52	20.60	1	1	1	-.0645	+ .998	+ 1.53	- 1.53	0
6.43	3.59	"	19.85	0.475	1.02	0.485	+.728	+ .685	- 17.3	- 1.05	- 8.9
5.93	3.44	"	19.00	0.202	1.04	0.211	+.999	+ .026	- 23.75	+ 0.04	- 5.01
5.43	3.3	"	18.20	0.091	1.09	0.099	+.643	- .766	- 15.28	+ 1.18	- 1.4
4.93	3.14	"	17.34	0.038	1.14	0.043	+.211	- .977	- 5.03	+ 1.5	- 0.152

These results, along with those for radial deflection and change of slope have been graphed and are shown in Fig.13. The graphs are interesting and show definitely the rapidity with which the edge effects are damped out. Similar results may be obtained for distortions and stresses due to effects at edge (A).

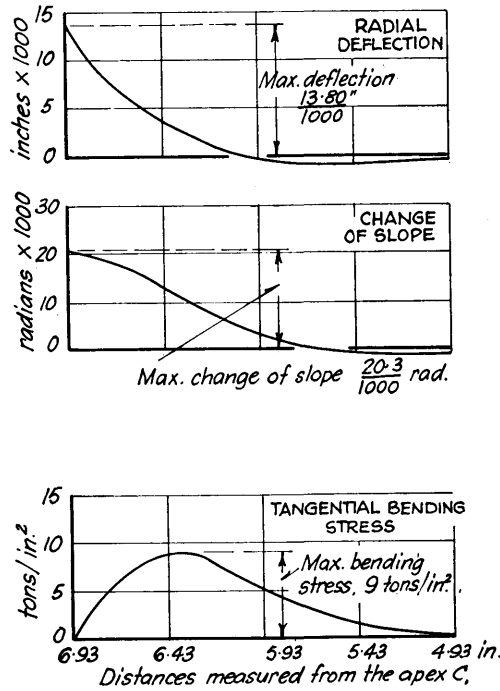

FIG. 13.

Extensional Effects.

At $x = x_A$, $p = -\frac{P\cos\lambda}{2\pi r_A \cos\lambda} = +\frac{a_1}{x_A}$ $\therefore a_1 = -1.47$ tons per in.²

$\therefore p_A = \frac{a_1}{x_A} = -0.6366$ tons per in.²

$\therefore p_B = \frac{a_1}{x_B} = -0.2122$ " "

at $x = x_B$, $u\sin\lambda = z\cos\lambda$

from which $b_1 = -\frac{a_1}{E}\{\log x_B + \sigma\sin^2\lambda\} = \frac{0.276}{10^3}$ in.

With a_1 and b_1 known, it is a simple matter to determine the values u and z. The displacements at the boundaries due to extensional and edge effects are combined in the following table:-

At Edge (A).	Extensional.	Edge Effect.	Total.
Radial displacement, u.	$-\frac{0.228}{10^3}$	$-\frac{7.97}{10^3}$	$-\frac{8.198}{10^3}$ in.
Tangential " , z.	$+\frac{0.168}{10^3}$	$-\frac{0.1154}{10^3}$	$+\frac{0.0526}{10^3}$ "
At Edge (B)	**Extensional.**	**Edge Effect.**	**Total.**
Radial displacement, u.	$+\frac{0.016}{10^3}$	$+\frac{13.8}{10^3}$	$-\frac{13.816}{10^3}$ in.
Tangential " , z.	$+\frac{0.0211}{10^3}$	$-\frac{0.1154}{10^3}$	$-\frac{0.094}{10^3}$ "

The/

The tangential displacement, z, due to edge effects is generally assumed to be zero. The assumption is obviously permissible.

Relative vertical deflection between edges (A) and (B)

$$= (u_A - u_B) \sin\lambda$$

$$= \frac{12.3}{10^3} \text{ in. per ton.}$$

Experimental reading $= \frac{12.6}{10^3}$ " " "

Increase of horizontal radius at base of cone

$$= u_B \cos\lambda + Z_B \sin\lambda$$

$$= \frac{6.82}{10^3} \text{ in. per ton.}$$

The conclusions from this problem show the critical stresses to be the tangential bending stress, p', and the circumferential direct stress, f, the important movements to be the radial displacement u, and the change of slope, i; all of which occur at, or near, the edges of the coned plate.

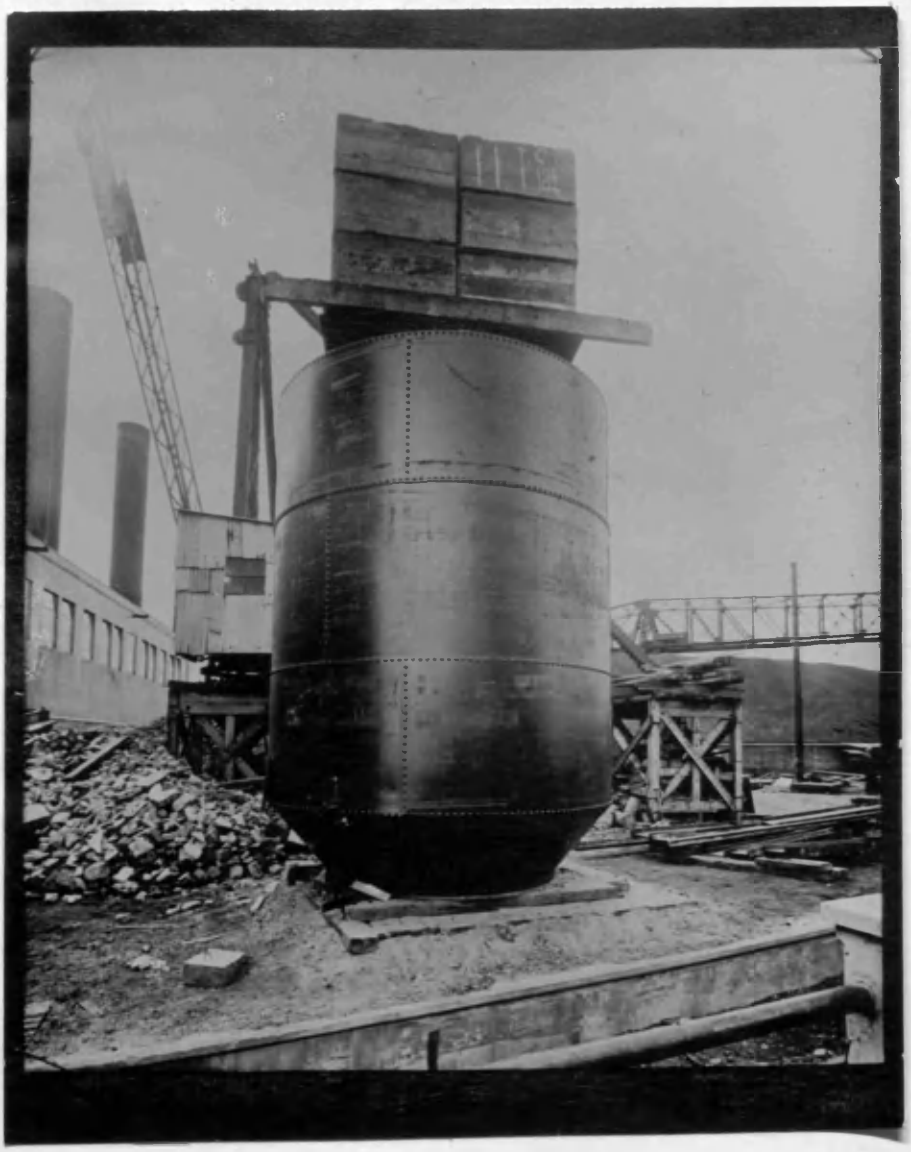

FIG. 14.

GENERAL ARRANGEMENT OF GRIT SEPARATOR

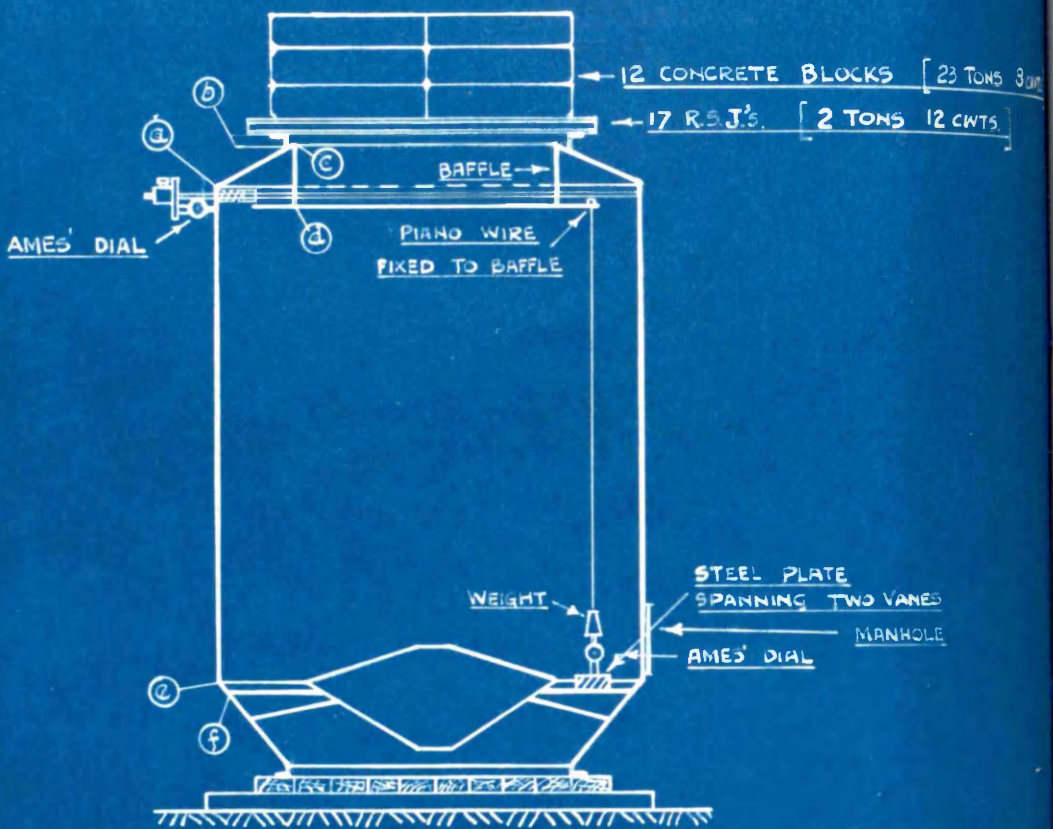

GENERAL VIEW OF SEPARATOR UNDER TEST

FIG. 15

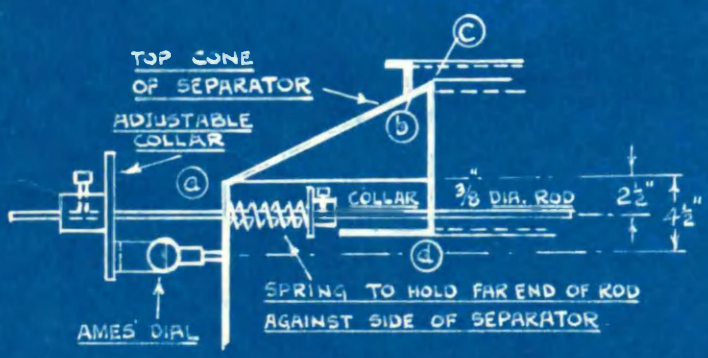

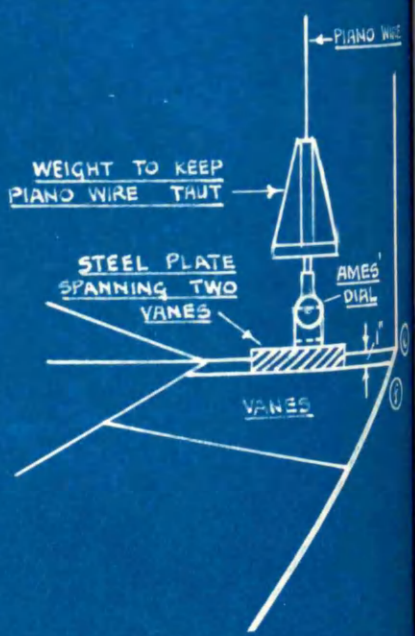

DETAILS OF MEASURING DEVICES

FIG. 16

Applications to Experimental Cases.

(11) Load Test on a Coned Separator Casing. An opportunity was afforded to record the distortions in the shell of a grit separator supporting a load of 26 tons, representing the weight of a chimney. Fig. 14 shows a photograph of the separator under full load, while the general arrangement is given in Fig. 15. A ring welded to the upper conical wall at (b) supports the load. This cone is connected to the outer cylinder by a single riveted lap joint at (a), while it is reinforced by an inner cylinder (c.d.) attached by a welded joint at (c). The bottom conical wall, forming the base of the separator, is heavily reinforced by vanes terminating at (f); and the connection to the outer cylinder at (e) is similar to the one at (a).

Experimental Observations: The two important movements of this separator recorded during the load test were:-

(1) Radial Deflections of cylinder (a.e) near joint (a).

(11) Relative Vertical Deflection between (f), near the top of the vanes in the bottom cone, and (d), the foot of the inner cylinder (c.d).

The details of the measuring devices are fully shown in Fig.16. The readings recorded on the Ames' dials are given below:-

Load W.	Readings (i)		Readings (ii)	
	Loading.	Unloading.	Loading.	Unloading.
51 cwts.	41 x 10^{-3} in.	38 x 10^{-3} in.	10 x 10^{-3} in.	17 x 10^{-3} in.
207 "	34.5 " "	31.5 " "	24 " "	30 " "
363 "	29 " "	27 " "	42 " "	44 " "
519 "	23 " "	23 " "	60 " "	60 " "

From Fig. 16 it will be noticed that the dial records the sum of the radial deflections at x = $2\frac{1}{2}$ in. and x = $4\frac{1}{2}$ in.; x being measured along the cylindrical wall (ae), from (a). The

separate/

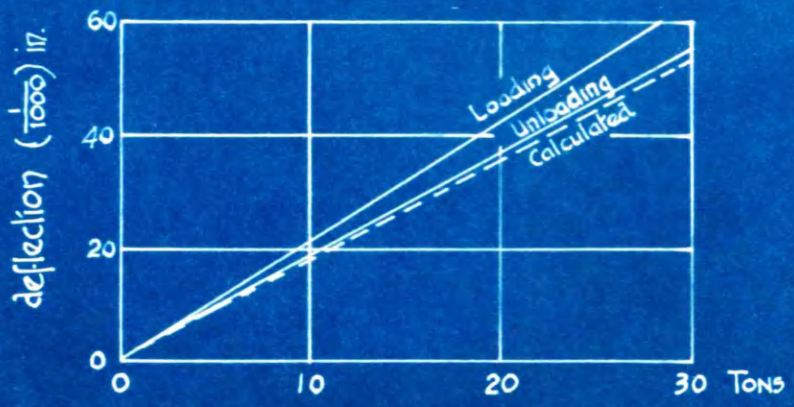

RELATIVE VERTICAL DEFLECTIONS
between points (d) and (f)

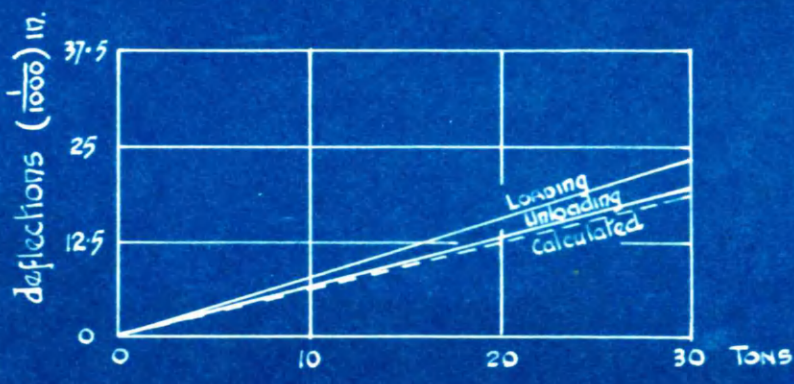

SUM OF RADIAL DEFLECTIONS
at 2½" and 4½".

FIG. 17

separate results are plotted on a load base as shown in Fig. 17. The difference between the loading and unloading readings is to be expected in a structure of this form. The cylindrical wall (ae) is built up in three sections, riveted together, and the ends of the wall are attached to the conical walls by a single riveted lap joint. While there may be other causes contributing to the difference in the loading and unloading deflections, the principal one would be slipping between the joints.

Analytical Investigation: For the purposes of calculation certain assumptions must be made. These assumptions, with a brief explanatory note attached to each, are:-

(a) The existence of a dust chamber and manhole is ignored. The readings are located to give the best average values.

(b) The load is assumed to be a vertical ring load applied at (b). The small bending moment on the short cylindrical wall formed by the angle leg is neglected.

(c) The conditions at (f) are taken to be rigid. Owing to the shortness of time available for the test and the unforeseen circumstances which prevented the use of a concrete foundation, the experimental observations on the bottom conical wall to check this assumption had to be discounted.

(d) The welded and riveted joints are assumed to realize the conditions of a continuous plate. The reinforcement effect in a welded joint can only be obtained by experi-:ment. As regards the single riveted lap joint under the action of edge loading, the assumption will not cause any great error. It may be pointed out here, however, that this is not true for such a joint subject to internal or external pressure. (Discussed in Section V)

(e) The value of the modulus, E, is taken to be 29.2×10^6 lb per in.^{2}. The only information which could/

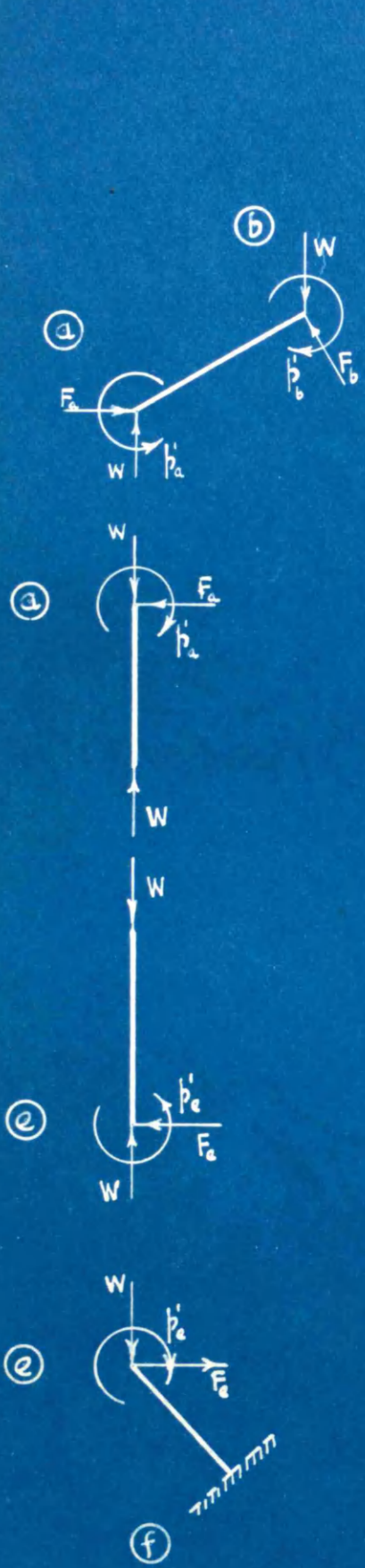

FORCES ACTING ON COMPONENT PARTS

FIG. 18

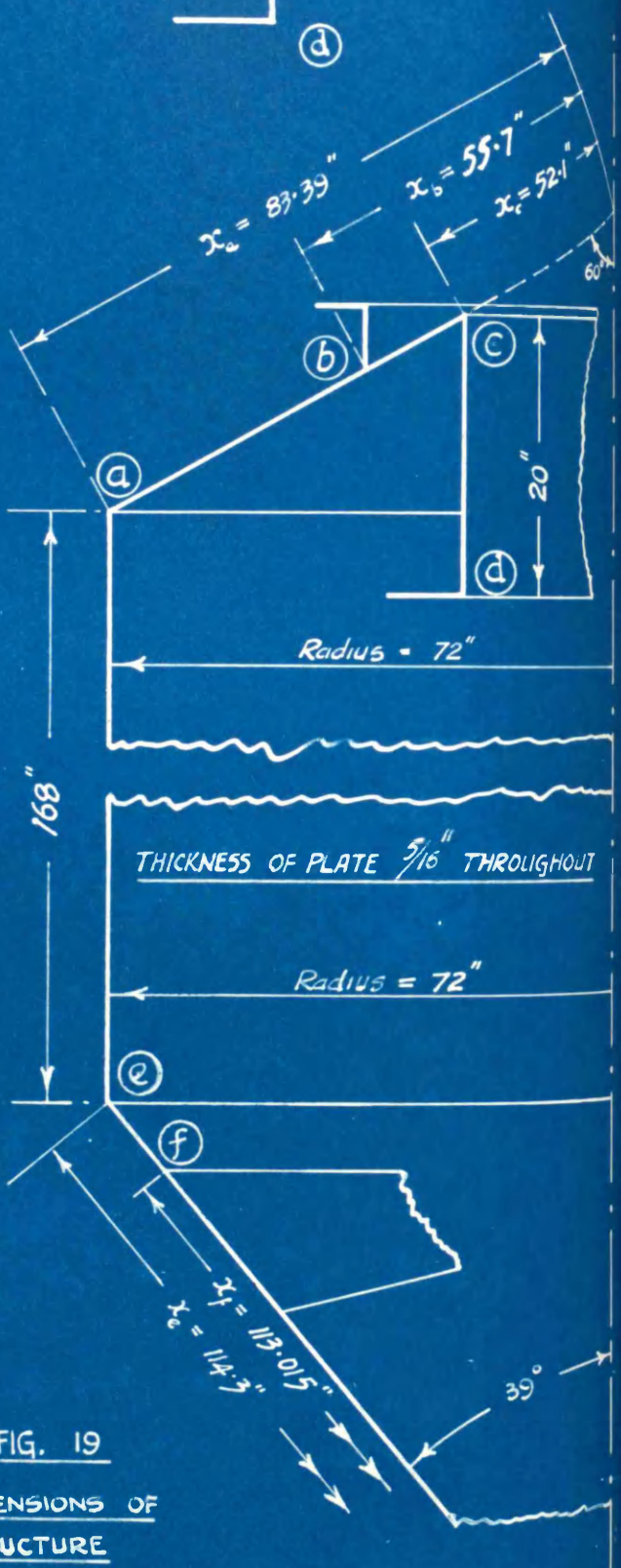

FIG. 19

DIMENSIONS OF STRUCTURE

could be obtained was that the material satisfied the requirements of the specification with a modulus value between 28 x 10^6 lb. per in.^{2} and 32 x 10^6 lb. per in.^{2}. The percentage error possible will not be very large.

The method of breaking up the component parts and the assumed forces and stresses acting are indicated in Fig.18. All the necessary dimensions are given in Fig. 19.

In this example certain cylindrical wall equations are required. These equations correspond to and are identical with the equations (25), (27), (28) and (29) given for conical walls, with the following substitutions:-

$b = \sin n x$, $q = \cos nx$, $\varepsilon = e^{2nx}$, $n' = \sqrt{\frac{\gamma^2}{6^2 r^2}}$

The radius r is constant and x is the distance measured along the cylindrical wall from any suitable origin.

Extensional Effects: Except for the cylindrical wall (ae), these effects are negligible. Due to the direct loading on this wall, the relative vertical deflection between joints (a) and (e) is $\frac{WL}{AE}$, where the direct load W = 26 tons; the length of wall L = 168 in., the sectional area A = 141.5 in.^{2}; and the modulus E = 29·^{2} x 10^6 lb. per in.^{2}. Hence putting in these values:-

$$\frac{WL}{AE} = 2.375 \times 10^{-3} \text{ in.} \qquad \ldots\ldots(4)$$

Edge Effects: The constants for the different parts are given below.

Cylinder (ae) - The length, L, of the cylinder is such that $nL > \pi$; Therefore the constants A, B, C and D may be evaluated in pairs A and B, C and D. Simplification is obtained by taking the origin in the first place at (a), dealing with the conditions at (a); and in the second place at (e), dealing with the conditions at (e). Thus the same pair of constants serve in both cases. These constants may be selected from Table II in the previous section and are:-

$$C = \beta' \; ; \qquad D = \beta' - \frac{6s}{\gamma\sqrt{6}r}.$$

The/

The appropriate bending and shear stresses are inserted according to the particular joint, (a) or (e), under consideration.

Cylinder (cd) - In this case $nL > \pi$ and the constants are similar to those for the wall (ae) but obtained in terms of the bending and shear stresses at (c).

Conical wall (ab) :- the length $(x_a - x_b) = L_1$ is such that $\sqrt[4]{m^3} \cdot e^{nL\left\{\frac{1-\sqrt{m}}{1-m}\right\}2\sqrt{\cos\alpha}} > e^{\pi}$, hence the constants may be determined in pairs in terms of the bending and shear stresses (or forces) at (a) and (b) respectively from equations (25) and (27) in the following manner:-

$$\left.\begin{aligned} p'_a &= \sqrt{\Sigma_a}\left\{A q_a + B b_a\right\} \\ S_a &= -\frac{v}{6}\sqrt{\frac{E}{r}}\left[\sqrt{\Sigma_a}\left\{(B+A)q_a + (B-A)b_a\right\}\right] \end{aligned}\right\} \quad \text{---- (2a)}$$

Hence

$$\left.\begin{aligned} A\sqrt{\Sigma_a} &= p'_a(b_a + q_a) + \frac{6S_a}{v\sqrt{E/r_a}} \\ B\sqrt{\Sigma_a} &= -p'_a(q_a - b_a) - \frac{6S_a}{v\sqrt{E/r_a}} \end{aligned}\right\} \quad \text{--- (3a)}$$

Similarly

$$\left.\begin{aligned} C/\sqrt{\Sigma_b} &= p'_b(q_b - b_b) + \frac{6S_b}{v\sqrt{E/r_b}} \\ D/\sqrt{\Sigma_b} &= p'_b(q_b + b_b) - \frac{6S_b}{v\sqrt{E/r_b}} \end{aligned}\right\} \quad \text{--- (4a)}$$

Conical wall (ef) :- In this case $(x_e - x_f) = L_1$ is such that $\sqrt[4]{m^3} \cdot e^{nL\left\{\frac{1-\sqrt{m}}{1-m}\right\}2\sqrt{\cos\alpha}} < e^{\pi}$, therefore the four constants must be determined simultaneously. The conditions existing at the edges of this wall are:-

At edge (e), $p' = p'e$; $s = s_e$;

At edge (f), $u = o$; $i = o$.

The equations from these conditions allow the constants $(A,B,C,D)_{ef}$ to be obtained in terms of p'_e and s_e.

Conical wall (bc) :- The length $(x_b - x_c) = L_1$ is such that the four constants must be obtained simultaneously. The conditions at the edges are:-

At edge (b), $p' = p'b$; $s = s_b$;

At edge (c), $p' = p'_e$; $s = s_c$;

The/

The details of the necessary calculation are given briefly. From equations (25) and (27) there is obtained the four equations:-

$$\left.\begin{aligned} p'_b &= \sqrt{\Sigma_b}\left\{Aq_b + Bb_b\right\} + \frac{1}{\sqrt{\Sigma_b}}\left\{Cq_b + Db_b\right\} \\ S_b &= -\frac{\nu}{6}\sqrt{\frac{r}{r_b}}\left[\sqrt{\Sigma_b}\left\{(B+A)q_b + (B-A)b_b\right\} + \frac{1}{\sqrt{\Sigma_b}}\left\{(D-C)q_b - (D+C)b_b\right\}\right] \\ p'_c &= \sqrt{\Sigma_c}\left\{Aq_c + Bb_c\right\} + \frac{1}{\sqrt{\Sigma_c}}\left\{Cq_c + Db_c\right\} \\ S_c &= -\frac{\nu}{6}\sqrt{\frac{r}{r_c}}\left[\sqrt{\Sigma_c}\left\{(B+A)q_c + (B-A)b_c\right\} + \frac{1}{\sqrt{\Sigma_c}}\left\{(D-C)q_c - (D+C)b_c\right\}\right] \end{aligned}\right\} \quad \ldots (5_2)$$

These equations may be rewritten thus:-

$$\left.\begin{aligned} A + B\frac{b_b}{q_b} + \frac{C}{\Sigma_b} + \frac{D}{\Sigma_b}\cdot\frac{b_b}{q_b} &= \frac{p'_b}{q_b\sqrt{\Sigma_b}} \\ A + B\left(\frac{q_b+b_b}{q_b-b_b}\right) - \frac{C}{\Sigma_b}\left(\frac{q_b+b_b}{q_b-b_b}\right) + \frac{D}{\Sigma_b} &= -\frac{6S_b}{\nu\sqrt{r/r_b}\cdot(q_b-b_b)\sqrt{\Sigma_b}} \\ A + B\frac{b_c}{q_c} + \frac{C}{\Sigma_c} + \frac{D}{\Sigma_c}\cdot\frac{b_c}{q_c} &= \frac{p'_c}{q_c\sqrt{\Sigma_c}} \\ A + B\left(\frac{q_c+b_c}{q_c-b_c}\right) - \frac{C}{\Sigma_c}\left(\frac{q_c+b_c}{q_c-b_c}\right) + \frac{D}{\Sigma_c} &= -\frac{6S_c}{\nu\sqrt{r/r_c}\cdot(q_c-b_c)\sqrt{\Sigma_c}} \end{aligned}\right\} \quad \ldots (6_2)$$

Inserting the arithmetical values:-

$R_b = \sqrt{2x_b} = 10.56$ in. , $R_c = \sqrt{2x_c} = 10.208$ in. , $n' = \sqrt{\frac{2\nu^2}{r^2\tan^2\lambda}} = 2.46$

$\Sigma_b = \frac{1}{R_b^3}\cdot e^{2n'R_b}$; $\Sigma_c = \frac{1}{R_c^3}\cdot e^{2n'R_c}$, $\therefore \frac{\Sigma_b}{\Sigma_c} = 5.508$

$n'R_b = 26$, $\therefore b_b = \sin n'R_b = 0.77$, $q_b = \cos n'R_b = 0.6374$

$n'R_c = 25.1$, $\therefore b_c = \sin n'R_c = 0$, $q_c = \cos n'R_c = 1$

the equations become:-

$$\left.\begin{aligned} A + 1.206B + \frac{C}{\Sigma_b} + 1.206\frac{D}{\Sigma_b} &= 1.57\frac{p'_b}{\sqrt{\Sigma_b}} \\ A - 10.64B + 10.64\frac{C}{\Sigma_b} + \frac{D}{\Sigma_b} &= 6.15\,F_b/\sqrt{\Sigma_b} \\ A + \frac{C}{\Sigma_c} &= p'_c/\sqrt{\Sigma_c} \\ A + B - \frac{C}{\Sigma_c} + \frac{D}{\Sigma_c} &= -0.448\,F_c/\sqrt{\Sigma_c} \end{aligned}\right\} \quad \ldots (7_2)$$

The values of the constants may be expressed finally as follows:-

(see over)

Constant.	p'c	p'b	F_c	F_b
$A\sqrt{\Sigma_b}$	- 5.4	+ 6	+ 0.956	+ 2.16
$B\sqrt{\Sigma_b}$	+ 1.104	- 0.727	- 0.133	- 0.82
$C/\sqrt{\Sigma_c}$	+ 3.3	- 2.565	- 0.416	- 0.918
$D/\sqrt{\Sigma_c}$	+ 5.12	- 4.85	- 1.2	- 1.481.

The values of the constants for the different walls may be similarly expressed in terms of the indeterminate forces acting at the respective edges.

Determination of the Edge Forces.

At Joint (a): the conditions are:-

(1) change of slope i, (cone) = change of slope i, (cylinder).

(11) increase in diam.at base of cone = diametral deflection of cylinder.

Therefore from (1)

$$-\frac{V^3}{6E}\sqrt{\frac{r_a}{h}}\left[\sqrt{\Sigma_a}\left\{-2(B-A)q_a+2(B+A)b_a\right\}\right] = -\frac{V^3}{6E}\sqrt{\frac{r}{h}}\left[\frac{1}{\sqrt{\Sigma_o}}\left\{2(D+C)q_o+2(D-C)b_o\right\}\right] \quad (8_2)$$

Inserting the values of the constants there results:-

$$p'_a\left[2\sqrt{\frac{r_a}{r}}+2\right] = \frac{6W\tan\lambda}{2\pi h r\sqrt{hr}}$$

$$\therefore p'a = +4.66 \text{ tons per in}^2. \quad \ldots\ (9_2)$$

From (11)

$$u\cos\lambda + z\sin\lambda \text{ (cone)} = u \text{ (cylinder)}. \quad (10_2)$$

but z may be taken as zero, therefore

$$u\cos\lambda \text{ (cone)} = u \text{ (cylinder)}. \quad (11_2)$$

$$\therefore \frac{r_a V^2}{6E}\left[\sqrt{\Sigma_a}\left\{2Bq_a-2Ab_a\right\}\right]\cos\lambda = \frac{rV^2}{6E}\left[\sqrt{\Sigma_o}\left\{2Bq_o-2Ab_o\right\}\right] \quad (12_2)$$

from which

$$\frac{F_a\cos\lambda - W\sin\lambda}{2\pi hr} = -\frac{F_a}{2\pi hr}\cdot\sqrt{\cos\lambda}$$

$$\therefore F_a = +18.7 \text{ tons} \quad (13_2)$$

The constants for the cylinder, origin at (a), are obtained from:- $C = p'_a$; $D = p'_a - \frac{6s}{\sqrt{r}\sqrt{h/r}}$, where $S = \frac{F_a}{2\pi hr}$

$$\therefore C = +4.66, \quad D = -4.71.$$

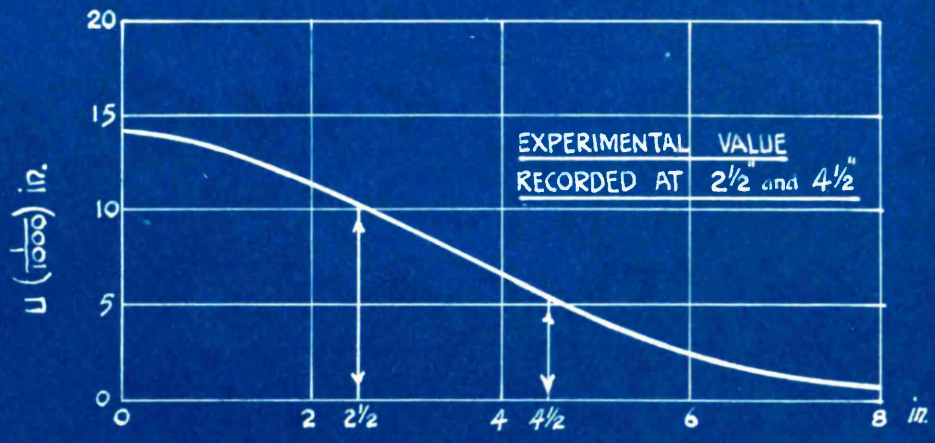

CALCULATED RADIAL DEFLECTIONS ALONG CYLINDRICAL WALL (ac) FROM EDGE (a)

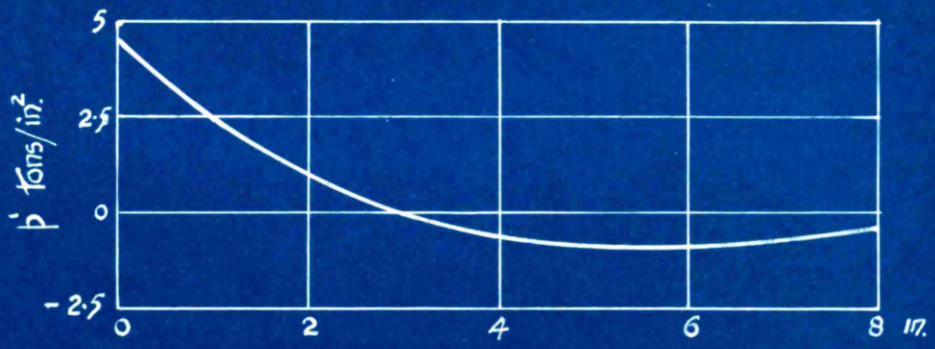

RADIAL BENDING STRESSES ALONG CYLINDRICAL WALL (ac) FROM EDGE (a)

FIG. 20

Radial deflection of the cylinder (ae), origin at (a), is given by:-

$$U = \frac{rv^2}{6E} \cdot \frac{1}{\sqrt{\Sigma_o}} \left\{ -2Dq_o + 2Cb_o \right\} \qquad \ldots\ldots (14_2)$$

This quantity is plotted on a base of x values from o to 8 in., as shown in Fig. 20, for W = 26 tons. The sum of the radial deflections at x = $2\frac{1}{2}$ in. and x = $4\frac{1}{2}$ in. is 16.2 x 10^{-3}in. Therefore when W = 519 cwts. - 51 cwts. = 23.4 tons, $U_{[x=2\frac{1}{2}+x=4\frac{1}{2}]}$ = 14.6 x 10^{-3}in. This value is to be compared with the actual experimental reading when unloading, which is 15 x 10^{-3}in.

The radial deflection U, at x = o, is 14.4 x 10^{-3}in. for W = 26 tons. Therefore, relative vertical deflection of joint (a) to joint (d) is:-

$$U \tan\lambda = 25 \times 10^{-3}\text{in.} \qquad \ldots\ldots (15_2)$$

At Joints (b) and (c): the conditions are:-

At joint (b):-

change of slope, i (cone bc) = change of slope, i (cone ba)

radial deflection u (" ") = radial deflection u (" ")

At joint (c):-

change of slope, i (cone cb) = change of slope, i (cylinder cd)

horizontal radial deflection (" ") = radial deflection, u (" ")

From these conditions, the following equations are obtained:-

$$\left.\begin{aligned}
B - A\left\{\frac{q_b+b_b}{q_b-b_b}\right\} + \frac{C}{\Sigma_b} + \frac{D}{\Sigma_b}\left\{\frac{q_b+b_b}{q_b-b_b}\right\} &= \frac{D'}{\Sigma_b}\left\{\frac{q_b+b_b}{q_b-b_b}\right\} + \frac{C'}{\Sigma_b} \\
B - A\frac{b_b}{q_b} + \frac{C}{\Sigma_b}\cdot\frac{b_b}{q_b} - \frac{D}{\Sigma_b} &= -\frac{D'}{\Sigma_b} + \frac{C'}{\Sigma_b}\cdot\frac{b_b}{q_b} \\
B - A + \frac{C}{\Sigma_c} + \frac{D}{\Sigma_c} &= \sqrt{\frac{\cos\lambda}{\Sigma_c}}\left\{D'' + C''\right\} \\
B - \frac{D}{\Sigma_c} &= -D''/\sqrt{\Sigma_c}
\end{aligned}\right\} \quad \ldots (16_2)$$

Where A, B, C, D are constants for the conical wall (bc); D', C', constants for the conical wall (ab); D", C", constants for the cylinder (cd).

These constants are all known in terms containing

p'_b/

p'_b, p'_c, F_b, F_c. Solving for these indeterminate reactions there results:-

p'_b = - 3.88 tons per in.^{2}; p'_c = + 2.88 tons per in.^{2};

F_b = 13.7 tons; F_c = 10.4 tons.

The constants for the cylinder (cd) are then obtained from:-

$$C'' = -p'_c \; ; \qquad D'' = -p'_c - \frac{6s}{\sqrt{2}h/r} \; , \text{ where } s = -\frac{F_c}{2\pi h r_c \cos\lambda}$$

$\therefore$ C'' = - 2.88 ; D'' = + 3.77.

In evaluating constants, careful attention has to be given to the assumed directions of the indeterminate reactions and reference made to the sign convention.

Radial deflection U, of the cylinder (cd), origin at (c), is given by:-

$$U = \frac{\gamma v^2}{6E}\left[\frac{1}{\sqrt{2}}\left\{-2D''q + 2C''b\right\}\right] \qquad (17_2)$$

When x = o, $U = \frac{\gamma v^2}{6E}\left\{-2D''\right\} = -7.22 \times 10^{-3}$ in.

Therefore vertical deflection of joint (c) is given by:-

$$U \tan\lambda = 12.5 \times 10^{-3} \text{ in.} \qquad \ldots (18_2)$$

$\therefore$ Vertical deflection of joint (d) = 12.5 x 10^{-3} in. (19_2)

At Joints (e) and (f): the conditions at edge (e) are:-

(1) change of slope, i (cone ef) = change of slope i (cylinder ea).

(11) Horizontal radial deflection (" ") = radial deflection u (cylinder ea).

The equations from these conditions include constants, the values of which are known in terms of p'_e and F_e. Solving for the indeterminate reactions there obtains:-

p'_e = + 1.97 tons per in.^{2}; F_e = 8.91 tons.

$\therefore$ Constant D for the cylinder (ea) is obtained from:-

$$D = p'_e - \frac{6s}{\sqrt{2}h/r} \; , \text{ where } s = \frac{F_e}{2\pi h r}$$

$\therefore$ D = - 2.5.

Radial deflection U of cylinder (ea), origin at (e) is given by:-

$$U = \frac{\gamma v^2}{6E}\left[\frac{1}{\sqrt{2}}\left\{-2Dq + 2Cb\right\}\right] \qquad \ldots (20_2)$$

$\therefore$ Radial deflection at (e) is $U_e = \frac{rv^2}{6E} - 2D = + 7.64 \times 10^{-3}$ in.

$\therefore$ Vertical deflection at joint (e) relative to (f) is given by:-

$$U_e \tan \quad = 6.1 \times 10^{-3} \text{in.} \qquad (21_2)$$

Collecting the results as given by equations (1_2), (15_2), (19_2), (21_2), the deflection of (d) relative to (f) is obtained.

Due to extensional effects on the cylinder (ae) = 2.375×10^{-3} in.

" " edge " at (a) = 25.00 " "

" " " " " (c) = 12.50 " "

" " " " " (e) = 6.10 " "

Total = 45.975×10^{-3} in.

This deflection is calculated for W = 26 tons, hence for W = (519 - 51) cwts. = 23.4 tons.

Deflection of (d) relative to (f) = 41.5×10^{-3} in. (22_2)

This value is to be compared with the actual reading taken for unloading which is 43×10^{-3} in.

The sum of the radial deflections for the cylinder (ae), origin at (a), for values at x = $2\frac{1}{2}$ in. and x = $4\frac{1}{2}$ in., and the relative vertical deflections between (d) and (f), calculated for different loads, have been plotted on Fig. 17 to allow a ready comparison between the experimental and theoretical results. The close agreement between the latter and the readings recorded for unloading would indicate certain compensating effects as regards the assumptions made. In spite of these assumptions, the test must be regarded as satisfactory, from a practical point of view, and indicates the maximum stress, occurring at (a), to be approximately 5 tons per in.^{2}

The variation of the radial bending stress along part of the cylindrical wall (ae) is shown in Fig. 20. With the values of the constants determined, similar diagrams, showing the variation of movements and stresses in all parts of the structure may be obtained.

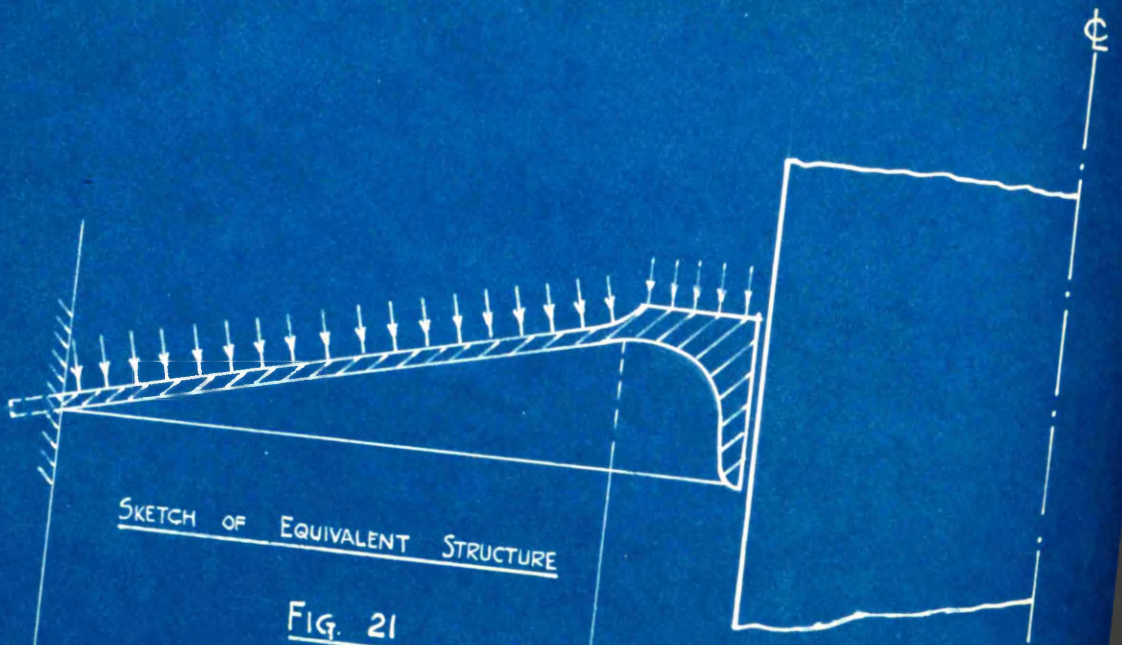

SKETCH OF EQUIVALENT STRUCTURE

FIG. 21

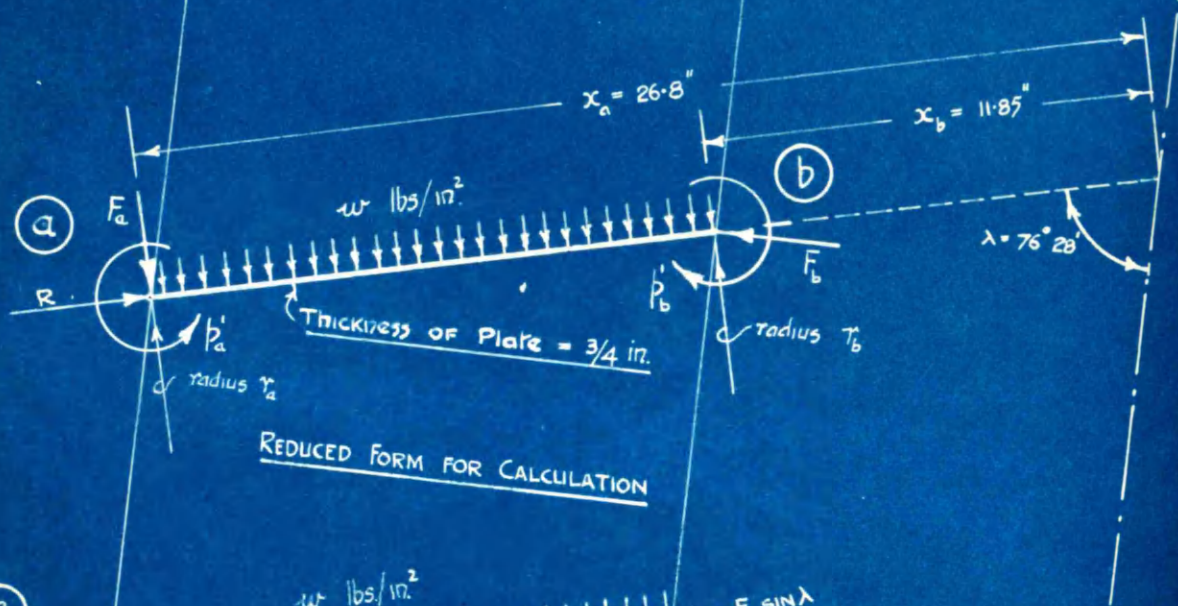

REDUCED FORM FOR CALCULATION

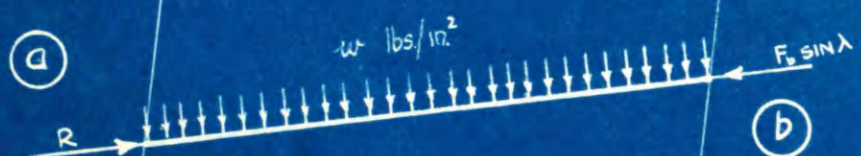

FORCES IN EXTENSIONAL SOLUTION

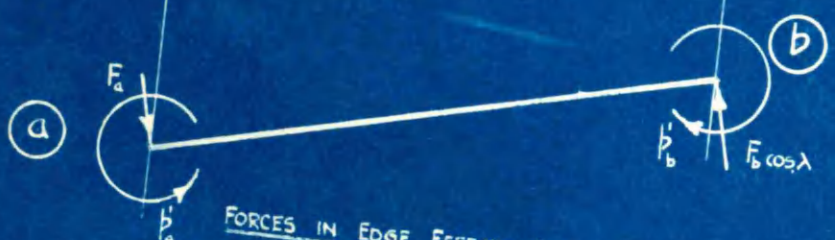

FORCES IN EDGE EFFECT SOLUTION

FIG. 22.

Investigation of Stresses in a Coned Turbine Diaphragm.

It is a well known fact that when a flat circular plate is slightly dished into a conical form, its strength is increased. This application demonstrates the variation in bending stress throughout the length of plate in a turbine diaphragm under pressure, and compares the radial bending stresses for three conical forms with those in a disc. The thickness h of the plate is uniform. The problem may be reduced to the arrangement shown in Fig. 21, in which the outer edge of the plate is rigidly fixed, while the inner edge is directionally fixed but laterally free. The loading and assumed edge forces together with the method of separating these for the purpose of determining the extensional and edge effects are given in Fig.22.

Extensional Effects: The conditions are:-

at edge (b), $p_b = -\frac{F_b \sin\lambda}{2\pi h r_b \cos\lambda}$

at edge (a), $Z_a = 0.$

∴ from equation (9)

$$-\frac{F_b \sin\lambda}{2\pi h r_b \cos\lambda} = -\frac{P r_b}{2h} + \frac{a_1}{x_b} \qquad \ldots (1_3)$$

from which $a_1 = -0.212\, F_b + 388\, P.$ $\ldots (2_3)$

∴ from equation (12)

$$0 = -\frac{(1-2\sigma) P r_a}{4hE} \cdot x_a + \frac{a_1}{E} \log_e x_a + b_1 \qquad \ldots (3_3)$$

from which $b_1 E = +0.701\, F_a - 878\, P.$ $\ldots (4_3)$

Edge Effects: The conditions are:-

at edge (b), $i_b = 0$; $S_b = \frac{F_b \cos\lambda}{2\pi h r_b \cos\lambda}$

at edge (a), $i_a = 0$; $S_a = \frac{F_a}{2\pi h r_a \cos\lambda}$

Hence from equations (27) and (28), four simultaneous equations are obtained:-

$$\left.\begin{aligned}
\frac{F_b}{2\pi\sqrt{rr_b}} &= -\frac{\nu}{6}\sqrt{\frac{r}{r_b}}\left[\sqrt{\xi_b}\left\{(B+A)q_{rb}+(B-A)b_b\right\}+\frac{1}{\sqrt{\xi_b}}\left\{(D-C)q_{rb}-(D+C)b_b\right\}\right]\\
\frac{F_a}{2\pi\sqrt{rr_a}\cos\lambda} &= -\frac{\nu}{6}\sqrt{\frac{r}{r_a}}\left[\sqrt{\xi_a}\left\{(B+A)q_{ra}+(B-A)b_a\right\}+\frac{1}{\sqrt{\xi_a}}\left\{(D-C)q_{ra}-(D+C)b_a\right\}\right]\\
0 &= -\frac{\nu^3}{6E}\sqrt{\frac{r_b}{r}}\left[\sqrt{\xi_b}\left\{2(B-A)q_{rb}-2(B+A)b_b\right\}+\frac{1}{\sqrt{\xi_b}}\left\{2(D+C)q_{rb}+2(D-C)b_b\right\}\right]\\
0 &= -\frac{\nu^3}{6E}\sqrt{\frac{r_a}{r}}\left[\sqrt{\xi_a}\left\{2(B-A)q_{ra}-2(B+A)b_a\right\}+\frac{1}{\sqrt{\xi_a}}\left\{2(D+C)q_{ra}+2(D-C)b_a\right\}\right]
\end{aligned}\right\}\quad(5_3)$$

Inserting the arithmetical values the equations become:-

$$\left.\begin{aligned}
0.097B^1 - 0.19A^1 - 1.26D^1 - 0.642C^1 &= +0.163F_b.\\
1.26B^1 - 0.642A^1 - 0.097D^1 - 0.19C^1 &= -0.465F_a.\\
0.19B^1 + 0.097A^1 - 0.642D^1 + 1.26C^1 &= 0.\\
0.642B^1 + 1.26A^1 - 0.19D^1 + 0.097C^1 &= 0.
\end{aligned}\right\}\quad(6_3)$$

where $A^1 = A\sqrt{\xi_a}$, $B^1 = B\sqrt{\xi_a}$, $C^1 = C/\sqrt{\xi_b}$, $D^1 = D/\sqrt{\xi_b}$.
The solution to these equations gives the values of the constants as:-

$$A\sqrt{\xi_a} = 0 + 0.1435F_a; \qquad C/\sqrt{\xi_b} = -0.051F_b + 0.009F_a.$$
$$B\sqrt{\xi_a} = -0.016F_b - 0.299F_a; \quad D/\sqrt{\xi_b} = -0.105F_b - 0.049F_a.$$

All the constants are now in terms of F_a, F_b and P. The indeterminate reactions F_a and F_b are obtained from the conditions:-

$$\left.\begin{aligned}
&\text{At edge (b),} && z_b\sin\lambda = -u\cos\lambda\\
&\text{At edge (a),} && u_a = 0
\end{aligned}\right\}\quad(7_3)$$

Combining extensional and edge effects, (12) with (32) and (11) with (29), the equations in group (7_3) may be expressed as:-

At edge (b), /

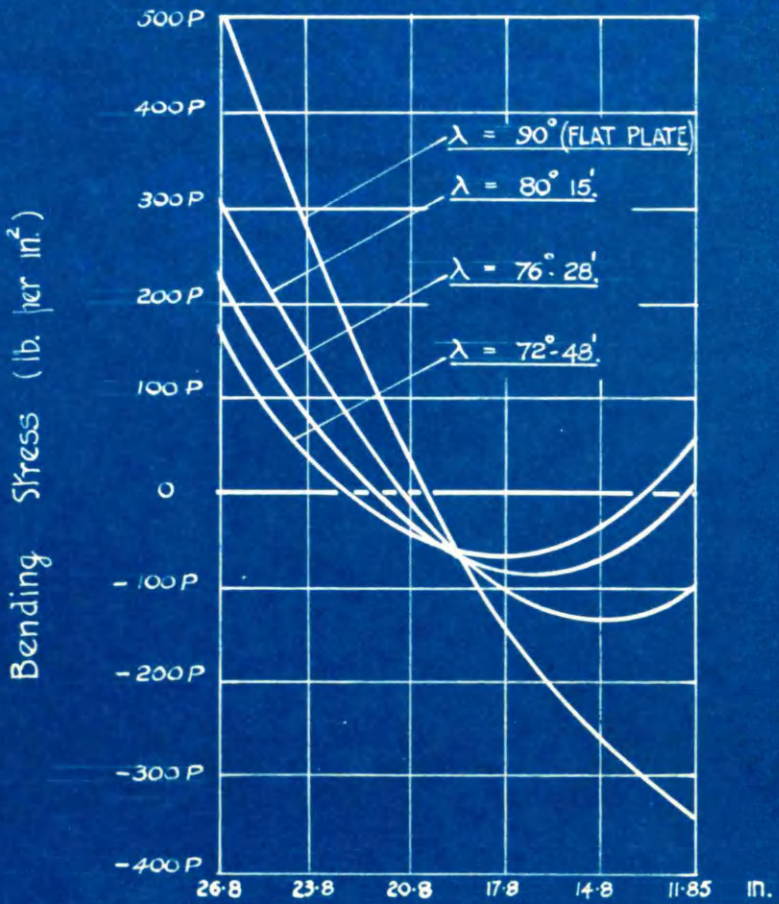

RADIAL BENDING STRESSES

FIG. 23 a.

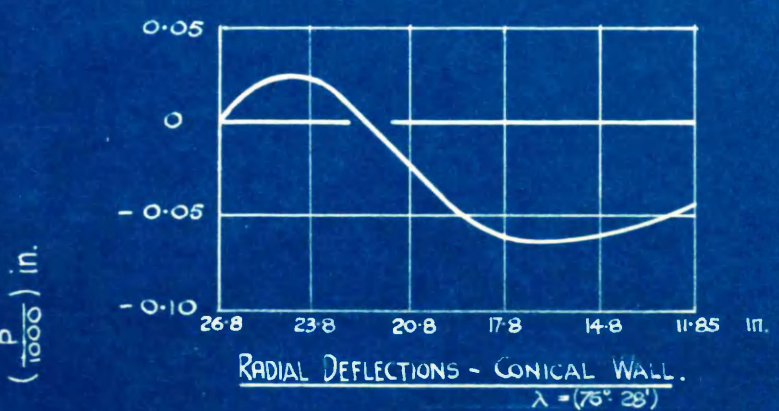

RADIAL DEFLECTIONS - CONICAL WALL.
λ = (76° 28')

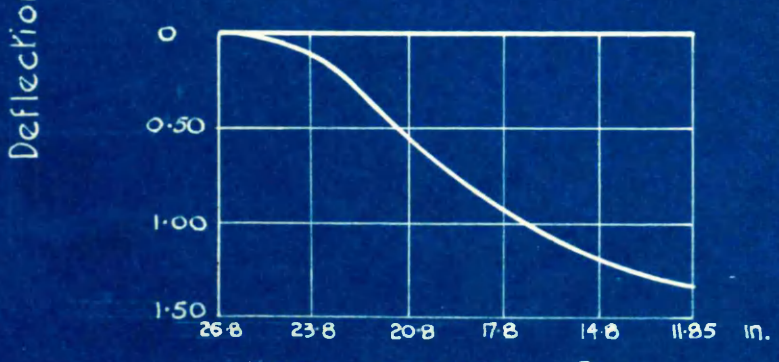

VERTICAL DEFLECTIONS - DISC.

FIG. 23 b.

TABLE II.

$R=\sqrt{2x}$	$\left(\frac{R_b}{R}\right)^{3/2}$	$\frac{R_b - R}{R_b}$	$n'(R_b-R)$	$e^{n'(R_b-R)}$	θ°	C'_q	D'_b	$-C'_q+D'_b$	$b'_{[c',d']}$	Total Bending Stress p'_t
7.32	0.54	- 2.45	- 2.53	0.08	72° ∠	- 23.9	- 83.6	- 107.5	- 4.67	+ 230 P
6.9	0.592	- 2.03	- 2.10	0.12	48°"	- 51.8	- 65.3	- 117.1	- 8.5	+ 73 P
6.45	0.658	- 1.58	- 1.63	0.20	22°"	- 71.8	- 33	- 104.8	- 13.5	- 28 P
5.96	0.74	- 1.09	- 1.124	0.33	8° <	- 76.7	+ 12.2	- 64.5	- 15.4	- 80 P
5.44	0.848	- 0.57	- 0.58	0.56	39°"	- 60.2	+ 55.4	- 4.8	- 2.3	- 71 P
4.87	1.00	0	0	1	72°"	- 23.9	+ 83.6	+ 59.7	+ 59.7	+ 11.3 P

The variation in radial bending stress is plotted on a base of distances x, measured from the apex of the cone, and is given in Fig. 23a. Comparisons are effected for $\lambda = 72^\circ 48'$, $80^\circ 15'$ and 90°; the last representing the flat circular disc.

The variation in radial deflections U, is obtained from:-

$$u = \frac{3Pr^2}{4\pi E} - \frac{a_1}{E}(\sigma + \log_e x)\tan\lambda - b_1\tan\lambda + \frac{\nu r}{6E}\left[\sqrt{\xi}\left\{2Bq - 2Ab\right\} + \frac{1}{\sqrt{\xi}}\left\{-2Dq + 2Cb\right\}\right] \quad \text{------}(12_3)$$

The values are plotted on a similar base and are compared with the vertical deflections for the disc: Fig. 23b. The scale for the former is ten times greater than that for the latter. The direct circumferential stresses are small compared with the radial bending stresses and have not been included.

Approximate Solution for Maximum Stress: While the variations in distortions and stresses along the length of wall are interesting, the designer is mainly concerned with the maximum stress and a rapid method for obtaining a fair approximation of this value is necessary.

An examination of the graphs in Fig. 23a shows the maximum stress to be at edge (a). From the tables it is seen that the contribution to this stress from the force effects/

effects at edge (b) is very small; the ratio being $-\frac{4.67}{230}$.

Therefore an approximation for the stress at edge (a), neglecting the effect of edge forces at (b), is all that is required; and the result will err on the safe side. This approximation is given below:-

Extensional Effects: These are as obtained in the more exact solution, but the general terms are retained. Hence

$$a_1 = -\frac{F_b}{2\pi h} + \frac{P r_b x_b}{2h} \qquad (13_3)$$

$$b_1 E = \frac{(1-2\sigma)}{4h} \cdot P r_a x_a - a_1 \log_e x_a \qquad (14_3)$$

Edge Effects: The conditions are

$$\text{at edge (a)}, \quad i_a = 0; \quad s_a = \frac{F_a}{2\pi h r_a \cos\lambda}$$

Hence from equations (27) and (28), omitting terms containing the constants C and D.

$$\frac{F_a}{2\pi h r_a \cos\lambda} = -\frac{\nu}{6}\sqrt{\frac{h}{r_a}}\left[\sqrt{\xi_a}\left\{(B+A)q_a + (B-A)b_a\right\}\right] \qquad \ldots\ldots(15_3)$$

$$0 = -\frac{\nu^3}{6E}\sqrt{\frac{r_a}{h}}\left[\sqrt{\xi_a}\left\{2(B-A)q_a - 2(B+A)b_a\right\}\right] \qquad \ldots\ldots(16_3)$$

From these equations the values of the constants A^1 and B^1 are obtained as:-

$$\left.\begin{aligned} A^1 = A\sqrt{\xi_a} &= -\frac{F_a}{2\pi h r_a \cos\lambda} \cdot \frac{6}{\nu}\sqrt{\frac{r_a}{h}} \cdot \frac{q_a - b_a}{2} \\ B^1 = B\sqrt{\xi_a} &= -\frac{F_a}{2\pi h r_a \cos\lambda} \cdot \frac{6}{\nu}\sqrt{\frac{r_a}{h}} \cdot \frac{q_a + b_a}{2} \end{aligned}\right\} \qquad \ldots\ldots(17_3)$$

The radial bending stress p^1 at edge (a) is given by

$$p'_a = \sqrt{\xi_a}(Aq_a + Bb_a) \qquad \ldots\ldots(18_3)$$

$$= \frac{F_a}{4\pi h r_a \cos\lambda} \cdot \frac{6}{\nu}\sqrt{\frac{r_a}{h}} \qquad \ldots\ldots(19_3)$$

The condition at edge (a) gives $U_a = 0$. $\qquad \ldots\ldots(20_3)$

$$\therefore \quad -\frac{3Pr_a^2}{4hE} - \frac{a_1}{E}(\sigma + \log_e x_a)\tan\lambda - b_1\tan\lambda + \frac{\nu^2 r_a}{6E}\left[\sqrt{\xi_a}\left\{2Bq_a - 2Ab_a\right\}\right] = 0 \qquad \ldots(21_3)$$

$$\frac{3Pr_a^2}{4hE} + \frac{P}{2hE}\left\{\sigma r_b x_b + \frac{(1-2\sigma)r_a x_a}{2}\right\}\tan\lambda = -F_a \cdot \frac{\nu}{2\pi h E \cos\lambda}\sqrt{\frac{r_a}{h}} + F_b \cdot \frac{\sigma\tan\lambda}{2\pi h E} \qquad (22_3)$$

F_a and F_b are numerically nearly equal, hence neglecting the F_b term:-

$$\frac{Pr_a^2}{2h}\left\{\frac{3}{2}+\sigma\frac{r_b^2}{r_a^2}+\frac{(1-2\sigma)}{2}\right\} = -F_a\left\{\frac{v\sqrt{r_a/h}}{2\pi h\cos\lambda}\right\} \qquad ----(23_3)$$

Neglecting the middle term on the left hand side:-

$$\frac{Pr_a^2}{4h}\left\{4-2\sigma\right\} = -F_a\left\{\frac{v\sqrt{r_a/h}}{2\pi h\cos\lambda}\right\} \qquad -----(24_3)$$

giving

$$F_a = -\left\{\frac{2\pi\cos\lambda}{v\sqrt{r_a/h}}\right\} 0{\cdot}85\,Pr_a^2 \qquad -----(25_3)$$

Substituting this value of F_a in equation (19_2):-

$$p^1_a = \left\{\frac{2{\cdot}55}{v^2}\right\}\cdot\frac{Pr_a}{h}$$

$$= K\cdot\frac{Pr_a}{h} \qquad ---- (26_3)$$

where K is a constant.

With $\lambda = 76^\circ 28'$, the calculated value of $p^1 = 230$ P. Using this value and putting $K^1\cdot\frac{Pr_a}{h} = 230$ P, $K^1 = 1.55$. Neglecting the effect of edge forces at (b), $p^1_a = 235$P. Hence equating $K''\cdot\frac{Pr_a}{h} = 235$P, $K'' = 1.585$. The value of K as derived is $K = \frac{2{\cdot}55}{v^2} = 1.54$. A sufficiently accurate value of the maximum radial bending stress is obtained from the rule

$$p^1_a = K\cdot\frac{Pr_a}{h} \qquad \text{where } K = 1.53.$$

A comparison of the calculated and approximate values of the radial bending stress at edge (a) is given in the table below:-

λ	p^1_a (calculated).	p^1_a (approx.) K= 1.53.	Percentage error.
80° - 15'	309.7P	313P	+ 1.06
76° - 28'	230P	226.5P	- 1.52
72° - 48'	177.8P	179P	+ 0.68

The variation in the percentage error shows that this value of K = 1.53 can be used for angle λ varying from 72° to 80°, when the error will not exceed ± 1.52. per cent.

The plates in this type of problem usually increase in thickness/

thickness from the apex to the base of the cone. The reason for this is obvious from the graphs in Fig. 23[a], and tends towards a minimum stress distribution.

SECTION IV.

THIN SPHERICAL WALLS.

Thin Spherical Walls.

Restatement of general equations:-

$$E\left(\frac{z\cot\theta}{R_1}+\frac{u}{R_1}\right) = f-\sigma p \qquad \frac{d}{d\theta}(pR_1\sin\theta) - fR_2\cos\theta - (sR_1\sin\theta) = -\frac{1}{2\pi h}\cdot\frac{dQ}{d\theta}$$

$$E\left(\frac{1}{R_1}\cdot\frac{dz}{d\theta}+\frac{u}{R_2}\right) = p-\sigma f \qquad pR_1\sin\theta + fR_2\sin\theta + \frac{d}{d\theta}(sR_1\sin\theta) = \frac{1}{2\pi h}\cdot\frac{dW}{d\theta}$$

$$E\cdot\frac{h}{2}\cdot\frac{i\cot\theta}{R_1} = f'-\sigma p' \qquad sR_1R_2\sin\theta = -\frac{h}{6}\cdot\frac{d}{d\theta}(p'R_1\sin\theta) + \frac{h}{6}f'R_2\cos\theta$$

$$E\cdot\frac{h}{2}\cdot\frac{1}{R_2}\cdot\frac{di}{d\theta} = p'-\sigma f' \qquad i = -\frac{1}{R_2}\cdot\frac{du}{d\theta} + \frac{z}{R_2}$$

Derivation of Stress-strain relations from general equations.

In spherical walls, $R_1 = R_2 = r$ = constant. Hence the equations are re-written in the form:-

$$\frac{E}{r}(z\cot\theta + u) = f-\sigma p \qquad (1)\quad \frac{d}{d\theta}(p\sin\theta) - f\cos\theta - s\sin\theta = -\frac{1}{2\pi hr}\cdot\frac{dQ}{d\theta} \qquad (5)$$

$$\frac{E}{r}\left(\frac{dz}{d\theta}+u\right) = p-\sigma f \qquad (2)\quad (p+f)\sin\theta + \frac{d}{d\theta}(s\sin\theta) = \frac{1}{2\pi hr}\cdot\frac{dW}{d\theta} \qquad (6)$$

$$\frac{Eh}{2r}\cdot i\cot\theta = f'-\sigma p' \qquad (3)\quad sr\sin\theta = -\frac{h}{6}\cdot\frac{d}{d\theta}(p'\sin\theta) + \frac{h}{6}f'\cos\theta \qquad (7)$$

$$\frac{Eh}{2r}\cdot\frac{di}{d\theta} = p'-\sigma f' \qquad (4)\quad i = -\frac{1}{r}\cdot\frac{du}{d\theta} + \frac{z}{r} \qquad (8)$$

Derivation of equations for extensional effect.

From equations (1) and (2)

$$p = \frac{E}{(1-\sigma^2)r}\left\{\frac{dz}{d\theta} + \sigma z\cot\theta + (1+\sigma)u\right\} \qquad (9)$$

$$f = \frac{E}{(1-\sigma^2)r}\left\{\sigma\frac{dz}{d\theta} + z\cot\theta + (1+\sigma)u\right\} \qquad (10)$$

Substituting the values of p and f from (9) and (10) in (6,) and neglecting the shear term:-

$$u = -\frac{1}{2}\cdot\frac{dz}{d\theta} - \frac{1}{2}z\cot\theta + \frac{1}{4\pi h}\cdot\frac{(1-\sigma)}{E\sin\theta}\cdot\frac{dW}{d\theta} \qquad (11)$$

p and f may now be expressed in terms of Z and W. Substituting in (5) and neglecting the shear term:-

$$\frac{d^2z}{d\theta^2} + \cot\theta\cdot\frac{dz}{d\theta} + z(1-\cot^2\theta) = \frac{(1+\sigma)}{2\pi hE\sin\theta}\left\{-\frac{d^2W}{d\theta^2} + \cot\theta\cdot\frac{dW}{d\theta} - 2\frac{dQ}{d\theta}\right\} \cdots (12)$$

The solution[1] of (12) is simplified by putting $Z = Z_0\sin\theta$ and is finally:-

$$z = b_1\sin\theta - \frac{a_1}{2}(\cot\theta - \sin\theta\log_e\tan\tfrac{\theta}{2}) + \frac{1+\sigma}{2\pi hE}\sin\theta\int\operatorname{cosec}^3\theta\left[\int\sin\theta\left(\cot\theta\frac{dW}{d\theta} - 2\frac{dQ}{d\theta} - \frac{d^2W}{d\theta^2}\right)d\theta\right]d\theta \cdots (13)$$

For/

[1] Ibid p.576.

For any specific problem, once the load term in (13) is evaluated, u, p and f follow from (11), (9) and (10).

When the plate is subject to an internal pressure P, the equations become:-

$$p = \frac{E}{2r(1+\sigma)} \cdot \frac{a_1}{\sin^2\theta} + \frac{Pr}{2h} \qquad (14)$$

$$f = -\frac{E}{2r(1+\sigma)} \cdot \frac{a_1}{\sin^2\theta} + \frac{Pr}{2h} \qquad (15)$$

$$u = -b_1\cos\theta - \frac{a_1}{2}\left(1+\cos\theta \log_e \tan\frac{\theta}{2}\right) + \frac{(1-\sigma)}{2hE} \cdot Pr^2 \qquad (16)$$

$$z = b_1\sin\theta - \frac{a_1}{2}\left(\cot\theta - \sin\theta \log_e \tan\frac{\theta}{2}\right) \qquad (17)$$

Derivation of equations for edge effect. Load terms and integration constants which have appeared in the extensional solution may now be omitted.

From (5) and (6), p and f may be determined in terms of S.

$$p = -S\cot\theta \quad \ldots (18) \quad , \qquad f = -\frac{dS}{d\theta} \quad \ldots (19)$$

From (3) and (4) p' and f' are given by:-

$$p' = \frac{Eh}{2(1-\sigma^2)r}\left\{\sigma i \cot\theta + \frac{di}{d\theta}\right\} \qquad (20)$$

$$f' = \frac{Eh}{2(1-\sigma^2)r}\left\{i\cot\theta + \sigma\frac{di}{d\theta}\right\} \qquad (21)$$

Using equations (20) and (21), and substituting for $\frac{d}{d\theta}(p'\sin\theta)$ and $f'\cos\theta$ in (7), there results:-

$$\frac{d^2i}{d\theta^2} + \cot\theta\frac{di}{d\theta} - i(\sigma + \cot^2\theta) = -\frac{12r^2(1-\sigma^2)}{Eh^2} \cdot S \quad \ldots (22)$$

From (1) and (8):-

$$\frac{d}{d\theta}\left(\frac{r}{E}\{f-\sigma p\}\right) = \frac{d}{d\theta}\{z\cot\theta + u\} = \frac{d}{d\theta}(z\cot\theta) + z - ir = \cot\theta\left(\frac{dz}{d\theta} - z\cot\theta\right) - ir \quad \ldots (23)$$

But from (1) and (2):-

$$\left\{\frac{dz}{d\theta} - z\cot\theta\right\} = \frac{r(1+\sigma)}{E}\{p - f\} \quad \ldots (24)$$

Therefore substituting this value in (23), we have:-

$$\frac{d}{d\theta}\left\{\frac{r}{E}(f-\sigma p)\right\} = \cot\theta \cdot \frac{r(1+\sigma)}{E}\{p-f\} - ir \quad \ldots (25)$$

Substituting the values of p and f from (18) and (19), we finally obtain:-

$$\frac{d^2S}{d\theta^2} + \cot\theta\frac{dS}{d\theta} - (\cot^2\theta - \sigma)S = Ei \quad \ldots (26)$$

The/

The solutions for the equations(22) and(26):-

$$\left.\begin{aligned} \frac{d^2i}{d\theta^2} + \cot\theta\,\frac{di}{d\theta} - i\,(\cot^2\theta+\sigma) &= -\frac{12r^2(1-\sigma^2)}{Eh^2}\cdot s \\ \frac{d^2s}{d\theta^2} + \cot\theta\,\frac{ds}{d\theta} - s\,(\cot^2\theta-\sigma) &= E\,i \end{aligned}\right\} \quad \cdots\cdots(27)$$

are given as:-

$$i = \frac{2\bar{K}^2}{(\sin\theta)^{\frac{1}{2}}}\left\{\sqrt{\xi}\,(K_1\cos\phi + H_1\sin\phi) + \frac{1}{\sqrt{\xi}}\,(K_1'\cos\phi + H_1'\sin\phi)\right\} \quad \cdots(28)$$

$$S = \frac{E}{(\sin\theta)^{\frac{1}{2}}}\left\{\sqrt{\xi}\,(-H_1\cos\phi + K_1\sin\phi) + \frac{1}{\sqrt{\xi}}\,(H_1'\cos\phi - K_1'\sin\phi)\right\} \quad \cdots(29)$$

where $\bar{K} = \sqrt[4]{\frac{3(1-\sigma^2)r^2}{h^2}}$; $\phi = (\bar{K}+\frac{1}{2})\theta$; $\xi = e^{2\bar{K}\theta}$

The formation of these equations is permissible from the basic assumption that h is small compared with r.

$$p' = \frac{Eh}{2(1-\sigma^2)}\cdot\frac{1}{r}\left\{\sigma i\cot\theta + \frac{di}{d\theta}\right\} \quad (30)$$

$$= \frac{Eh}{2(1-\sigma^2)r}\frac{2\bar{K}^3}{(\sin\theta)^{\frac{1}{2}}}\left[\sqrt{\xi}\left\{(cK_1+H_1)\cos\phi + (cH_1-K_1)\sin\phi\right\} + \frac{1}{\sqrt{\xi}}\left\{(-c'K_1'+H_1')\cos\phi + (-c'H_1'-K_1')\sin\phi\right\}\right] \cdots(31)$$

To obtain similarity with the equations for radial bending stress in cylindrical and conical walls this may be written:-

$$p' = \sqrt{\xi}\left\{(cK+H)q + (cH-K)b\right\} + \frac{1}{\sqrt{\xi}}\left\{(-c'K'+H')q + (-c'H'-K')b\right\} \quad \cdots(32)$$

where $\sqrt{\xi}$, associated with K and H $= e^{\bar{K}\theta}/(\sin\theta)^{\frac{1}{2}}$ and with K' and H' , $= e^{\bar{K}\theta}\cdot(\sin\theta)^{\frac{1}{2}}$.

where $q = \cos\phi$, $b = \sin\phi$, $c = (1 - \frac{\cot\theta}{\bar{K}}\cdot\frac{1}{2-\sigma})$, $c' = (1 + \frac{\cot\theta}{\bar{K}}\cdot\frac{1}{2-\sigma})$

The contribution of the term i cot θ to the expression for the radial bending stress p' is represented by $\frac{\sigma\cot\theta}{\bar{K}}$. Unless θ is very small this quantity is negligible and equation (30) may be written:-

$$p' = \frac{Eh}{2(1-\sigma^2)}\cdot\frac{1}{r}\left\{\frac{di}{d\theta}\right\}$$

It follows, to a lesser degree, that:-

$$f' = \frac{Eh}{2(1-\sigma^2)}\cdot\frac{1}{r}\left\{\sigma\cdot\frac{di}{d\theta}\right\} = \sigma p' \quad \cdots\cdots(33)$$

For the majority of practical cases, this is sufficiently accurate.

From equation (24),

$$\left\{\frac{dz}{d\theta} - z\cot\theta\right\} = \frac{r(1+\sigma)}{E}\left\{p - f\right\}$$

Substituting the values for p and f from(18) and(19) respectively,

Z/

[1] Ibid p.579 et seq.

Z is expressed in terms of S as:-

$$Z = \frac{r(1+\sigma)s}{E} \qquad \ldots\ldots (34)$$

From equation (1):-

$$u = \frac{r}{E}\left\{f - \sigma p\right\} - z\cot\theta$$

$$= \frac{r}{E}\left\{-\frac{ds}{d\theta} + s\cot\theta\right\} \qquad \ldots\ldots (35)$$

In much the same way that i cot θ is negligible compared with $\frac{di}{d\theta}$, so is s cot θ with $\frac{ds}{d\theta}$; therefore:-

$$u = \frac{r}{E}\left\{-\frac{ds}{d\theta}\right\}, \qquad \therefore \quad f = E\,u/r. \qquad \ldots\ldots (36)$$

From the full equation (35) u is obtained as:-

$$u = -r\bar{K}\left[\sqrt{2}\left\{(-gH_1 + K_1)\cos\phi + (gK_1 + H_1)\sin\phi\right\} + \frac{1}{\sqrt{2}}\left\{(-g'H_1' - K_1')\cos\phi + (g'K_1' - H_1')\sin\phi\right\}\right] \qquad \ldots\ldots (37)$$

where $g = \left(1 + \frac{\cot\theta}{2\bar{K}}\right)$, $\qquad g' = \left(1 - \frac{\cot\theta}{2\bar{K}}\right)$.

All the edge effect equations are now known and are expressed in the group below so as to complete the similarity, as far as the form of plate permits, obtained in the corresponding groups for cylindrical and conical walls.

Edge effect equations:-

$$p' = \sqrt{2}\left\{(cK + H)q + (cH - K)b\right\} + \frac{1}{\sqrt{2}}\left\{(-c'K' + H')q + (-c'H' - K')b\right\} \qquad (38)$$

$$f' = \sigma p' \qquad (39)$$

$$s = -\frac{r}{6}\sqrt{\frac{r}{t}}\left[\sqrt{2}\left(2Hq - 2Kb\right) + \frac{1}{\sqrt{2}}\left(-2H'q + 2K'b\right)\right] \qquad (40)$$

$$i = -\frac{r^3}{6E}\sqrt{\frac{r}{t}}\left\{\sqrt{2}\left(-4Kq - 4Hb\right) + \frac{1}{\sqrt{2}}\left(-4K'q + 4H'b\right)\right\} \qquad (41)$$

$$u = \frac{rv^2}{6E}\left[\sqrt{2}\left\{(2gH - 2K)q + (-2gK - 2H)b\right\} + \frac{1}{\sqrt{2}}\left\{(2g'H' + 2K')q + (-2g'K' + 2H')b\right\}\right] \qquad (42)$$

$$f = E\frac{u}{r} \qquad (43)$$

$$p = -s\cot\theta \qquad (44)$$

$$Z = \frac{(1+\sigma)rs}{E} \qquad (45)$$

When θ is such that cot θ is negligible compared to $\bar{K}$, c = c' = g = g' = unity. Then putting (K + H), (H - K), (H' - K') and (-H' - K') equal to A, B, C and D respectively, equations/

equations(38)(40)(41)and(42)are exactly similar to the corresponding equations for cylindrical and conical walls.

Evaluation of the Constants.

For determining the constants it is generally necessary, owing to the form of the plate, to combine the extensional equations as obtained from(9)(10)(11)and(13) with the equations (44)(43)(42)and(45). This would seem to introduce complications, but when it is observed that the equations for 'p^1', 's' and 'i', do not contain the extensional constants a_1 and b_1, this essential step, peculiar to spherical walls is not serious. This feature is illustrated in the examples.

Particular cases, such as a spherical bowl subject to fluid or internal pressure, and supported at the edges by tangential forces may be solved by the use of extensional equations above.

Simplification in the determination of the constants is possible when the spherical plate exceeds a certain length measured along the meridian. This is equivalent to case II as outlined for cylindrical walls. Let the edges (1) and (2) of a spherical wall subtend an angle at the centre $(\theta_2 - \theta_1)$. In the general equations the term, corresponding to $\sqrt{\xi}$ for the cylinder is $\sqrt{\xi_2|\xi_1}$

$$\sqrt{\xi} = e^{nL} \quad ; \qquad \sqrt{\xi_2|\xi_1} = \left(\frac{\sin\theta_1}{\sin\theta_2}\right)^{\frac{1}{2}} \cdot e^{\bar{K}(\theta_2-\theta_1)} \quad .$$

In comparing the quantities $\sqrt{\xi}$ and $\sqrt{\xi_2|\xi_1}$, the thickness, h, and radius, r, for the cylindrical and spherical walls are taken as equal:-

$$n = \sqrt[4]{\frac{3(1-\sigma^2)}{h^2 r^2}} \quad , \qquad \bar{K} = \sqrt[4]{\frac{3(1-\sigma^2)r^2}{h^2}}$$

When the value of L is such that $nL \geq \pi$ the constants A and B for the cylindrical wall may be determined independently of the constants C and D. Therefore, in order that the constants H and K for the spherical wall, may be determined independently of the constants H' and K', $\sqrt{\xi_2|\xi_1} = \sqrt{\xi} = e^{nL} = e^{\pi}$

and $\sqrt{\xi_2|\xi_1} = \left(\frac{\sin\theta_1}{\sin\theta_2}\right)^{\frac{1}{2}} \cdot e^{\bar{K}(\theta_2-\theta_1)} = \sqrt{m'} \cdot e^{nL_1}$

Where/

where:-

$$m' = \frac{\sin\theta_1}{\sin\theta_2} \qquad \text{and } L_1 = r(\theta_2 - \theta_1)$$

Knowing the length L_1 of the spherical wall, the constants H and K may be determined independently of H' and K', provided:-

$$\sqrt{m'} \cdot e^{nL_1} \geqq e^{\pi}.$$

In all other cases, the arithmetical solution is simplest; the only difference from the conical wall examples being the inclusion of the constants a_1 and b_1.

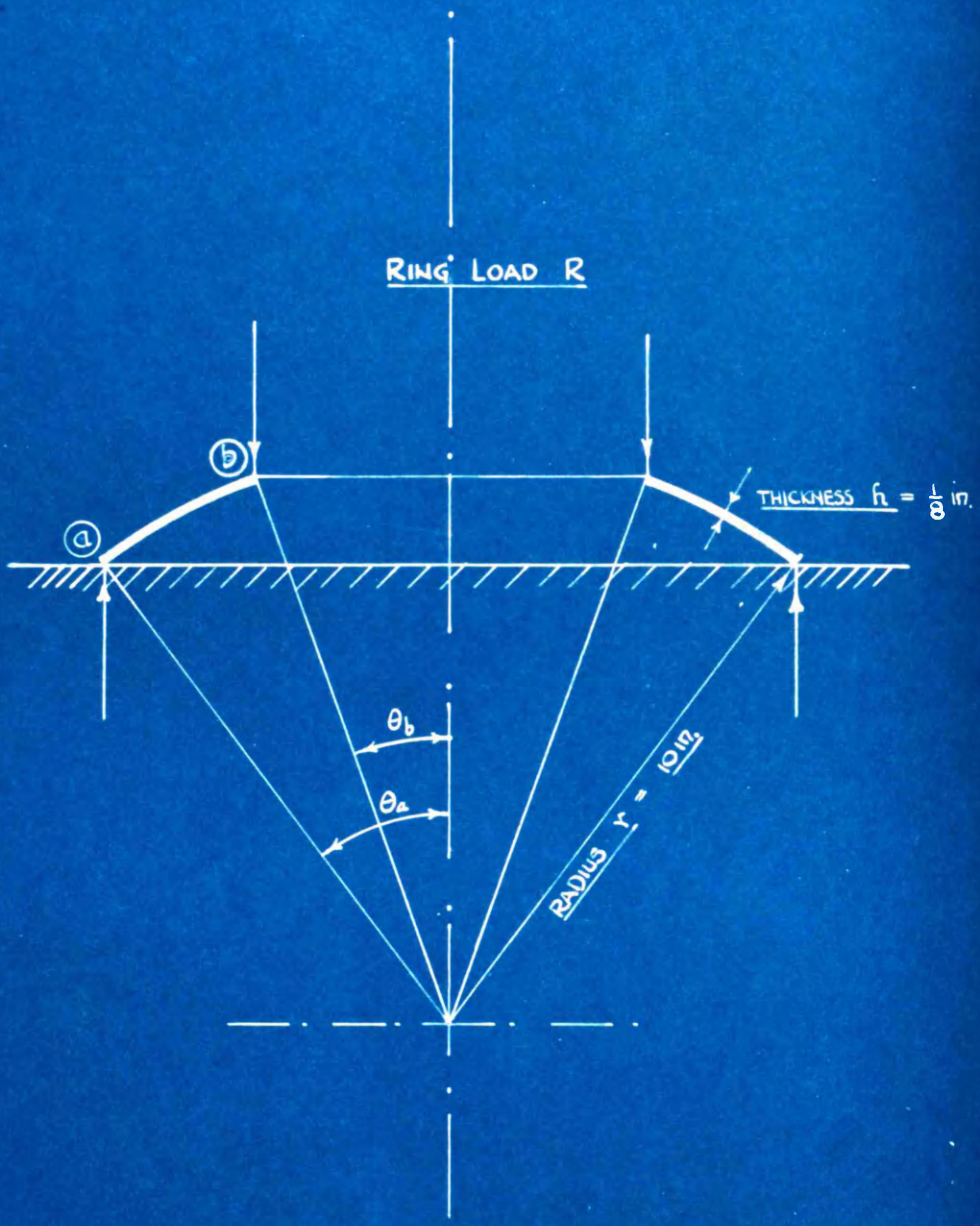

FIG. 24.

Application to Experimental Cases.

(1) Vertical Ring Load on a Spherical Shell: A spherical shell of the form shown in Fig. 24 carries a vertical ring load, R, at edge (b) and is simply supported at edge (a). Frictional effects are assumed to be zero, the surfaces in contact being highly polished. Readings were taken of the relative vertical deflections between the edges, for various loads, by means of an Ames' dial reading to $\frac{1}{1000}$ in. (See Fig.10).

Experimental Observations: The experimental values of the relative deflections, shown in Fig. 25, are plotted on a load base up to value of 0.9 tons.

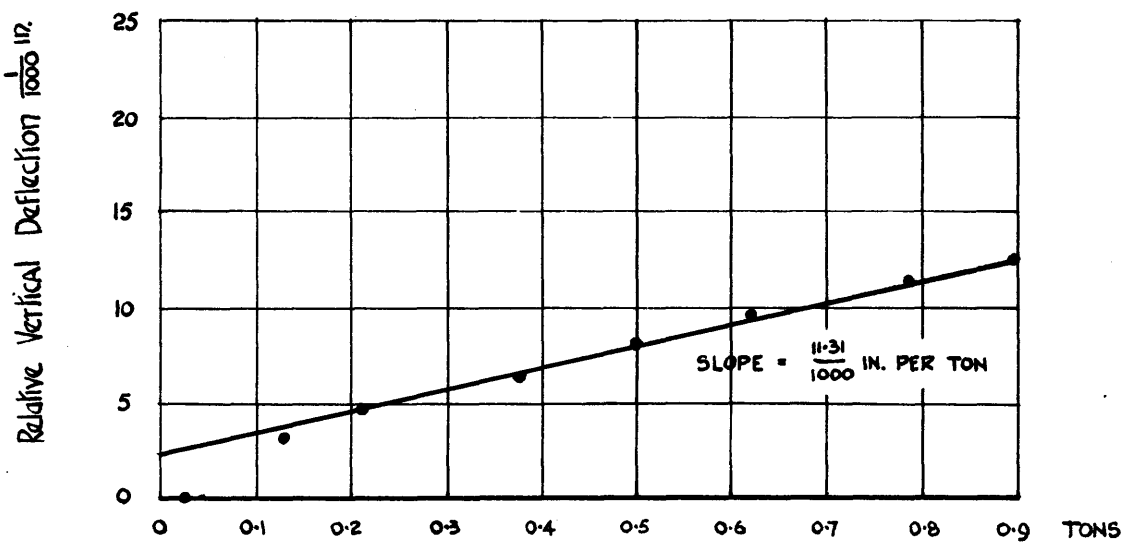

VERTICAL RING LOAD APPLIED AT EDGE.

FIG. 25

The straight line drawn through these points is the slope of the deflection - load graph, giving a value of 11.31 $x \cdot 10^{-3}$ in. per ton load. Zero errors, similar to those for a thin conical wall under the action of a ring load, are observed/

observed.

Analytical Investigation: To determine whether the forces at edge (a) are effective at edge (b), apply the criterion

$$\sqrt{\varepsilon_a/\varepsilon_b} \gtrless e^{\pi}.$$

$h = 0.125$ in., $r = 10$ in., $\therefore \bar{K} = \sqrt[4]{\frac{3(1-\sigma^2)r^2}{h^2}} = 11.47.$

$\theta_a = 36^\circ 54'$, $\theta_b = 19^\circ 43'$, $\therefore (\theta_a - \theta_b) = 0.299$

$\sqrt{m'} = \left(\frac{\sin\theta_b}{\sin\theta_a}\right)^{\frac{1}{2}} = 0.751$, $\therefore \sqrt{\varepsilon_a/\varepsilon_b} = \sqrt{m'} \cdot e^{\bar{K}(\theta_a - \theta_b)} = 23.2$

$e^{n\lambda} = e^{\pi} = 23.17$ $\therefore \sqrt{\varepsilon_a/\varepsilon_b} \fallingdotseq e^{n\lambda}.$

which means that it is permissible to assume that the forces at edge (a) have a negligible effect at edge (b) and vice-versa. It also allows the constants H and K to be determined independently of the constants H' and K'.

As there is no surface loading, the extensional equations for this example are:-

$$p = \frac{E}{2r(1+\sigma)} \cdot \frac{a_1}{\sin^2\theta} \quad \ldots\ldots\ldots (1_1)$$

$$f = -\frac{E}{2r(1+\sigma)} \cdot \frac{a_1}{\sin^2\theta} \quad \ldots\ldots\ldots (2_1)$$

$$u = -b_1\cos\theta - \frac{a_1}{2}\left(1 + \cos\theta \log_e \tan\frac{\theta}{2}\right) \quad \ldots\ldots (3_1)$$

$$z = b_1\sin\theta - \frac{a_1}{2}\left(\cot\theta - \sin\theta \log_e \tan\frac{\theta}{2}\right) \quad \ldots\ldots (4_1)$$

The equations $(1_1 - 4_1)$ are, of course, to be combined with the edge effect equations.

At edge (a) the conditions are:-

$$(I)\ p_a = -\frac{R\sin\theta_a}{2\pi hr\sin\theta_a};\ (II)\ p'_a = 0;\ (III)\ s_a = -\frac{R\cos\theta_a}{2\pi hr\sin\theta_a};\ (IV)\ u_a\cos\theta_a = z_a\sin\theta_a$$

where R is the total vertical load.

$$\therefore (I) \quad -\frac{R}{2\pi hr} = \frac{E}{2r(1+\sigma)} \cdot \frac{a_1}{\sin^2\theta} - s_a\cot\theta_a \quad \ldots (5_1) \qquad \therefore a_1 = -\frac{R(1+\sigma)}{\pi hE} \quad \ldots (6_1)$$

$$\therefore (II) \quad 0 = \sqrt{\varepsilon_a}\left[(c_aK + H)q_a + (c_aH - K)b_a\right] \quad \ldots (7_1) \qquad \therefore K = -H\left(\frac{q_a + c_ab_a}{c_aq_a - b_a}\right) \ldots (8_1)$$

$$\therefore (III) \quad -\frac{R\cos\theta_a}{2\pi hr\sin\theta_a} = -\frac{\nu}{6}\sqrt{\frac{h}{r}}\left[\sqrt{\varepsilon_a}\left(2Hq_a - 2Kb_a\right)\right] \ldots (9_1) \quad \text{and substituting for K}$$

$$\sqrt{\varepsilon_a}\cdot H = \frac{R\cos\theta_a}{2\pi hr\sin\theta_a} \cdot \frac{3}{\nu} \cdot \sqrt{\frac{r}{h}} \cdot \frac{c_aq_a - b_a}{c_a} \quad \ldots\ldots\ldots (10_1)$$

$$\sqrt{\varepsilon_a}\cdot K = -\frac{R\cos\theta_a}{2\pi hr\sin\theta_a} \cdot \frac{3}{\nu} \cdot \sqrt{\frac{r}{h}} \cdot \frac{q_a + c_ab_a}{c_a} \quad \ldots\ldots\ldots (11_1)$$

Substituting these values in (42):-

$$u_a\left[\text{edge effect}\right] = \frac{r\nu^2}{6E} \cdot \sqrt{\varepsilon_a}\left[(2q_aH - 2K)q_a + (-2q_aK - 2H)b_a\right] \quad \ldots (12_1)$$

$$= \frac{R\cot\theta_a}{2\pi hE} \cdot \nu \cdot \sqrt{\frac{r}{h}}\left[\frac{c_aq_a + 1}{c_a}\right] \quad \ldots (13_1)$$

(IV)/

(IV) $\quad U_a \cos\theta_a = Z \sin\theta_a$

$$\therefore \frac{R\cot\theta_a \cdot \cos\theta_a}{2\pi hE} \cdot \nu \cdot \sqrt{\frac{r}{h}}\left[\frac{c_a q_a + 1}{c_a}\right] - b_1\cos^2\theta_a - \frac{a_1}{2}\left(\cos\theta_a + \cos^2\theta_a \log_e \tan\frac{\theta_a}{2}\right)$$

$$= b_1 \sin^2\theta_a - \frac{a_1}{2}\left(\cos\theta_a - \sin^2\theta_a \cdot \log_e \tan\frac{\theta_a}{2}\right) + \frac{r(1+\sigma)}{E} \cdot S_a \sin\theta_a \quad \ldots\ldots(14_1)$$

from which

$$b_1 = \frac{R(1+\sigma)}{2\pi hE}\left[\log_e \tan\frac{\theta_a}{2} + \cos\theta_a + \frac{\nu}{1+\sigma} \cdot \frac{\cos^2\theta_a}{\sin\theta_a}\sqrt{\frac{r}{h}}\left(\frac{c_a q_a + 1}{c_a}\right)\right] \quad \ldots(15_1)$$

Evaluating for the constants a_1 and b_1:-

$$a_1 = -\frac{0.286R}{10^3}\ ; \qquad b_1 = \frac{2.77R}{10^3}\ .$$

$$\therefore u_a = \frac{rv^2}{6E}\sqrt{\varepsilon_a}\left[\left(2q_aH - 2K\right)q_a + \left(-2q_aK - 2H\right)b_a\right] - b_1\cos\theta_a - \frac{a_1}{2}\left(1 + \cos\theta \log_e \tan\frac{\theta_a}{2}\right)$$

$$= + \frac{1.313R}{10^3}. \qquad \ldots\ldots(16_1)$$

$\therefore$ Relative vertical deflection between edges (a) and (b), due to the forces at (a) $= u_a \cos\theta_a = \frac{1.05}{10^3} R.$ $\qquad \ldots\ldots\ldots(17_1)$

<u>At edge (b)</u> the conditions are:-

(1) $p_b = -\frac{R\sin\theta_b}{2\pi hr\sin\theta_b}$; (11) $p_b' = 0$; (111) $s_b = -\frac{R\cos\theta_b}{2\pi hr\sin\theta_b}$.

(1) This gives as for conditions at edge (a), $a_1 = -\frac{R(1+\sigma)}{\pi hE}$

(11) and (111) give H' and K' in terms of R and hence the radial deflection is found from:-

$$U_b = \frac{rv^2}{6E} \cdot \frac{1}{\sqrt{\varepsilon_b}}\left[\left(2q_b'H' + 2K'\right)q_b + \left(-2q_b'K' + 2H'\right)b_b\right] - b_1\cos\theta_b - \frac{a_1}{2}\left(1 + \cos\theta_b \log_e \tan\frac{\theta_b}{2}\right)$$

$$= -\frac{9.61R}{10^3} \qquad \ldots\ldots(18_1)$$

$\therefore$ Vertical deflection $= U_b \cos\theta_b = -\frac{9.05R}{10^3}$ $\qquad \ldots\ldots(19_1)$

$$Z_b = b_1 \sin\theta_b - \frac{a_1}{2}\left(\cot\theta_b - \sin\theta_b \log_e \tan\frac{\theta_b}{2}\right) + \frac{(1+\sigma)rS_b}{E}$$

$$= \frac{1.79R}{10^3} \qquad \ldots\ldots(20_1)$$

$\therefore$ vertical deflection $= Z_b \sin\theta_b = \frac{0.605R}{10^3}$ $\qquad \ldots\ldots(21_1)$

Total relative vertical deflection between edges (a) and (b)

$$= U_a \cos\theta_a - U_b \cos\theta_b + Z_b \sin\theta_b.$$

$$= (1.05 + 9.61 + .605)\ R/10^3 \text{ in.}$$

$$= \frac{11.265}{10^3} R \text{ in.}$$

$$= 11.265/10^3 \text{ in. per ton.} \qquad \ldots\ldots (22.)$$

Experimental value $= 11.31/10^3$ in. per ton.

The bending stress due to the forces at edge (a) is given by:-

$$p' = \sqrt{\xi}\left[(cK+H)q + (cH-K)b\right]$$

$$= \frac{3R}{2\pi h r v}\cdot\sqrt{\frac{r}{h}}\cdot \cot\theta_a \sqrt{\frac{\xi}{\xi_a}}\left[-\left(c+\frac{1}{c_a}\right)\sin(\phi_a-\phi) + \left(1-\frac{c}{c_a}\right)\cos(\phi_a-\phi)\right] \quad \ldots\ldots (23.)$$

For the evaluation of the bending stress at various sections the following tabular scheme is drawn up:-

$$\bar{K} = \sqrt[4]{\frac{3(1-\sigma^2)r^2}{h^2}} = 11.47\ ; \quad \sqrt{\xi} = e^{\bar{K}\theta}/(\sin\theta)^{\frac{1}{2}}\ ; \quad \phi = (\bar{K}+\tfrac{1}{2})\theta\ ;$$

$$C = \left\{1 - (\tfrac{1}{2}-\sigma)\cdot\frac{\cot\theta}{\bar{K}}\right\}.$$

θ°	θ	$\bar{K}\theta$	$\bar{K}(\theta-\theta_a)$	$e^{\bar{K}(\theta-\theta_a)}$	$(\bar{K}+\frac{1}{2})\theta$	$\phi_a-\phi$	$\sin(\phi_a-\phi)$	$\cos(\phi_a-\phi)$	$c+\frac{1}{c_a}$	$1-\frac{c}{c_a}$	$\left(\frac{\sin\theta_a}{\sin\theta}\right)^{\frac{1}{2}}$	p' tons/in.^{2}
$36^\circ 52^1$	.644	7.48	0	1	7.79	0	0	1	1.999	0	1	0
33	.576	6.69	- .79	.454	6.97	47°	.731	.682	1.995	.005	1.005	- 2.48
30	.524	5.09	-1.39	.249	6.34	83°	.993	.122	1.992	.006	1.095	- 1.93
27	.471	5.47	-2.01	.134	5.7	60.5°	.87	-.492	1.988	.01	1.15.	- .951
24	.419	4.86	-2.62	.073	5.07	24°	.407	-.913	1.983	.015	1.215	- .257
21	.366	4.25	-3.23	.039	4.43	12.5°	-.216	-.976	1.977	.022	1.29	+ .077
$19^\circ 43^1$	.34	3.95	-3.53	.029	4.11	31°	-.515	-.857	1.973	.025	1.34	+ .142

The bending stress due to the forces at edge (b) is given by:-

$$p' = \frac{1}{\sqrt{\xi}}\left[\left(-c'K'+H'\right)q + \left(-c'H'-K'\right)b\right]$$

$$= \frac{3R}{2\pi h r v}\sqrt{\frac{r}{h}}\cdot\cot\theta_b\sqrt{\frac{\xi_b}{\xi}}\left[\left(c'+\frac{1}{c_b'}\right)\sin(\phi-\phi_b) - \left(1-\frac{c'}{c_b'}\right)\cos(\phi-\phi_b)\right] \quad \ldots\ldots (24.)$$

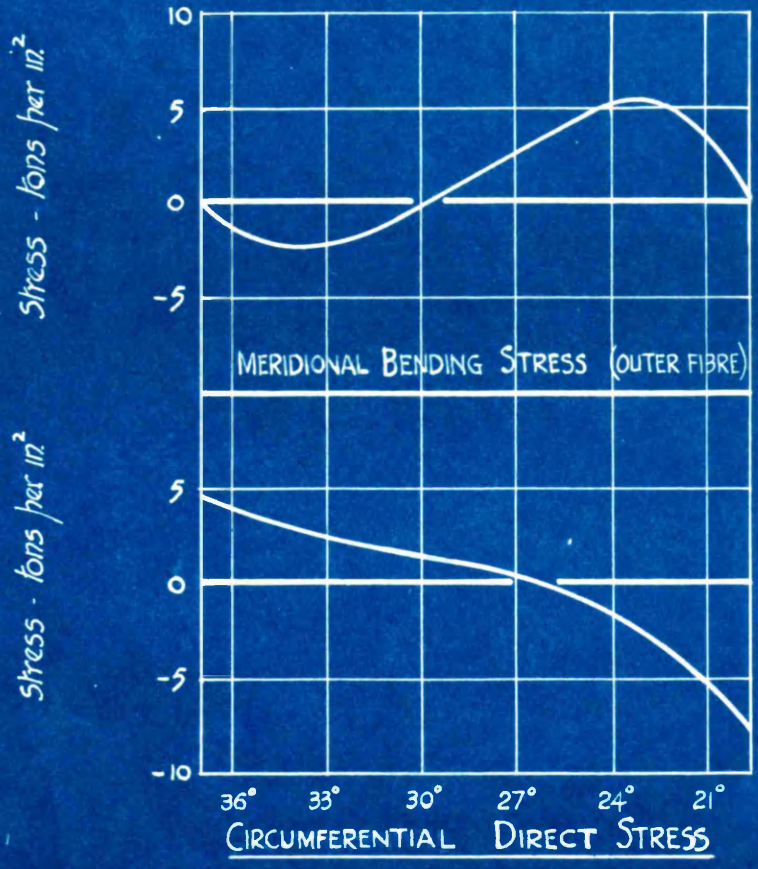
Stress - tons per in.²
10
5
0
-5
MERIDIONAL BENDING STRESS (OUTER FIBRE)
Stress - tons per in.²
5
0
-5
-10
36°
33°
30°
27°
24°
21°
CIRCUMFERENTIAL DIRECT STRESS

FIG. 26.

A table similar to that for the forces at edge (a) may be drawn up and the effects added.

θ	Edge (b) p'	Edge (a) p'	Total p' $\frac{\text{tons}}{\text{in}^2}$
36°52'	- .302	0	- .302
35°	- .121	- 1.89	- 2.011
33°	+ .332	- 2.48	- 2.148
30°	+ 1.705	- 1.93	- .225
27°	+ 3.86	- .951	+ 2.909
24°	+ 5.5	- .257	+ 5.243
21°	+ 3.56	+ .0768	+ 3.637
19°43'	0	+ .142	+ .142

Actually at θ = 36°52' and 19°43', p' should be zero. The error involved is due to method of evaluating the constants, and shows it to be reasonably accurate when $\sqrt{\varepsilon_a/\varepsilon_b} = e^{\pi}$.

The circumferential stress $f = -\frac{E}{2r(1+\sigma)} \cdot \frac{a_1}{\sin^2\theta} + \frac{E}{r} \cdot u$ (edge effect).

The radial deflection u may be expressed:-

$$u \text{ (edge effect)} = \frac{rv^2}{6E} 2\sqrt{\xi}\left[H(gq-b) - K(q-gb)\right] + \frac{rv^2}{6E} \cdot 2\frac{1}{\sqrt{\xi}}\left[H'(g'q+b) + K'(q-g'b)\right] \quad \cdots\cdots (25.)$$

Neglecting small terms such as $(c_a - g)\sin(\phi_b - \phi)$, where $(c_a - g) \neq$ zero, the circumferential direct stress is given by:-

$$f = \frac{R}{2\pi hr\sin^2\theta} + \frac{vR}{\pi hr} \cdot \sqrt{\frac{r}{h}}\left[\cot\theta_a\sqrt{\frac{\xi}{\varepsilon_a}} \cdot \cos(\phi_a - \phi) - \cot\theta_b\sqrt{\frac{\xi_b}{\xi}}\cos(\phi - \phi_b)\right] \quad \cdots\cdots (26.)$$

A tabular scheme similar to that for radial bending stresses is necessary for evaluation. The circumferential direct and radial bending stresses for the whole wall are shown in Fig.26 for R = 1 ton. A test piece of the material gave the modulus E = 11,600 tons per in^2.

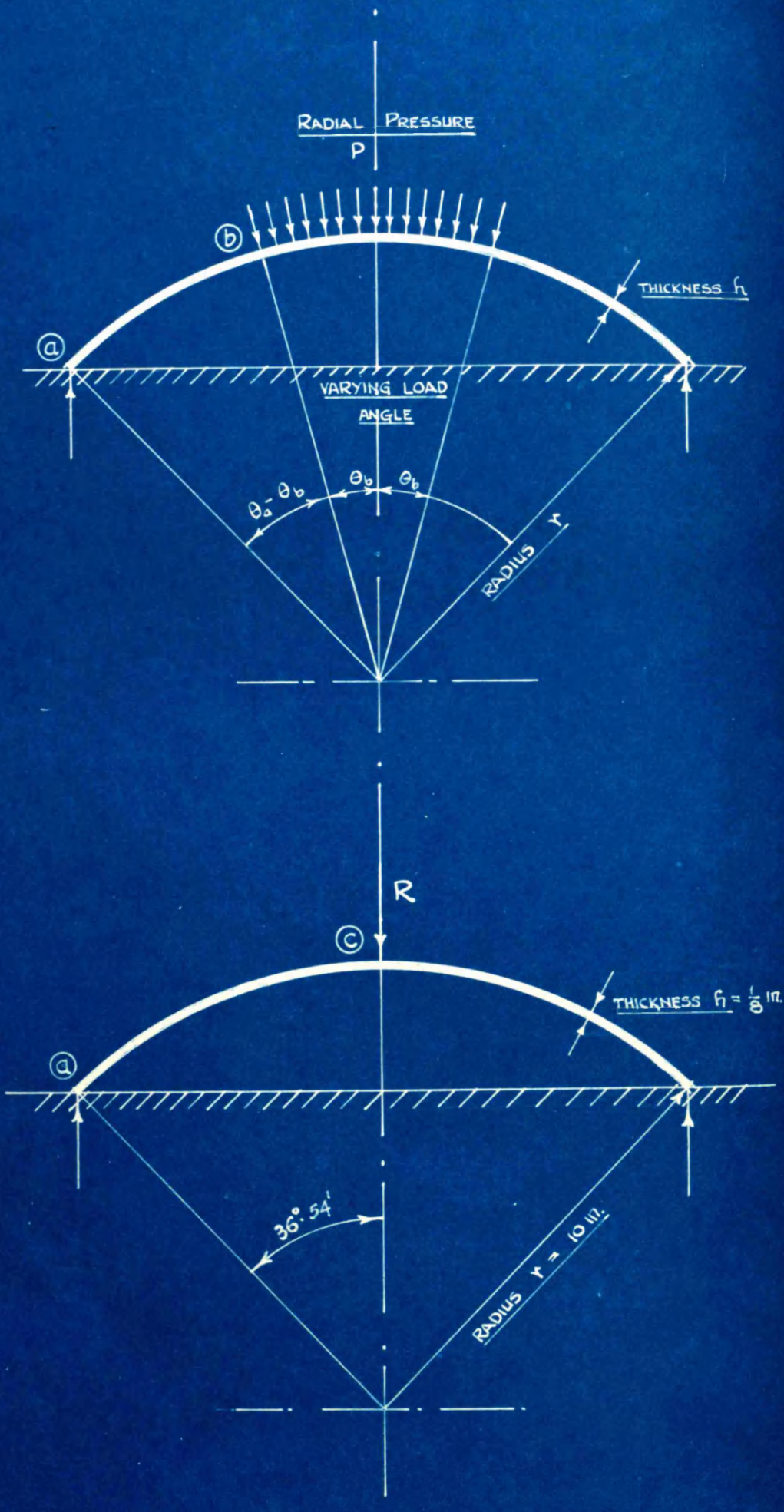
RADIAL PRESSURE
P
b
THICKNESS h
a
VARYING LOAD
ANGLE
θa - θb
θb
θb
RADIUS r
R
c
THICKNESS h = 1/8 in.
a
36° 54'
RADIUS r = 10 in.

FIG. 27.

Application to Experimental Cases.

(11) Vertical Concentrated Load applied at the crown of a Spherical Shell: A vertical load R is applied at the crown (c) of a spherical shell which is simply supported at the edge (a). The relative vertical deflection between the crown and the edge (a) for different loads were obtained by means of an Ames' dial.

Experimental Observations: The experimental values of the relative deflections, shown in Fig. 28, are plotted on a load base up to the value of 0.7 tons.

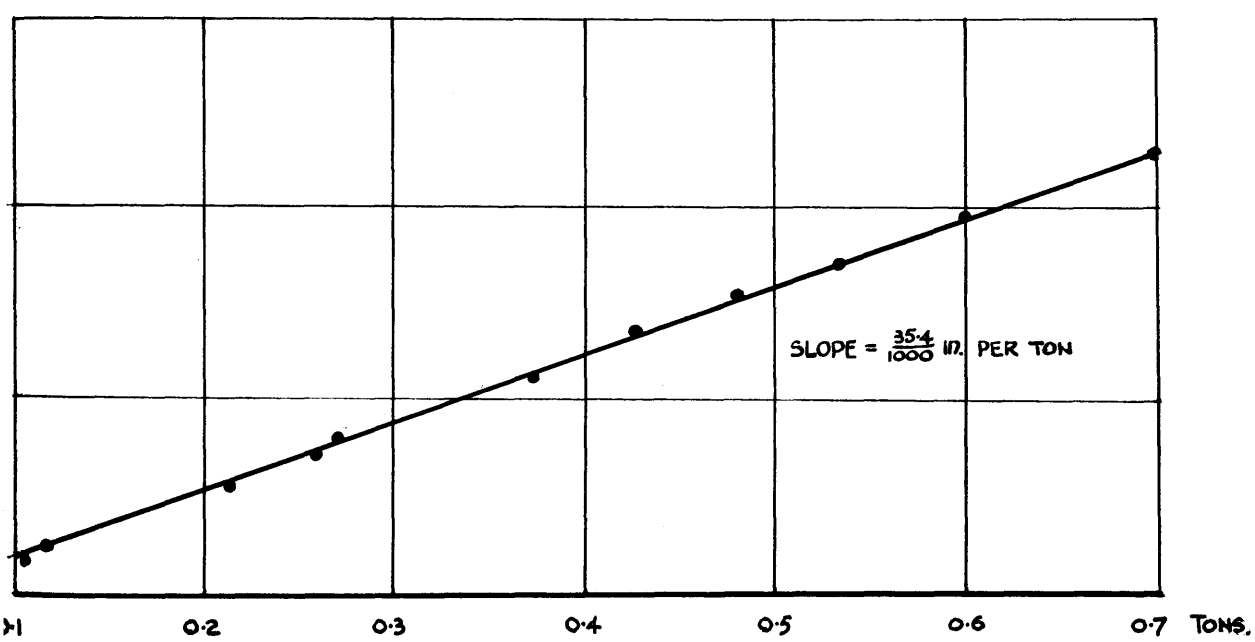

RELATIVE VERTICAL DEFLECTION BETWEEN LOAD POINT (C) AND EDGE (a)

FIG. 28.

The straight line drawn through these points is the slope of the deflection load graph, giving a value of 35.4×10^{-3} in. per ton load.

Analytical Investigation: Consider part of a thin spherical shell subject to the action of a radial pressure P. The load

area/

area is symmetrical about the crown and subtends an angle $2\theta_b$ at the centre of the sphere (Fig.27). The dome is simply supported at edge (a). It is required to find the radial deflection at edge (b). The length of the meridian (a b) is such that the conditions at (a) do not affect the distortions and stresses at (b). The dome is of uniform thickness, h, and radius r.

The conditions at edge (a) are:-

(I) $p_a = -\frac{R\sin\theta_a}{2\pi rh\sin\theta_a}$; (II) $s_a = -\frac{R\cos\theta_a}{2\pi rh\sin\theta_a}$; (III) $p'_a = 0$; (IV) $z\sin\theta_a = u\cos\theta_a$

where $R = \pi r^2\sin^2\theta_b \cdot P$ = total vertical force

from (I), $-\frac{R\sin\theta_a}{2\pi rh\sin\theta_a} = \frac{E}{2r(1+\sigma)}\cdot\frac{a_1}{\sin^2\theta_a} - s\cot\theta_a$ .... (1_2) $\quad\therefore a_1 = -\frac{(1+\sigma)R}{\pi hE}$ ...(2_2)

from (II), $s_a = -\frac{\nu}{6}\sqrt{\frac{E}{r}}\left[\sqrt{\Sigma_a}\left(2Hq_a - 2Kb_a\right)\right]$

from (III), $0 = \sqrt{\Sigma_a}\left[(c_aK+H)q_a + (c_aH-K)b_a\right]$ $\Big\}$ ...(3_2)

$\therefore$ from (3_2)

$$H\sqrt{\Sigma_a} = -\frac{6s_a}{2\nu\sqrt{h/r}}\cdot\frac{c_aq_a - b_a}{c_a} \quad \text{.....}(4_2)$$

$$K\sqrt{\Sigma_a} = +\frac{6s_a}{2\nu\sqrt{h/r}}\cdot\frac{c_ab_a + q_a}{c_a} \quad \text{.....}(5_2)$$

$$\therefore\ u_a[\text{edge effect}] = \frac{r\nu^2}{6E}\sqrt{\Sigma_a}\left[2(q_aH-K)q_a - 2(q_aK+H)b_a\right]$$

$$= -\frac{r\nu s_a}{E\sqrt{h/r}}\cdot\frac{c_aq_a+1}{c_a} \quad \text{.....}(6_2)$$

from (IV), $z\sin\theta_a = u\cos\theta_a$

$$\therefore \left\{b_1\sin\theta_a - \frac{a_1}{2}\left(\cot\theta_a - \sin\theta_a\log_e\tan\frac{\theta_a}{2}\right) + \frac{r(1+\sigma)}{E}\cdot s_a\right\}\sin\theta_a$$

$$= \left\{-\frac{r\nu s_a}{E\sqrt{h/r}}\cdot\frac{c_aq_a+1}{c_a} - b_1\cos\theta_a - \frac{a_1}{2}\left(1+\cos\theta_a\log_e\tan\frac{\theta_a}{2}\right)\right\}\cos\theta_a \quad (7_2)$$

$$\therefore b_1 = \frac{R(1+\sigma)}{2\pi hE}\left\{\cos\theta_a + \log_e\tan\frac{\theta_a}{2} + \frac{\cos^2\theta_a}{\sin\theta_a}\cdot\frac{q_ac_a+1}{c_a(1+\sigma)}\cdot\frac{\nu}{\sqrt{h/r}}\right\} \quad \text{.....}(8_2)$$

The conditions at edge (b) give:-

$$p' = p'_b, \qquad s = s_b.$$

The following constants are then obtained in terms of p'_b and s_b. For the lower part of the shell:-

$$\left.\begin{aligned}\frac{1}{\sqrt{\Sigma_b}}\cdot H' &= \frac{6s_b}{2\nu\sqrt{h/r}}\cdot\frac{b_b + c'_bq_b}{c'_b} - p'_b\cdot\frac{b_b}{c'_b}\\ \frac{1}{\sqrt{\Sigma_b}}\cdot K' &= \frac{6s_b}{2\nu\sqrt{h/r}}\cdot\frac{q_b - c'_bb_b}{c'_b} - p'_b\cdot\frac{q_b}{c_b}\end{aligned}\right\} \quad \text{.....}(9_2)$$

For/

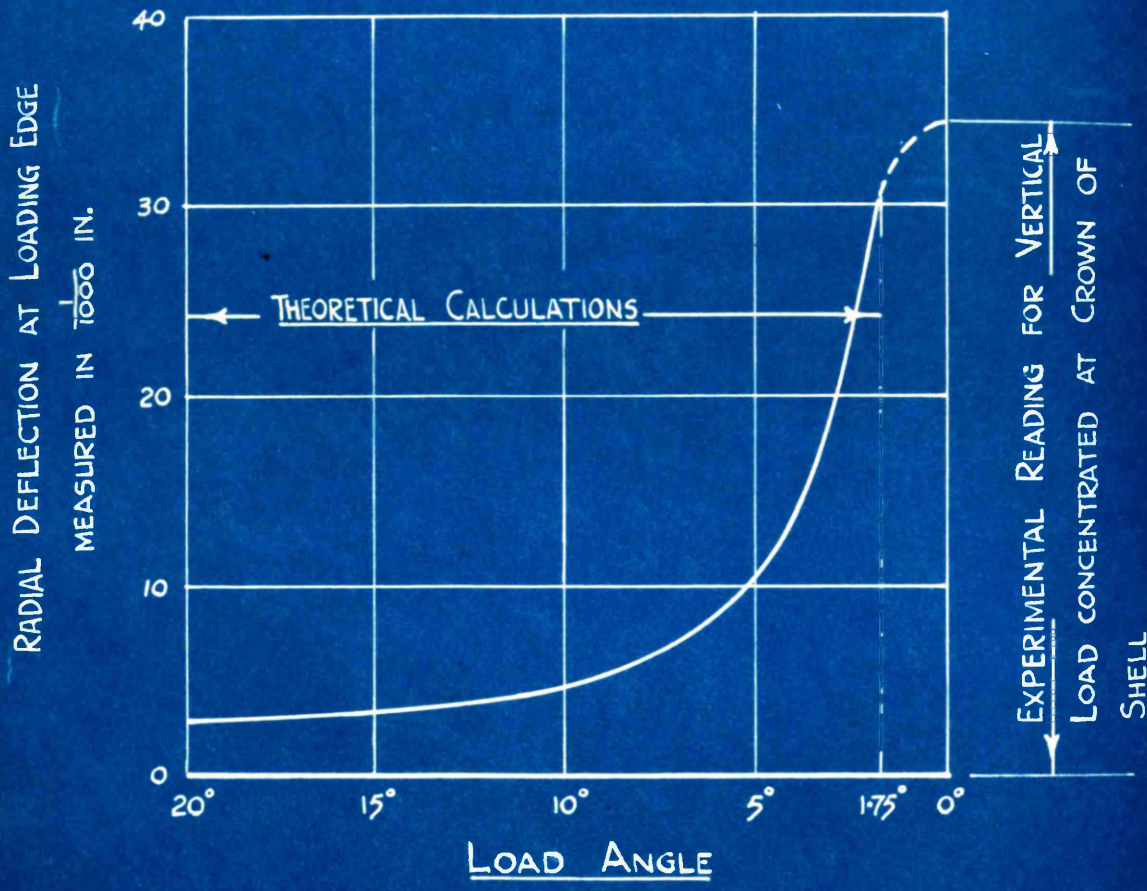
RADIAL DEFLECTION AT LOADING EDGE
MEASURED IN 1/1000 IN.
40
30
20
10
0
THEORETICAL CALCULATIONS
EXPERIMENTAL READING FOR VERTICAL
LOAD CONCENTRATED AT CROWN OF
SHELL
20°
15°
10°
5°
1·75°
0°
LOAD ANGLE

FIG. 29.

For the upper portion of the shell:-

$$\left.\begin{aligned} H\sqrt{\varepsilon_b} &= -\frac{6s_b}{2v\sqrt{h/r}}\cdot\frac{c_b q_b - b_b}{c_b} + p'_b\cdot\frac{b_b}{c_b} \\ K\sqrt{\varepsilon_b} &= +\frac{6s_b}{2v\sqrt{h/r}}\cdot\frac{q_b + c_b b_b}{c_b} + p'_b\cdot\frac{q_b}{c_b} \end{aligned}\right\} \quad \ldots\ldots (10_2)$$

The tangential displacement, Z, at (b) for the upper and lower walls of the dome are equal.

$$\therefore \quad b_2\sin\theta_b - \frac{a_2}{2}(\cot\theta_b - \sin\theta_b \log_e\tan\tfrac{\theta_b}{2}) + \frac{r(1+\sigma)}{E}\cdot s_b$$

$$= b_1\sin\theta_b - \frac{a_1}{2}(\cot\theta_b - \sin\theta_b\log_e\tan\tfrac{\theta_b}{2}) + \frac{r(1+\sigma)}{E}s_b \quad \ldots\ldots (11_2)$$

But the upper wall, being continuous, $a_2 = 0$

$$\therefore (b_2 - b_1)\cos\theta_b = \frac{R(1+\sigma)}{2\pi hE}\left\{\cot^2\theta_b - \cos\theta_b\log_e\tan\tfrac{\theta_b}{2}\right\} \quad \ldots\ldots (12_2)$$

Equating the change of slope, i, at (b)

$$-\frac{v^3}{6E}\sqrt{\frac{r}{h}}\left\{\sqrt{\varepsilon_b}\left(-4Kq_b - 4Hb_b\right)\right\} = -\frac{v^3}{6E}\sqrt{\frac{r}{h}}\left\{\frac{1}{\sqrt{\varepsilon_b}}\left(-4K'q_b - 4H'b_b\right)\right\} \quad \ldots\ldots (13_2)$$

from which

$$p'_b = \frac{6s_b}{2v\sqrt{h/r}}\left\{\frac{c_b - c'_b}{2}\right\}. \quad \ldots\ldots (14_2)$$

Equating the radial deflections, u, at edge (b) there is obtained:-

$$\frac{rv^2}{6E}\left[\sqrt{\varepsilon_b}\left\{2(g_bH - K)q_b - 2(g_bK + H)b_b\right\}\right] - b_2\cos\theta_b - \frac{(1-\sigma)}{2hE}\cdot Pr^2$$

$$= \frac{rv^2}{6E}\left[\frac{1}{\sqrt{\varepsilon_b}}\left\{2(g'_bH' + K')q_b - 2(g'K' - H')b_b\right\}\right] - b_1\cos\theta_b - \frac{a_1}{2}\left(1 + \cos\theta_b\log_e\tan\tfrac{\theta_b}{2}\right) \quad (15_2)$$

from which

$$s_b = -\frac{R\,\mathrm{cosec}^2\theta_b}{4\pi vr\sqrt{h/r}}. \quad \ldots\ldots (16_2)$$

The radial deflection, u, at edge (b) may now be obtained from

$$u_b = \frac{rv^2}{6E}\left[\frac{1}{\sqrt{\varepsilon_b}}\left(2(g'_bH' + K')q_b - 2(g'_bK' - H')b_b\right\}\right] - b_1\cos\theta_b - \frac{a_1}{2}(1 + \cos\theta_b\log_e\tan\tfrac{\theta_b}{2})$$

$$= -\frac{R\,\mathrm{cosec}^2\theta_b}{8\pi hE}\left\{1 + g'_b\right\} - b_1\cos\theta_b - \frac{a_1}{2}(1 + \cos\theta_b\log_e\tan\tfrac{\theta_b}{2}) \quad \ldots\ldots (17_2)$$

Keeping a constant vertical force R = 1 ton, the values of U_b are shown in Fig. 29 plotted on a base of the load angle θ_b varying from 20° to 1.75°. Beyond the latter value, $\{1 + g'_b\}$ is negative and the values for U_b become meaningless due to approximate solution of equations (27).

The experimental value obtained for the relative vertical/

vertical deflection between the crown and edge (a) for a vertical load R applied at the crown was $\frac{35.4}{1000}$in. per ton. The contribution to this value from the movement at edge (a) is obtained from:-

$$u_a \cos\theta_a = \left\{\frac{rv^2}{bE}\sqrt{\xi_a}\left[2(g_a H - K)q_a - 2(g_a K + H)b_a\right] - b_1\cos\theta_a - \frac{a_1}{2}\left(1+\cos\theta_a \log_e \tan\frac{\theta_a}{2}\right)\right\}\cos\theta_a$$

$$= \frac{1.05}{1000}\text{in. per ton load.}$$

Therefore the vertical deflection of the crown is:-

$$\left(\frac{35.4}{1000} - \frac{1.05}{1000}\right)\text{in. per ton load} = \frac{34.35}{1000}\text{in.}$$

Plotting this value on the graph in Fig. 29 it would appear that a reasonable continuation of the graph for calculated values is obtained.

This experiment shows the importance of the coefficients c, c', g and g' attached to the constants. Their influence on any result depends on the ratio $\cot\theta/2\bar{K}$ compared with unity. As $\bar{K}$ is usually large it will be sufficiently accurate in most practical cases to put $c = c' = g = g' = 1$ for values of $\theta > 30^\circ$.

Similar coefficients are attached to the constants in the equations for the conical walls when the distance, x, measured along the wall from the apex is small. The occasion for which these should be introduced is not practical and they have been entirely omitted, but mention is made here in order to complete the similarity between the conical and spherical walls.

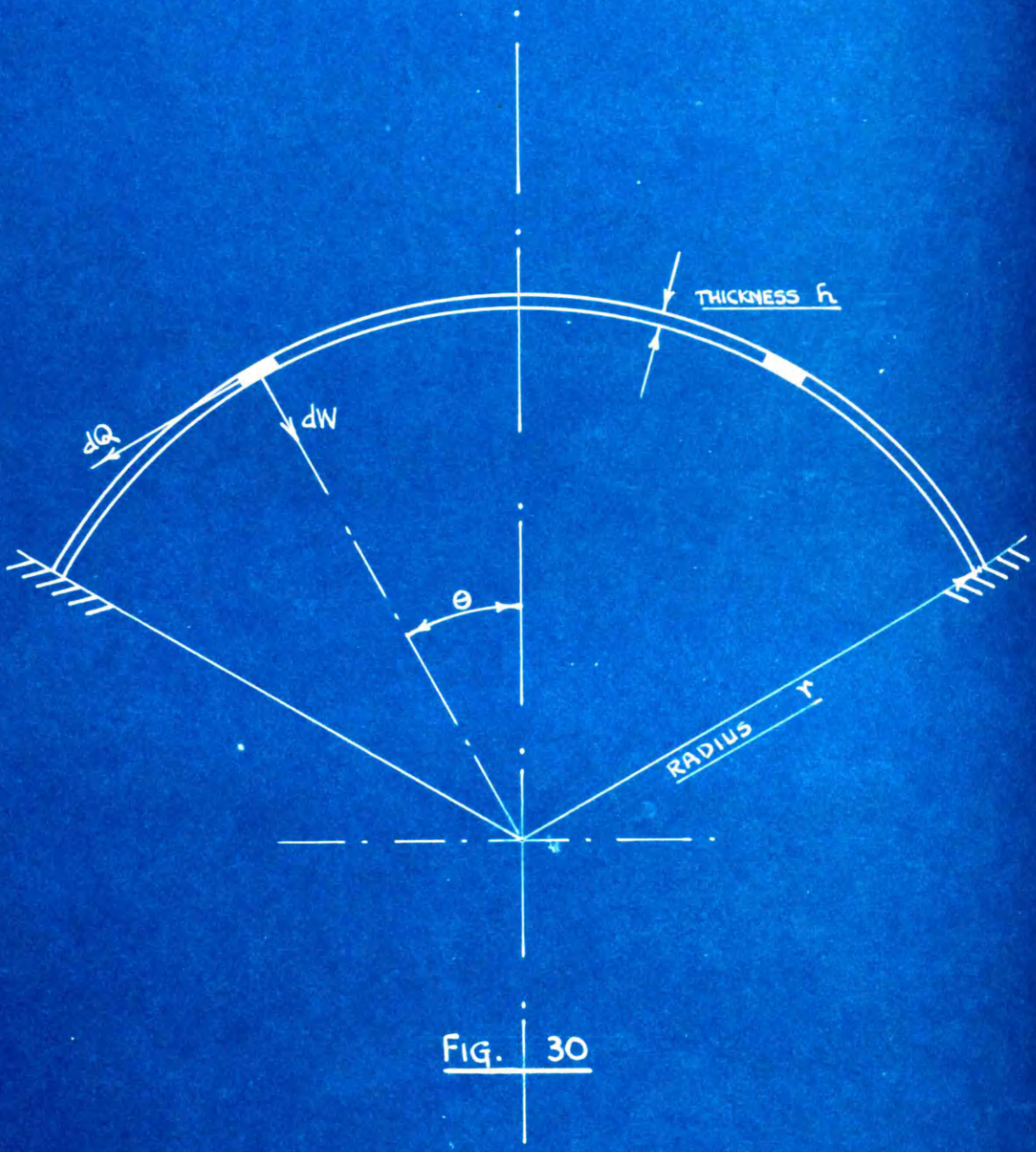

FIG. 30

Investigation of Dome Weight Effect on the meridional bending and circumferential direct stresses. Fig. 30 shows part of a segmental dome rigidly fixed at the base, having a uniform thickness, h, and radius r. dW and dQ represent the radial and tangential forces due to the weight of a complete annular element.

The extensional equations. From the general equations, the tangential displacement is given by (13)

$$Z = b_1 \sin\theta - \frac{a_1}{2}(\cot\theta - \sin\theta \log_e \tan\tfrac{\theta}{2}) + \frac{1+\sigma}{2\pi r h E} \sin\theta \int \operatorname{cosec}^3\theta \left[\int \sin\theta \left(\cot\theta \frac{dW}{d\theta} - 2\frac{dQ}{d\theta} - \frac{d^2W}{d\theta^2} \right) d\theta \right] d\theta \quad \cdots (1_3)$$

Putting in $\frac{dW}{d\theta} = -\pi r^2 h w \sin 2\theta$; $\frac{dQ}{d\theta} = +2\pi r^2 h w \sin^2\theta$

and evaluating

$$Z = b_1 \sin\theta - \frac{a_1}{2}(\cot\theta - \sin\theta \log_e \tan\tfrac{\theta}{2}) - \frac{(1+\sigma) w r^2}{E} \left[\operatorname{cosec}\theta - \sin\theta \log_e \sin\theta \right] \quad \cdots (2_3)$$

To make this finite for Z = o

$$-\frac{a_1}{2} - \frac{(1+\sigma) w r^2}{E} = 0 \qquad \therefore \quad a_1 = -\frac{W(1+\sigma)}{\pi r h E}, \quad \cdots (3_3)$$

Where W is the total weight of the dome.

$$\therefore \quad Z = b_1 \sin\theta - \frac{a_1}{2}\left[\frac{\cos\theta - 1}{\sin\theta} + \sin\theta \log_e (1+\cos\theta) \right] \quad \cdots (4_3)$$

Substituting for Z in (11), (9) and (10) the equations for radial deflection, meridional and circumferential direct stress are obtained. The complete set of extensional equations are then:-

$$\left.\begin{aligned}
p &= \frac{E}{2(1+\sigma)} \cdot \frac{a_1}{2} \cdot \frac{(2+\cos\theta)(1-\cos\theta)}{(1+\cos\theta)} - \frac{wr\cos\theta}{2} \\
f &= -\frac{E}{2(1+\sigma)} \cdot \frac{a_1}{2} \cdot \frac{(2+\cos\theta)(1-\cos\theta)}{(1+\cos\theta)} - \frac{wr\cos\theta}{2} \\
u &= -b_1 \cos\theta - \frac{a_1}{2}\left[1 - \frac{\cos\theta}{2} - \cos\theta \log_e \sqrt{1+\cos\theta} \right] - \frac{(1-\sigma)}{2} \cdot \frac{wr^2\cos\theta}{E} \\
z &= b_1 \sin\theta - \frac{a_1}{2}\left[\frac{\cos\theta - 1}{\sin\theta} + \sin\theta \log_e \sqrt{1+\cos\theta} \right]
\end{aligned}\right\} \quad \cdots (5_3)$$

The equations in group (5_3) combined with the edge effect equations are sufficient to solve the more common problems concerning domes of uniform thickness.

Numerical Example: A semi-spherical dome of uniform thickness

9 in./

9 in. and radius 22 ft. is rigidly fixed at the edge. The important stresses are the meridional bending and circumferential direct stresses near the fixed edge. The solution for these stresses is as follows.

The conditions at the fixed edge, $\theta = \pi/2$, are:-

(I) $\phi = -\frac{W}{2\pi hr}$, (II) $\iota = 0$, (III) $u = 0$, (IV) $z = 0$.

$\therefore$ From (I) $-\frac{W}{2\pi hr} = \frac{E}{2r(1+\sigma)} \cdot \frac{a_1}{2} \cdot \frac{(2+\cos\pi/2)(1-\cos\pi/2)}{(1+\cos\pi/2)} - \frac{\omega r \cos\pi/2}{2} - S\cot\frac{\pi}{2}$ ....(6_3)

$\therefore a_1 = -\frac{W(1+\sigma)}{\pi h E}$ . . . . . (7_3)

$\therefore$ From (III) $-b_1\cos\pi/2 - \frac{a_1}{2}\left(1 - \frac{\cos\pi/2}{2} - \cos\pi/2 \log_e \overline{1+\cos\pi/2}\right) - \frac{(1-\sigma)\omega r^2\cos\pi/2}{2E} + \frac{2rv^2}{6E}\sqrt{\xi_a}\left[(H-K)q_a - (K+H)b_a\right] = 0$ (8_3)

$\therefore$ From (II) $-\frac{v^3}{6E}\sqrt{\frac{r}{h}}\sqrt{\xi_a}\left(-4Kq_a - 4Hb_a\right) = 0$ ....(9_3) $\therefore K = -H\cdot\frac{b_a}{q_a}$ ....(10_3)

$\therefore$ Substituting in (8_3)

$$\left.\begin{aligned} H\sqrt{\xi_a} &= \frac{3Eq_a}{2rv^2}\cdot a_1 \\ \therefore\ K\sqrt{\xi_a} &= -\frac{3Eb_a}{2rv^2}\cdot a_1 \end{aligned}\right\} \ldots\ldots (11_3)$$

$\therefore$ From (IV) $b_1\sin\frac{\pi}{2} - \frac{a_1}{2}\left[\frac{\cos\pi/2 - 1}{\sin\pi/2} + \sin\pi/2\,\log_e\overline{1+\cos\pi/2}\right] + \frac{(1+\sigma)r}{E}\cdot S_a = 0$ ....(12_3)

$$\therefore\ b_1 = \frac{a_1}{2} - \frac{r(1+\sigma)}{E}\cdot S_a \quad \ldots (13_3)$$

$$u\left[\text{edge effect}\right] = \frac{rv^2}{6E}\sqrt{\xi_a}\left[(H-K)q_a - (K+H)b_a\right]$$

$$= -\frac{W(1+\sigma)}{2\pi hE}\left[\sin(\phi_a - \phi) + \cos(\phi_a - \phi)\right]\sqrt{\frac{\xi}{\xi_{\pi/2}}} \quad \ldots\ldots (14_3)$$

The circumferential direct stress is given by:-

$$f = -\frac{E}{2r(1+\sigma)}\cdot\frac{a_1}{2}\cdot\frac{(2+\cos\theta)(1-\cos\theta)}{(1+\cos\theta)} - \frac{\omega r\cos\theta}{2} + \frac{E}{r}\cdot u\left[\text{edge effect}\right]$$

$$= \frac{W}{4\pi hr}\left[\frac{(2+\cos\theta)(1-\cos\theta)}{(1+\cos\theta)} - \cos\theta\right] + \frac{E}{r}\cdot u\left[\text{edge effect}\right]. \quad \ldots\ldots (15_3)$$

The meridional bending stress is given by:-

$$p' = \sqrt{\xi}\left[(K+H)q + (H-K)b\right]$$

$$= \frac{3W(1+\sigma)}{2\pi hrv^2}\left[\sin(\phi_a - \phi) - \cos(\phi_a - \phi)\right]\sqrt{\frac{\xi}{\xi_{\pi/2}}} \quad \ldots\ldots (16_3)$$

where $\sqrt{\xi} = e^{\bar{K}\theta}/(\sin\theta)^{\frac{1}{2}}$, $\phi = (\bar{K}+\frac{1}{2})\theta$ and $\bar{K} = \sqrt[4]{3(1-\sigma^2)}\frac{r^2}{h^2} = 6.96$.

The values of the meridional bending stresses and circumferential direct stresses are shown in Fig. 31. for values of θ from

90/

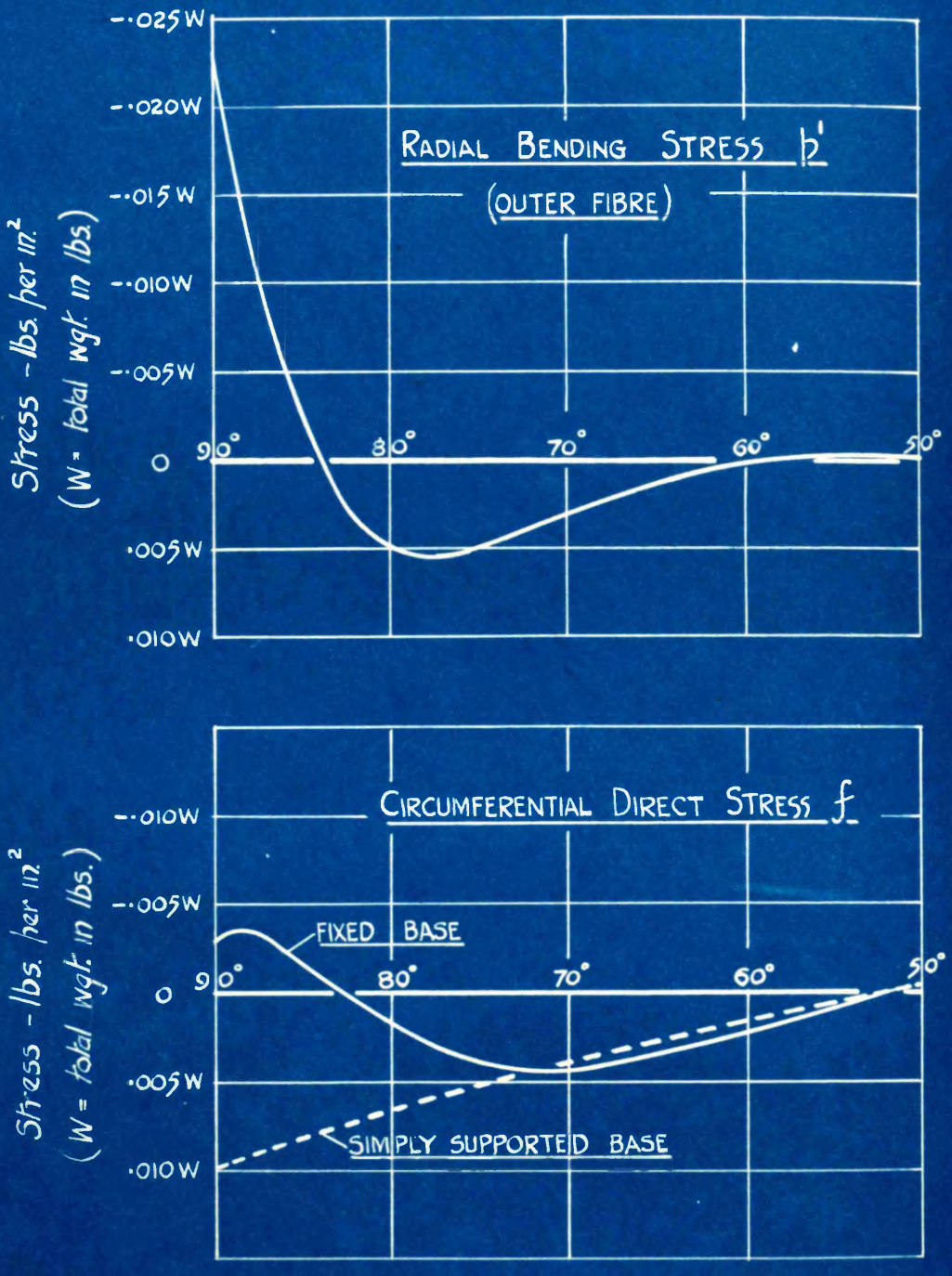
Stress - lbs. per in.²
(W = total wgt. in lbs.)
-·025W
-·020W
-·015W
-·010W
-·005W
0
·005W
·010W
RADIAL BENDING STRESS h'
(OUTER FIBRE)
90°
80°
70°
60°
50°
Stress - lbs. per in.²
(W = total wgt. in lbs.)
-·010W
-·005W
0
·005W
·010W
CIRCUMFERENTIAL DIRECT STRESS f
FIXED BASE
SIMPLY SUPPORTED BASE
90°
80°
70°
60°
50°

FIG. 31.

90^{o} to 50^{o}. The maximum circumferential stress is f + f', where f' = σp'. The value of θ for this maximum is between 70^{o} and 75^{o}, which is normally about the second or third course in a masonry dome. It is interesting to know that this is the zone where vertical cracks appear.

Architects, in their design of domes, usually assume the edge to be freely supported. Under these conditions the bending stress at any section is zero and the circumferential direct stress is given by:-

$$f = \frac{W}{4\pi hr}\left[\frac{(2+\cos\theta)(1-\cos\theta)}{(1+\cos\theta)} - \cos\theta\right] \qquad \ldots\ldots (17_3)$$

The values of f from equation (17_3) are also shown in Fig. 31. for the same range of θ values. When $\theta = 51^{o}- 50'$ f is zero. Contrasting the circumferential stresses for the cases when the dome is rigidly fixed and freely supported, it is observed that the zero values occur at approximately the same section, but the maximum values are neither equal nor do they occur at the same value of θ.

If the conditions at the edge are such that the dome may be taken as simply supported with a horizontal frictional force acting, the maximum circumferential stress at the outer fibre will differ from the circumferential direct stress for the case of a simply supported dome. The difference results from the action of the frictional force giving a meridional bending stress p', from which is obtained the circumferential bending stress f' = σp', a value to be added to f, the direct stress.

When the dome is not continuous and the opening at the crown subtends an angle 2α at the centre, the circumferential direct stress is given by:-

$$f = \frac{W'}{4\pi hr}\left[\frac{(2+\cos\theta)(1-\cos\theta)}{(1+\cos\theta)} - \frac{\cos\theta}{\cos\alpha}\right] \qquad \ldots\ldots\ldots (18_3)$$

where W' represents the total weight of the dome. In the edge effect equations W' replaces W.

<u>Equations for Lantern Effect on a Dome:</u> Fig. 32 shows the lantern/

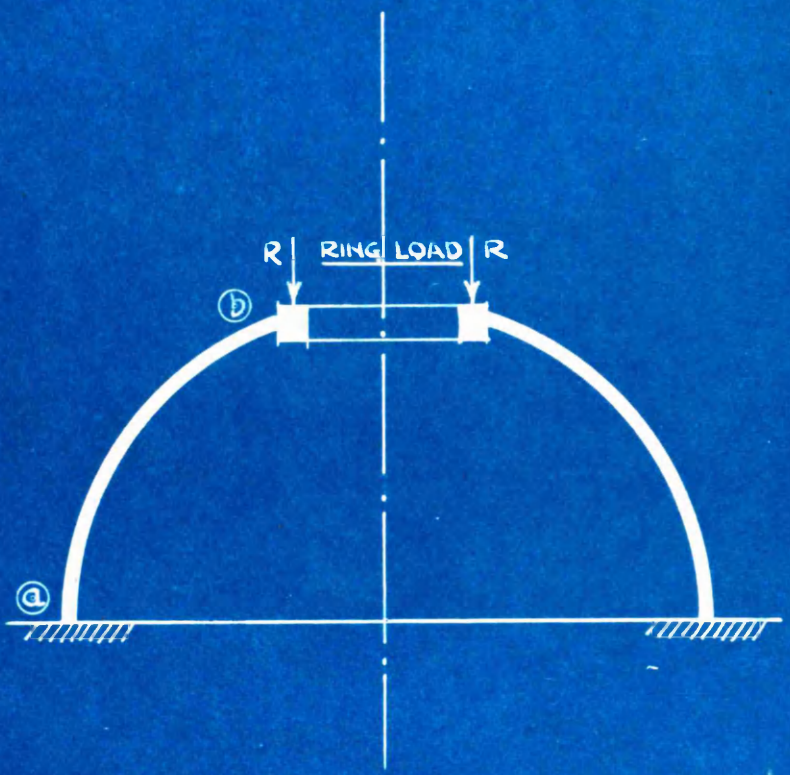

FIG. 32.

lantern represented by a vertical ring load R, supported on a rigid ring at edge (b). Taking a hemispherical dome, rigidly fixed at the base, the stresses induced by R may be obtained and are given below:-

<u>At edge (a)</u>, the conditions are, i = u = z = o.

$$\left.\begin{aligned} \therefore\ p' &= \frac{3R(1+\sigma)}{2\pi h r v^2}\left[\sin(\phi_a-\phi)-\cos(\phi_a-\phi)\right]\sqrt{\frac{\xi}{\xi_a}}\cdot \\ u(\text{edge effect}) &= -\frac{R(1+\sigma)}{2\pi h E}\left[\sin(\phi_a-\phi)+\cos(\phi_a-\phi)\right]\sqrt{\frac{\xi}{\xi_a}}\cdot \\ f &= \frac{R\,\mathrm{cosec}^2\theta}{2\pi h r}+\frac{E}{r}\cdot u\left[\text{edge effect}\right]. \end{aligned}\right\}\quad\ldots\ldots(19_3)$$

<u>At edge (b)</u>, the conditions are, i = o, z cos α = - u sin α .

$$\left.\begin{aligned} \therefore\ p' &= -\frac{3R(1+\sigma)}{2\pi h r v^2 B}\left[c'\sin(\phi_b-\phi)+\cos(\phi_b-\phi)\right]\sqrt{\frac{\xi_b}{\xi}}\cdot \\ u(\text{edge effect}) &= \frac{R(1+\sigma)}{2\pi h E\cdot B}\left[\sin(\phi_b-\phi)-g'\cos(\phi_b-\phi)\right]\sqrt{\frac{\xi_b}{\xi}}\cdot \\ f &= \frac{R\,\mathrm{cosec}^2\theta}{2\pi h r}+\frac{E}{r}\cdot u\left[\text{edge effect}\right]. \end{aligned}\right\}\quad\ldots\ldots(20_3)$$

where $B = \mathrm{cosec}^2\alpha\left(1+\frac{1}{2}\overline{+\sigma}\cdot\frac{\cot\alpha}{K}\right)$ and $\theta_b = \alpha$.

The assumptions in the derivation of the above equations are that the forces at edge (a) do not affect the distortions and stresses at edge (b) and vice-versa. The total stress at any section is obtained by adding the separate effects from groups (19_3) and (20_3). The term $\left\{\frac{R\,\mathrm{cosec}^2\theta}{2\pi h r}\right\}$ in the f equations is common to both groups and is not to be computed twice.

In masonry domes, the thickness usually increases from, h, near the crown, to 2h at the base. The equations derived above have not been extended to include this feature, being outside the scope of this paper. With the advent of reinforced concrete domes, however, where the thickness is uniform, they are definitely of some value, especially in regard to meridional bending stresses and the maximum circumferential stress. In design work it is usually assumed that the distribution steel is sufficient to take

meridional/

meridional bending stresses. In certain cases this may not be within the limits of safety.

Comparison of Spherical Dished Ends with Flat Circular Discs.

Circular flat discs and spherical plates of small curvature are the usual end covers for cylindrical vessels subject to internal pressure. It is desirable that the stresses induced in these forms should be contrasted. As the curvature of a spherical plate, with a fixed horizontal diameter, decreases, the form eventually becomes a circular flat plate. The problem then reduces to comparing the stresses in spherical plates subtending angles at the centre varying from 2θ to zero. In the combined form of the spherical plate attached to the cylindrical wall complications arise, due to the joint effect between the two forms, the nature of which are unknown. It is therefore proposed to study the simple case of a spherical plate rigidly fixed at the edges, which is of some interest.

Consider a circular flat plate, thickness $\frac{3}{4}$in. and radius 13.5in., rigidly fixed at the edge and subject to an upward lateral pressure of P lb. per sq. in. From the equations given in section I the condition of uniform pressure gives

$$\frac{3}{\pi h^3} \cdot W = \frac{3}{\pi h^3} \cdot \pi r^2 P = K_2' r^2 . \qquad \ldots\ldots (1_4)$$

The plate being continuous the integration constant $B' = 0$. From these conditions the bending stress equations appear as:-

Radial bending stress $p' = A' - \frac{3+\sigma}{8} \cdot K_2' r^2 .$ $\ldots (2_4)$

Circumferential " " $f' = A' - \frac{1+3\sigma}{8} \cdot K_2' r^2 .$ (3_4)

And from the condition $i = o$ at $r = r_e$

$$f_e' = \sigma p_e' \qquad \ldots\ldots\ldots (4_4)$$

where the suffix e denotes the edge of the plate. Substituting the value of f_e from (4_4) in (3_4) and eliminating A' from (2_4) and (3_4), the radial bending stress at the edge

is/

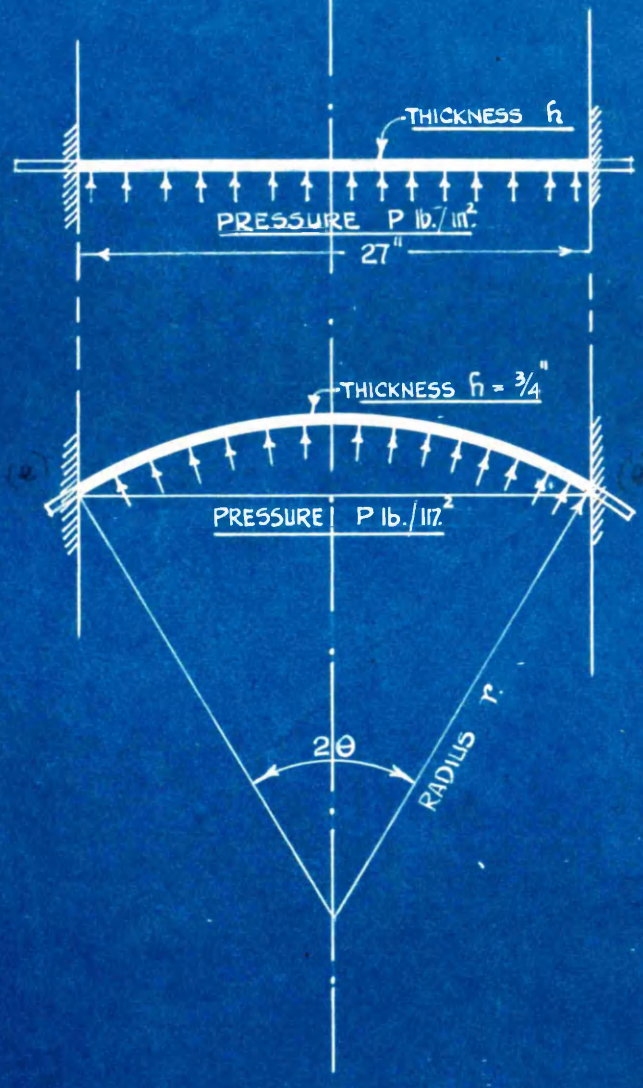
THICKNESS h
PRESSURE P lb./in.²
27"
THICKNESS h = 3/4"
PRESSURE P lb./in.²
2θ
RADIUS r.

FIG. 33.

is found as:-

$$p'_e = -\frac{3Pr^2}{4h^2} \quad \ldots\ldots\ldots \quad (5_4)$$

which is the maximum stress in the plate.

Consider the spherical plate (Fig.33), having a horizontal diameter 27ins. and a thickness $h = \frac{3}{4}$in., subject to an internal pressure P lb. per sq. in. Let the angle subtended by the plate at the centre be 2θ and the radius of the plate r.

The conditions at the edge are:-

(1) $z = o$; (11) $i = o$; (111) $u = o$.

The plate being continuous through the centre, the integration constant $a_1 = o$.

From (1) $$b_1 \sin\theta_e - \frac{a_1}{2}\left(\cot\theta_e - \sin\theta_e \log_e \tan\frac{\theta_e}{2}\right) + \frac{r(1+\sigma)}{E} \cdot S_e = o \quad \ldots\ldots (6_4)$$

$$\therefore b_1 = -\frac{r(1+\sigma)}{E} \cdot S_e \cdot \operatorname{cosec}.\theta_e \quad \ldots\ldots (7_4)$$

From (11) $$-\frac{v^3}{6E}\sqrt{\frac{r}{h}}\left\{\sqrt{\xi_e}\left(-4Kq_e - 4Hb_e\right)\right\} = o \quad \ldots\ldots (8_4)$$

$$\therefore K = -H \cdot \frac{b_e}{q_e}. \quad \ldots\ldots (9_4)$$

From (111) $$-b_1\cos\theta_e - \frac{a_1}{2}\left(1+\cos\theta_e \log_e \tan\frac{\theta_e}{2}\right) + \frac{(1-\sigma)Pr^2}{2hE} + \frac{rv^2}{6E}\sqrt{\xi_e}\left\{(2g_eH-2K)q_e - (2g_eK+2H)b_e\right\} = o$$

$$\therefore H\sqrt{\xi_e} = -\left\{\frac{(1-\sigma)}{2hE} \cdot Pr^2 - \frac{S_e \cdot r(1+\sigma)}{E} \cdot \cot\theta_e\right\} \cdot \frac{6Eq_e}{2rv^2 g_e}. \quad \ldots\ldots (11_4)$$

The shear stress S_θ is given by

$$S_e = -\frac{v}{6}\sqrt{\frac{h}{r}}\left\{\sqrt{\xi}\left(2Hq_e - 2Kb_e\right)\right\}$$

$$= -\frac{v}{6}\sqrt{\frac{h}{r}}\sqrt{\xi_e} \cdot \frac{2H}{q_e}. \quad \ldots\ldots (12_4)$$

Substituting the value of S_θ from (12_4) in (11_4) then

$$H\sqrt{\xi_e} = -\frac{3(1-\sigma)Pr}{2hv^2} \cdot q_e [B] \quad \ldots\ldots (13_4)$$

where $[B] = 1\Big/\left(g_e + \frac{1+\sigma}{K}\right)$.

The meridional bending stress p'e is given by

$$p'e = \sqrt{\xi_e}\left\{(c_eK+H)q_e + (c_eH-K)b_e\right\}$$

$$= H\sqrt{\xi_e}\Big/q_e \quad \ldots\ldots (14_4)$$

$$\therefore p'e = -\frac{3(1-\sigma)}{2hv^2} \cdot Pr \cdot [B]. \quad \ldots\ldots (15_4)$$

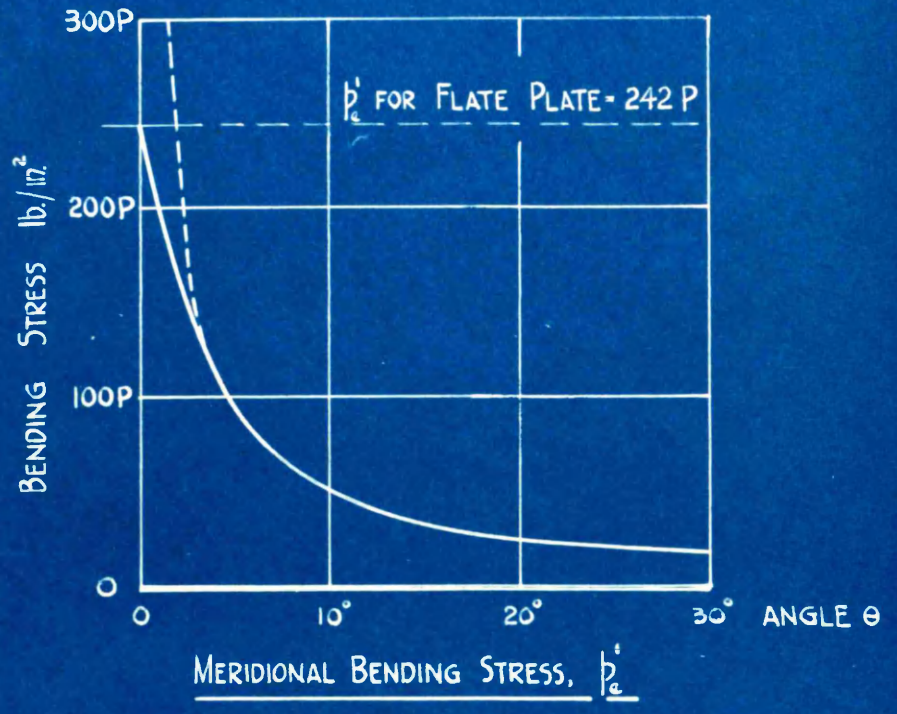
300P
200P
100P
0
BENDING STRESS lb./in.²
p_c' FOR FLATE PLATE - 242 P
0
10°
20°
30°
ANGLE θ
MERIDIONAL BENDING STRESS, p_c'

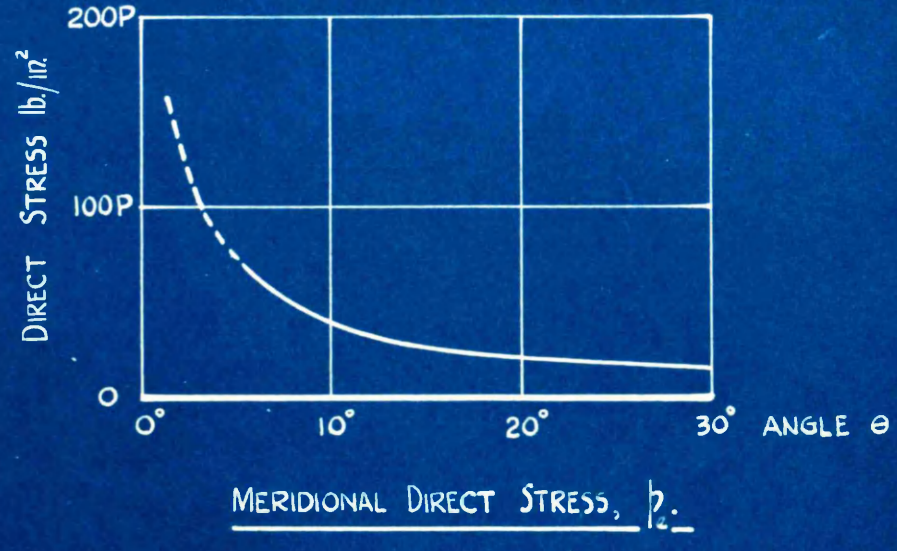
200P
100P
0
DIRECT STRESS lb./in.²
0°
10°
20°
30°
ANGLE θ
MERIDIONAL DIRECT STRESS, p_c

FIG. 34.

Varying the angle θ_e from 0° to 30° the corresponding radial bending stresses are obtained and shown in the graph (Fig.34). The following table gives a few selected values:-

θ	0°	2.5°	5°	10°	20°	30°
	Flat Plate, $p'_e = -\frac{3Pr^2}{4h^2}$	← Spherical Plate. →				
p'_e	- 242P	-176P	-95P	-51P	-26P	-18P

Owing to the approximations made, the solutions to the general equations do not hold for very small angles. In Fig. 34 the broken line indicates the calculated values of p'_e from equation for $\theta < 5^\circ$. The probable values are given by the full line which terminates at the value for flat plates at $\theta = 0^\circ$. Fig. 34 also shows the meridional direct stress obtained from:-

$$p_e = \frac{Pr}{2h} - S_e \cot \theta.$$

In practice the angle θ would be about 30°. At this value the maximum stress = 17.88P (bending) + $15.785\frac{P}{\lambda}$ (direct) = 33.665P. With a flat circular plate the thickness, h, required in order that this maximum stress be not exceeded, is obtained from:-

$$\frac{3Pr^2}{4h^2} = 33.665P.$$

$\therefore h = 2.05$in. compared with $h = 0.75$in. for the spherical plate.

SECTION V.

COMBINED FORMS.

Application: Page.

Discussion:

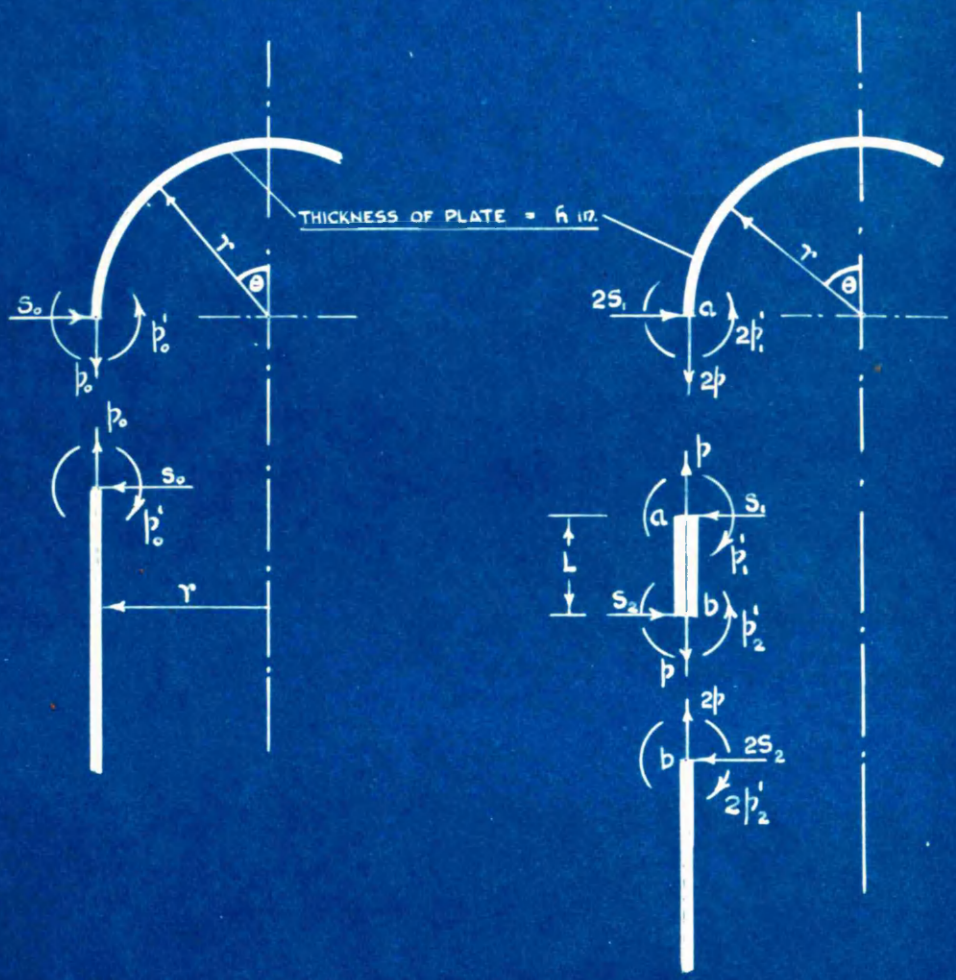

WELDED JOINT

RIVETED LAP JOINT

FIG. 35

Combined Forms.

The grit separator discussed in Section III is an example of the combined forms of a cylindrical wall and a conical wall. The most common construction in practice is perhaps the cylindrical shell with an end cover. The shape of these covers may be anything between a circular flat plate and an elliptical dished end. Whatever the form of the cover, however, one of the main difficulties encountered is that of assessing joint effect. The joint between the plates may be welded, riveted or bolted according to the material.

It is proposed here to compare the axial and meridional bending stresses set up in a cylindrical shell with a hemi-:spherical dished end, under pressure, when these forms are connected by (a) welding, (b) riveted lap joint.

(a) Welded Joint:- In this case the reinforcing effect of the weld is neglected and the plates taken as continuous. Fig.35 shows the dome and the cylindrical shell separated with the assumed bending and shear stresses acting at the edges. The cylinder may be taken as infinitely long and the constants can be obtained immediately from Table II (Section III) and are:-

$$C = p_o' \quad ; \qquad D = p_o' - \frac{6S_o}{v\sqrt{rh/r}} .$$

For the dome it is a simple matter expressing the constants H and K in terms of p'_o and S_o. These constants are:-

$$H\sqrt{\xi_{\pi/2}} = p'_o b_{\pi/2} - \frac{6S_o(q-b)\pi/2}{2v\sqrt{rh/r}} \quad ; \qquad K\sqrt{\xi_{\pi/2}} = p'_o q_{\pi/2} + \frac{6S_o(q+b)\pi/2}{2v\sqrt{rh/r}} .$$

At the junction of the plates the changes of slope are equal

$$\therefore \text{ i (cylinder)} = \text{i (dome)}.$$

$$\therefore -\frac{v^3}{6E}\sqrt{\frac{r}{h}}\frac{1}{\sqrt{\xi_o}}\left\{2(D+C)\cos\alpha_o + 2(D-C)\sin\alpha_o\right\} = -\frac{v^3}{6E}\sqrt{\frac{r}{h}}\sqrt{\xi_{\pi/2}}\left\{-4Kq_{\pi/2} - 4Hb_{\pi/2}\right\} \qquad (1)$$

from which $p'_o = 0$. . . . . (2)

Also, the radial deflections at the junction are equal

$$\therefore \text{ u (cylinder)} = \text{u (dome)}.$$

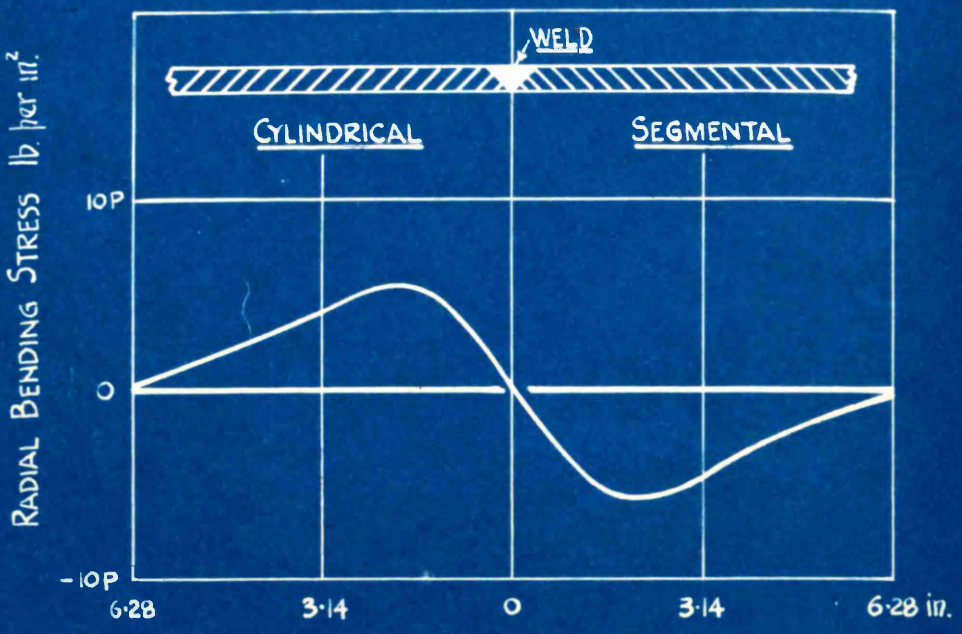
WELD
CYLINDRICAL
SEGMENTAL
RADIAL BENDING STRESS lb. per in.²
10P
0
-10P
6·28
3·14
0
3·14
6·28 in.

FIG. 36

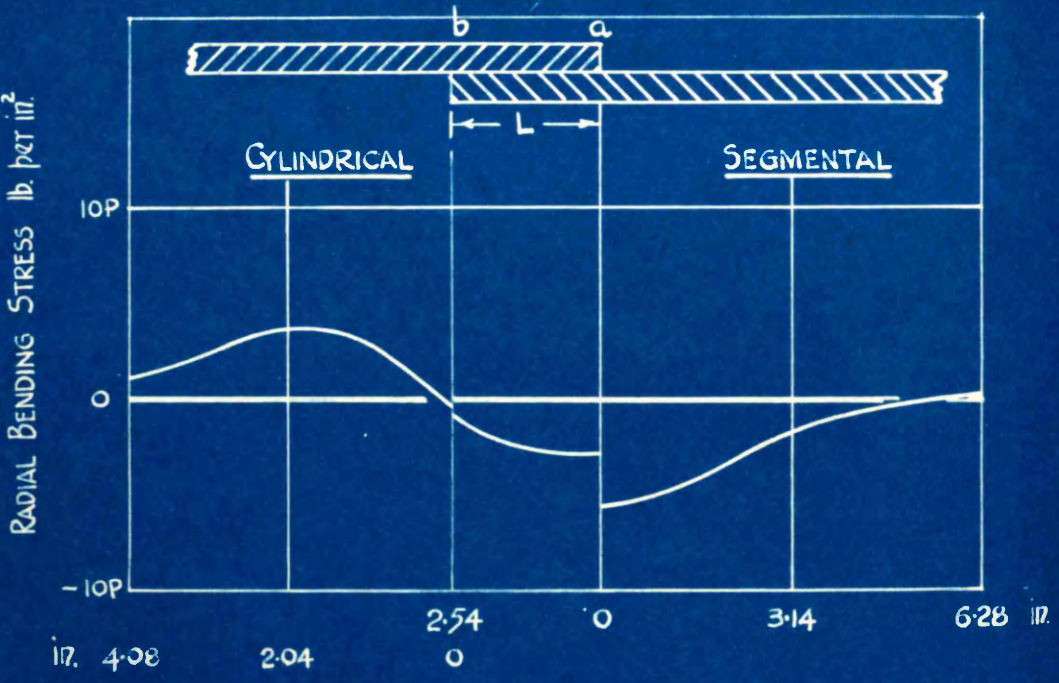
b
a
L
CYLINDRICAL
SEGMENTAL
RADIAL BENDING STRESS lb. per in.²
10P
0
-10P
2·54
0
3·14
6·28 in.
in. 4·08
2·04
0

FIG. 37.

$$\therefore \frac{v^2 r}{6E}\left[\frac{1}{\sqrt{\xi_0}}\left\{-2D\cos\alpha_0 + 2C\sin\alpha_0\right\}\right] + \frac{r}{2\pi hE}\cdot\frac{dW}{dx} - \frac{\sigma r}{E}\cdot a_1$$

$$= \frac{v^2 r}{6E}\left[\sqrt{\xi_0}\left\{(2H-2K)q_{\pi/2} + (-2K-2H)b_{\pi/2}\right\}\right] - b_1\cos\pi/2 - \frac{a_1}{2}\left(1+\cos\frac{\pi}{2}\log_e\tan\frac{\pi}{4}\right) + \frac{Pr^2}{2hE}(1-\sigma) \quad \cdots (3)$$

$$\frac{dW}{dx} = 2\pi r.P \ , \quad a_1(\text{cyl.}) = \frac{Pr}{2h} \ , \quad a_1(\text{dome}) = 0 \ , \quad b_1 = -\frac{r(1+\sigma)}{E}\cdot s_0 \ ,$$

from which

$$s_0 = -\frac{P}{8v}\cdot\sqrt{\frac{r}{h}} \qquad \cdots (4)$$

Hence the constants may now be rewritten thus:-

For the cylinder - $C = 0$; $D = \frac{3}{4}\cdot\frac{Pr}{hv^2}$.

For the dome - $\sqrt{\xi_{\pi/2}}\cdot H = \frac{3}{8}\cdot\frac{Pr}{hv^2}(q-b)_{\pi/2}$,

$\sqrt{\xi_{\pi/2}}\cdot K = -\frac{3}{8}\cdot\frac{Pr}{hv^2}(q+b)_{\pi/2}$.

The bending stress in the cylinder is obtained from:-

$$p' = \frac{1}{\sqrt{\xi}}(C\cos\alpha + D\sin\alpha)$$

$$= \frac{1}{\sqrt{\xi}}\cdot D\sin\alpha$$

$$= \frac{3Pr}{4hv^2}\left[\frac{\sin\alpha}{\sqrt{\xi}}\right]$$

where $\alpha = nx$, $\xi = e^{2nx}$.

The bending stress in the dome is obtained from:-

$$p' = \sqrt{\xi}\left[(cK+H)q + (cH-K)b\right]$$

$$= -\frac{3Pr}{8hv^2}\sqrt{\frac{\xi}{\xi_{\pi/2}}}\left[(c+1)\sin(\phi_{\pi/2}-\phi) + (c-1)\cos(\phi_{\pi/2}-\phi)\right]$$

But $C \doteq 1$ for all necessary values of θ in this case

$$\therefore p' = -\frac{3Pr}{4hv^2}\left[\sin(\phi_{\pi/2}-\phi)\right]\sqrt{\frac{\xi}{\xi_{\pi/2}}}.$$

where $\phi = (\bar{k}+\tfrac{1}{2})\theta$, $\sqrt{\xi} = e^{\bar{k}\theta}/(\sin\theta)^{\frac{1}{2}}$.

Taking the values h = $\frac{1}{8}$in., r = 18in., the variations of the radial bending stresses along the plates from the junction are shown in Fig. 36.

(b) <u>Riveted Joint:-</u> This case reduces to an infinitely long cylinder, radius r and thickness h, connected to a hemi-:spherical shell of radius r and thickness h, by means of a cylinder (ab) (Fig.37) of length L and thickness 2h. The cylinder (ab) is composed of two cylinders of equal length

and/

and thickness.

The method of solution is given briefly. The constants for the hemispherical wall can be expressed in terms of p_1' and s_1. The constants for the long cylinder can be expressed in terms of p_2' and s_2. And the constants for the cylindrical wall, length L, thickness 2h, may be expressed in terms of p_1', p_2', s_1 and s_2. The values for these constants can be obtained from Table II, Section II of this paper. To facilitate the work, the following values have been taken.

Radius r = 18in; thickness, h = $\frac{1}{2}$in; L = 2.58in.

The conditions at (a) and (b) furnish four equations, from which the bending and shear stresses can be evaluated. The equations are obtained from:-

$$\left.\begin{array}{ll} \text{At edge (a)} & i \text{ (spherical wall)} = i \text{ (cylinder L)} \\ & u \text{ (" ")} = u \text{ (" ")} \\ \text{At edge (b)} & i \text{ (long cylinder)} = i \text{ (" ")} \\ & u \text{ (" ")} = u \text{ (" ")} \end{array}\right\} \quad \ldots\ldots(8)$$

The arithmetical values of the bending and shear stresses are:-

$p_1' = -2.9P$; $s_1 = +0.0094P$; $p_2' = -0.355P$; $s_2 = -0.263P$;

Hence the values of the constants may be obtained:-

For the spherical wall,

$$\left.\begin{array}{l} H\sqrt{\xi_1} = -1.912P. \\ K\sqrt{\xi_1} = -5.2P. \end{array}\right\} \quad \ldots\ldots\ldots(9)$$

For the long cylinder,

$$\left.\begin{array}{l} C = -0.71P \\ D = +13.99P \end{array}\right\} \quad \ldots\ldots\ldots(10)$$

For the cylinder (ab),

$$\left.\begin{array}{ll} A'\sqrt{\xi'} = -11.64P, & C' = +2.44P \\ B'\sqrt{\xi'} = +8.42P, & D' = +3.62P \end{array}\right\} \quad \ldots\ldots(11)$$

The radial or axial bending stresses are obtained from the following equations.

<u>For the spherical wall</u> - neglecting c.

$$p' = \sqrt{\xi}\left[(H + K)q + (H - K)b\right] \quad \ldots\ldots\ldots(12)$$

<u>For the long cylinder.</u>

$$p' = \frac{1}{\sqrt{\xi}}\left[C\cos\alpha + D\sin\alpha\right] \quad \ldots\ldots\ldots(13)$$

For the cylinder (ab), origin at (a),

$$p' = \sqrt{\xi'}\left\{A'\cos\alpha' + B'\sin\alpha'\right\} + \frac{1}{\sqrt{2'}}\left\{C'\cos\alpha' + D'\sin\alpha'\right\} \quad \ldots\ldots (14)$$

The variations in the bending stresses along the plates are shown in Fig. 37.

The radial bending stresses in the spherical plate are due to the forces acting at the edge. While the maximum values in the two cases are practically equal, the stresses in case (a) are the result of the shearing force, while in case (b) they are due to the edge bending moment. These stresses are not so important in vessels of this form since the design is controlled by the circumferential direct stress in the cylinder. The point of interest, however, lies in the change of the edge force values from a zero edge moment accompanied by a large negative shear force for the welded joint to a high bending moment combined with a very small positive shear force for the riveted joint. In dished ends of a shape other than hemispherical, this feature may be very important.

Elliptical and Double Segmental Dished Ends.

The two types of dished ends in practice are the elliptical and the double segmental. The former has been discussed in various publications, and agreement between theoretical calculations and practical tests has been obtained where the cover is welded to the cylinder.

The extensional equations for the elliptical dished end are easily obtainable,[6] but the edge effect equations in use are those of the cylindrical wall with $ns = \sqrt[4]{\frac{3(1-\sigma^2)}{h^2}}\int_0^s \frac{ds}{\sqrt{R_1}}$ in place of $nx = \sqrt[4]{\frac{3(1-\sigma^2)}{h^2r^2}} \cdot x$.

When it is known that the important bending stresses occur in the zone of the end cover plate adjacent to the cylindrical wall, the reason why this adaption of the cylindrical/

[6] Transactions A.S.M.E. (A.P.M.) 1930 Vol. 52 (1).

cylindrical equations is so well supported by experimental results becomes apparent. The form of this portion of the elliptical plate does not differ greatly from that of the cylinder, and the stresses in the sections further removed from the edge are very small. The criticism of the equations is that no account is taken of the variation in the width of a strip in the elliptical shell, and therefore, their applicability to points some distance from the edge is not possible.

This fact is clearly demonstrated in spherical shells where the cylindrical edge effect equations can be applied to an edge subtending a large value of θ at the centre. The difference in the final results so obtained, and those given by the application of the spherical shell equations to the same edge is negligible. Where θ is small, however, the cylindrical equations cannot be applied. This is due to the effect which the coefficients c, c', g and g' have on the final values. These quantities are present in the spherical equations but absent in the cylindrical equations. In the former equations their value is approximately unity when θ is large. Therefore, while the cylindrical or spherical equations may be adapted for the elliptical shell and applied in the zone adjacent to the cylindrical wall, giving results which compare favourably with those obtained by experimental methods, the spherical equations only, can be adapted for the successive zones. As far as the determination of the maximum stress is concerned, there is no gain in adapting the latter equations; indeed, there is additional labour, for the origin of the shell would be at the crown; whereas, in adapting the cylindrical equations, the origin is at the edge; but a more uniform solution is obtained.

The nature of the difference in the equations lies in the 'nx' value for the cylinder or the Kθ value for the

sphere/

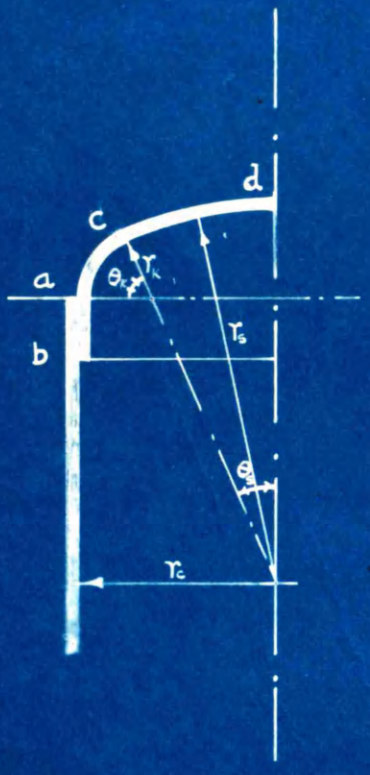

FIG. 38(a).

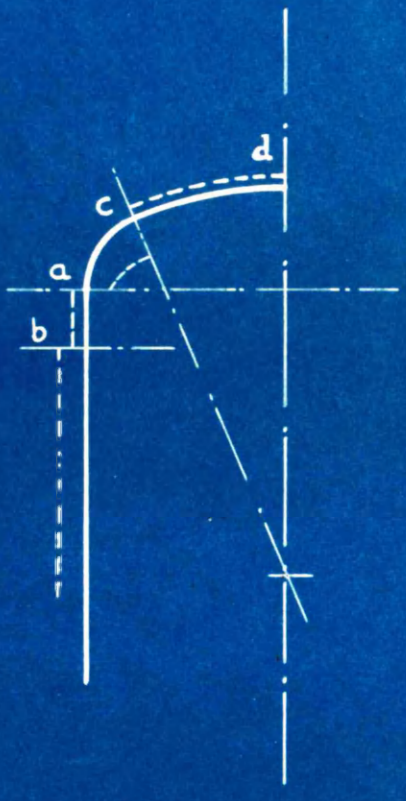

FIG. 38(b).

FULL LINES - MERIDIONAL SECTION OF VESSEL

BROKEN LINES - NORMAL DISPLACEMENTS (EXTENSIONAL EFFECTS.)

sphere. To maintain complete similarity in the elliptical shell equations the following development is given.

(1) Adapting the cylindrical equations:-

For the cylinder, $nx = \sqrt[4]{\frac{3(1-\sigma^2)}{h^2r^2}} \cdot x = N$

For the elliptical shell, $N = \sqrt[4]{\frac{3(1-\sigma^2)}{h^2}} \int_0^s \frac{ds}{\sqrt{R_1}}$

$$= \sqrt[4]{\frac{3(1-\sigma^2)}{h^2r^2}} \int_0^s \lambda\, ds$$

where $\lambda = \sqrt{\frac{r}{R_1}}$, $\therefore N = n\bar{s}$,

where $\bar{s}$ is the modified length of the elliptical shell under consideration, corresponding to x in the cylindrical shell.

(2) Adapting the spherical equations:-

For the spherical wall, $\bar{K}\theta = \sqrt[4]{\frac{3(1-\sigma^2)r^2}{h^2}} \cdot \theta = M$

For the elliptical wall $M = \sqrt[4]{\frac{3(1-\sigma^2)}{h^2}} \int_0^{\theta} \frac{R_2\, d\theta}{\sqrt{R_1}}$

$$= \sqrt[4]{\frac{3(1-\sigma^2)r^2}{h^2}} \int \lambda\, d\theta$$

where $\lambda = \frac{R_2}{\sqrt{R_1 \cdot r}}$, r = radius of the cylindrical wall

$$\therefore M = \bar{K}\bar{\theta}$$

where $\bar{\theta}$ is the modified angle subtended to the vertical through the crown by the section of elliptical shell under consideration. This value corresponds to θ in the spherical shell.

The analogy may be continued in the treatment of double segmental dished ends. Fig. (38a) shows such a form, the knuckle wall (ac) attaching the spherical shell to the cylindrical wall. The plate for the knuckle and spherical parts is continuous, but discontinuity stresses are set up at (c) due to the change in form. The joint at (a) may be welded or riveted. The latter is shown in this instance. While the cylindrical equations may be adapted and applied to the knuckle wall at edge (a), they cannot be applied with the same confidence at edge (c), and certainly definite errors

would/

would occur if they were adapted and applied to the spherical plate at the same edge, the angle θ being about 20°. It is more fitting that in this type of cover plate, the spherical equations should be adapted for the knuckle throughout.

The modification of the value $\bar{K}\theta$ to be used in the edge effect equations for the knuckle wall is obtained by a method similar to that given above.

For the knuckle:-

$$M = \sqrt[4]{\frac{3(1-\sigma^2)}{h^2}} \cdot \int_0^{\theta} \frac{R_1 d\theta}{\sqrt{R_1}} = \sqrt[4]{\frac{3(1-\sigma^2)R_1^2}{h^2}} \int_0^{\theta} \lambda \, d\theta .$$

where $\lambda = \sqrt{\frac{R_2}{R_1}}$, since R_2, the meridional radius for the knuckle is constant.

$$\therefore \quad M = \bar{K}_0 \bar{\theta}.$$

In the equations of stress and distortion, the circumferential radius r for the spherical shell, is replaced by R_1 which is variable. Graphical methods may be adopted for the evaluation of the quantity $\bar{\theta} = \int_0^{\theta} \lambda d\theta$. The most convenient way is to divide up the plate into a series of annular elements, for each of which the circumferential radius R_1 may be regarded as constant, and obtaining a straight-forward numerical integration. The value θ subtended by these elements may be taken as 5 degrees as a maximum, but should decrease as R_1 increases. Experience would be the best guide in the selection of this value.

The extensional equations for the knuckle wall are obtained in much the same way as those for the spherical shell. They are longer and more complicated but maintain similarity. Experiments on this type of dished end, subject to internal pressure, have been carried out by different firms. One set of results[7] has been published accompanied by an analytical solution which contains many doubtful assumptions and is rather incomplete. In other cases only the experimental results are given/

[7] Transactions A.S.M.E. (P.M.E.) 1931 Vol. 53.

given,[8] while some do not seem to have appeared in print at all. One outstanding feature of these publications is, that while the dimensions of the plate are carefully detailed, those for the joint are omitted. In one case,[7] the solution given assumes a welded joint between the knuckle and cylindrical walls, while a photograph of one of the vessels tested shows a double riveted joint of some description.

Fig. (38b) illustrates the radial deflections u of the different shells when supported by tangential forces at the edges. It will be observed that edge (a) is the junction between two short walls, the knuckle wall (ac) and the cylindrical wall (ab). The shearing force at this edge, owing to the nature of the free radial deflections of the separate plates, will always be high,and correspondingly high radial bending stresses are set up in the knuckle. The stresses due to the edge moment, in contrast to the case of the spherical-cylindrical vessel, are negligible in comparison. It is desirable, therefore, that this shearing force should be as small as possible.

The opportunities for effecting this are two-fold; the first being the length and thickness of the joint, or as it is treated in this case, the cylinder (ab); the second being the location of the edge (c). It requires no argument to show that the dimensions of (ab) and the length (ac) will have a definite effect on the forces at edge (a). An analytical demonstration of these facts would be very complicated, but it would not be difficult to give arithmetical illustrations showing for different dimensions the variation in the maximum bending stress in the knuckle.

This treatment of the joint (ab) as a short cylinder does not seem to have been developed, and while it cannot be assumed that the conditions in practice are similar, a good approximation for the restraint effect due to the lap may be

obtained/

[8] "The Strength of Dished Ends" A.E.S.D. 1923.
[7] Ibid.

obtained. The method of solution, while it entails much arithmetical work, is simple. The constants in the edge effect equations can be expressed in terms of the unknown bending and shear stresses at the edges, (a), (b) and (c). The conditions of radial deflection and change of slope at these points supply six equations to solve for six unknowns. The constants in the extensional equations are obtained from the conditions of tangential displacement and direct stress at the edges (a), (b) and (c). When it is remembered that the extensional and edge effect equations for the different walls are of a similar form, the labour in these computations is not so great as it would at first appear.

While it is possible for the knuckle wall to be of such a length that the conditions at edge (c) do not affect the forces at edge (a), it is not possible in the case of the cylinder (ab). As was seen in the problem of the overhung rim of a rotating wheel, there will be a ratio $L/\sqrt{rh}$ for the cylindrical wall (ab) which, in this case, will give a maximum reduction of the shearing force at the edge (a), determined as for a welded joint and a corresponding decrease in the radial bending stresses in the knuckle plate. In the usual design practice, while the restraint due to the riveted joint is recognized, no allowance appears to have been made for it. In the case of the spherical-cylindrical vessel, the shear stress at the joint changes from - 0.584P for the weld to + 0.0094P for the lap. While such a change is not possible in the vessels having a double segmental cover plate, the shearing forces in the two cases will be different.

An interesting fact which appeared in the discussion of a paper[7] was that the stress at the crown in a double segmental end was found to be higher in experimental results than the radial direct stress $\frac{Pr}{2h}$ which is usually assumed. This additional stress is, of course, a radial bending stress set up by the edge forces at c. In shallow spherical plates the rate at/

[7] Ibid.

at which edge force effects are damped out is not very rapid.

There are many features in a design of this type which require careful examination; but the main purpose of this Thesis has been fulfilled in formulating similar equations for the cylindrical, conical and spherical walls, and showing how this similarity may be extended to include forms of any shape. Various points in the former serve as excellent guides in the method of solution for the more complicated forms. And for all cases the method of attack is similar, no matter what the edge conditions may be. It has been mentioned that this method of solution is very laborious; any attempt at an exact analysis always is. The approximate solution, however, can only be reached through these labours, and in many cases an arithmetical computation is a more persuasive argument than an analytical discussion. When a number of solutions have been examined, the vital terms may be selected and so re-cast that a more simple formula for the critical stresses can be obtained. This was done in the problem of the turbine diaphragm. When the values and positions of the maximum stresses can be thus expressed, the design is more or less under complete control.

This work is so presented that the further problems of the variation of plate thickness and temperature effect may now be developed and put on record. When this analytical survey of the arched plate is allied with experimental work, much of which remains to be done, the whole should serve to have this important section of engineering design in a more satisfactory state.

The author desires to express his gratitude to Professor A. L. Mellanby, D.Sc. for arranging tests to be carried out in the engineering laboratories of the Royal Technical College; and for many opportunities afforded for the collection of data from various sources; also to Professor W. Kerr, Ph.D. for his unfailing interest, helpful criticisms and direction in the work so presented.

---- oOo ----

BIBLIOGRAPHY.

Boyd, I. S. "A Domed Pavilion - Its Construction and Stone Cutting". Architects Journal, April 1922, p.567.

Coates, W. M. "The State of Stress in Full Heads of Pressure Vessels". Transactions of American Society of Mechanical Engineers, Vol. 52(1) 1930.

Dunn, W. "Notes on the Stresses in Framed Spires and Domes". Journal of the Royal Institute of British Architects, May 1904, p. 401.
"Principles of Dome Construction". The Builder, February, 1909, p.63.

Engineering. Vol. 116, June 1923.

do. Vol. 121, June 1926.

Hobson, E. W. London, Philosophical Transactions of Royal Society. Vol. 187, 1897.

Hool, G. A. and Johnson, N.C. Handbook of Building Construction Vol. (1) 1920. McGraw - Hill Book Company.

Kerr, Professor W. "Direct and Bending Stresses in Circular Flat Plates". Journal of Royal Technical College, Glasgow, 1930.

Lorenz, R. Verein Deutscher Ingenieure. Vol. 52, 1908, p. 1706.

Love, A.E.H. Mathematical Theory of Elasticity , 1920. Cambridge University Press.
"Equilibrium of a Thin Elastic Spherical Bowl". Proceedings of the Royal Mathematical Society, 1897.

"Mechanical Engineering". Vol. 49, No. 2, February, 1927.

Pounder, C. C. "The Strength of Dished Ends". Association of Engineering and Shipbuilding Draughtsmen, 1923.

Prescott, J. Applied Elasticity - 1924. Longmans, Green and Company.

Reports of British Association. Edinburgh 1921, Liverpool 1923.

Rhys, C. O. "Stresses in Dished Heads of Pressure Vessels". Transactions of American Society of Mechanical Engineers, Vol. 53, December 1931.

Timoshenko, S. Strength of Materials, Part II 1931. Macmillan & Co.

Westphal, M. Verein Deutscher Ingenieure. Vol. 41, 1897. p. 1036.